

Field testing of railroad flatcar bridges on low-volume roads

by

Holly Ann Boomsma

A thesis submitted to the graduate faculty
in partial fulfillment of the requirements for the degree of
MASTER OF SCIENCE

Major: Civil Engineering (Structural Engineering)

Program of Study Committee:
F. Wayne Klaiber, Co-major Professor
Terry J. Wipf, Co-major Professor
Loren W. Zachary

Iowa State University

Ames, Iowa

2005

**Graduate College
Iowa State University**

**This is to certify that the master's thesis of
Holly Ann Boomsma
has met the thesis requirements of Iowa State University**

Signatures have been redacted for privacy

—

TABLE OF CONTENTS

LIST OF FIGURES	vi
LIST OF TABLES.....	ix
1. INTRODUCTION.....	1
1.1 Railroad Flatcar Bridges	1
1.1.1 RRFC Selection	1
1.1.2 RRFC Bridges.....	2
1.1.2.1 Tama County Bridge, IA	2
1.1.2.2 Buchanan County Bridge, IA.....	3
1.1.2.3 Winnebago County Bridge, IA.....	4
1.2 Objective and Scope of Project.....	5
2. BUCHANAN COUNTY BRIDGE 3 ON 270 th St.	7
2.1 Introduction.....	7
2.2 Design and Construction	9
2.3 BCB3 Field Testing.....	18
2.4 BCB3 Dead Load Analysis.....	26
2.5 BCB3 Field Testing Results	27
2.5.1 Static Testing	27
2.5.2 BCB3 Longitudinal Connection Behavior.....	33
2.5.3 Time History Analysis.....	36
2.5.4 Dynamic Testing	37
3. WINNEBAGO COUNTY BRIDGE 2 ON 460 th St.	42
3.1 Introduction.....	42
3.2 Design and Construction	43
3.3 WCB2 Field Testing.....	47

3.4 WCB2 Dead Load Analysis.....	58
3.5 WCB2 Field Testing Results	59
3.5.1 Static Testing	59
3.5.2 Time History Analysis.....	68
3.5.3 Dynamic Analysis.....	69
4. SUMMARY AND CONCLUSIONS	77
4.1 Summary	77
4.2 Conclusions	80
APPENDIX A: SHEET PILE ABUTMENTS	81
A.1 Background.....	82
A.1.1 Sheet Pile Abutment Feasibility	82
A.1.2 Case Studies of Sheet Pile Abutments	83
A.1.2.1 Highway Bridge over a Branch of the Moselle - Europe.....	83
A.1.2.2 Highway Bridge over a Railroad - Europe.....	83
A.1.2.3 Highway Bridge over a Port Facility - Europe	84
A.1.2.4 Taghkanic Creek Bridge, Columbia County, New York – United States.....	84
A.1.2.5 Banks Road Bridge, Tompkins County, New York – United States.....	84
A.1.2.6 Sprout Brook Bridge, Paramus, New Jersey – United States	85
A.1.3 Analysis and Design	85
A.1.3.1 Point Resistance	88
A.1.3.2 Frictional Resistance	89
A.2 Sheet Pile Abutment Design.....	89
A.2.1 Soil Properties	90
A.2.2 Earth Pressures.....	90
A.2.3 Pile Design	91

APPENDIX B: "SHOE" DESIGN FOR CONCRETE AND STEEL ABUTMENTS.....	104
REFERENCES	111
ACKNOWLEDGEMENTS	113

LIST OF FIGURES

Figure 2.1. Location of the Buchanan County RRFC Bridge 3.....	7
Figure 2.2. Original Buchanan County Bridge on 270 th St	8
Figure 2.3. Buchanan County RRFC Bridge 3.....	9
Figure 2.4. Details of the BCB3 concrete abutments	11
Figure 2.5. 66 ft – 2 in. RRFC cut from 89-ft RRFC	14
Figure 2.6. Bolted longitudinal connection.....	17
Figure 2.7. Built-up bearing sections at the abutments of the BCB3.....	18
Figure 2.8. Dimensions and weights of test truck used in BCB3 field tests.....	19
Figure 2.9. Test truck used in BCB3 bridge field test.....	20
Figure 2.10. Dynamic testing of the BCB3.....	20
Figure 2.11. Transverse locations of the truck used in field tests.	21
Figure 2.12. Photographs of the test truck on BCB3.....	22
Figure 2.13. Location of instrumentation used in BCB3 field test.....	23
Figure 2.14. Midspan deflections and strains for tandem truck in Lane 1	28
Figure 2.15. Midspan deflections and strains for tandem truck in Lane 2	29
Figure 2.16. Midspan deflections and strains for tandem truck in Lane 3	30
Figure 2.17. Comparison of midspan deflections and strains for Lanes 1, 2, and 3	31
Figure 2.18. Midspan cross-section of BCB3	34
Figure 2.19. Horizontal and vertical axes of bending	35
Figure 2.20. End view of the longitudinal connection joint during loading	35
Figure 2.21. Plan view of the longitudinal connection joint	36
Figure 2.22. Strain instrumentation locations for BCB3 time history analysis	36
Figure 2.23. Time history of bottom flange strains in the South RRFC interior girder.....	38

Figure 2.24. Comparison of the measured interior girder deflections of the North, Middle and South RRFCs from static and dynamic field tests (Lane 1 loading).....	39
Figure 2.25. Comparison of the measured interior girder bottom flange strains of the North, Middle, and South RRFCs from static and dynamic field tests (Lane 1 loading)	40
Figure 3.1. Location of the Winnebago County RRFC Bridge 2.....	42
Figure 3.2. Original three-span, timber bridge at the WCB2 site.....	43
Figure 3.3. Winnebago County RRFC Bridge 2.....	44
Figure 3.4. Longitudinal concrete beam connection used in the WCB2.....	46
Figure 3.5. Exterior girder supports for the WCB2.....	48
Figure 3.6. Dimensions and weights of truck used in WCB2 field test	50
Figure 3.7. Location of instrumentation used on the WCB2.....	52
Figure 3.8. Deflection and strain instrumentation on the WCB2	55
Figure 3.9. Transverse truck locations during the WCB2 load testing.....	56
Figure 3.10. Photographs of WCB2 field testing.....	57
Figure 3.11. WCB2 midspan deflections and strains when the truck was in Lane 1	60
Figure 3.12. WCB2 midspan deflections and strains when the truck was in Lane 2	61
Figure 3.13. WCB2 midspan deflections and strains when the truck was in Lane 3	62
Figure 3.14. WCB2 midspan deflections and strains when the truck was in Lane 4	63
Figure 3.15. Comparison of midspan deflections and strains for Lanes 1, 2, and 3	65
Figure 3.16. Strain instrumentation locations for WCB2 time history analysis	68
Figure 3.17. WCB2 strain vs. time for the South RRFC's interior girder bottom flange	70
Figure 3.18. Comparison of the measured interior girder deflections of the North, Middle, and South RRFCs from static and dynamic field tests (Lane 1 loading).....	71
Figure 3.19. Comparison of the measured interior girder bottom flange strains of the North, Middle, and South RRFCs from static and dynamic field tests (Lane 1 loading)	72

Figure 3.20. Comparison of field data from WCB1 and WCB2 (Lane 1)	74
Figure 3.21. Comparison of field data from WCB1 and WCB2 (Lane 2)	75
Figure 3.22. Comparison of field data from WCB1 and WCB2 (Lane 3)	76
Figure A.1. Design lateral forces for a cantilevered sheet pile	87
Figure A.2. Design lateral forces for an anchored sheet pile using free-earth method	87
Figure A.3. Point and frictional resistance	88
Figure A.4. Bounded and developed areas	88
Figure A.5. Theoretical WCB dimensions	89
Figure A.6. Sketch of sheet pile analysis	91
Figure A.7. Sheet pile abutment design for the theoretical WCB	94
Figure A.8. Theoretical WCB sheet pile abutment bearing support design	95
Figure A.9. Location of interior girder supports	96
Figure A.10. Location of exterior girder supports	97
Figure A.11. Exterior girder support at the sheet pile wall abutment	98
Figure A.12. Exterior girder support at reinforced concrete connection beam located at the sheet pile wall abutment	99
Figure A.13. Exterior girder support at the pier (bolster location)	100
Figure A.14. Exterior girder support at the reinforced concrete connection beam located at the pier (bolster location)	101
Figure A.15. Interior girder support at the sheet pile wall abutment	102
Figure A.16. Interior girder support at the pier (bolster location)	103
Figure B.1. 89-ft RRFC interior girder depths along length	105
Figure B.2. Bearing conditions for the RRFC interior girders	106
Figure B.3. Support at tapered end of RRFC interior girder for concrete abutment	107
Figure B.4. Support at tapered end of RRFC interior girder for steel abutment cap	109

LIST OF TABLES

Table 2.1. Inertias of various RRFC members.....32

Table 3.1. WCB2 bottom flange dead load stresses.....59

Table 3.2. WCB2 bottom flange total stresses.....67

1. INTRODUCTION

1.1 Railroad Flatcar Bridges

Previous research regarding the viability of using railroad flatcars (RRFCs) for low-volume road (LVR) bridge superstructures has been documented in the Iowa State University (ISU) 1999 feasibility study [1] and 2003 demonstration project [2]. This construction technique has been shown to provide an economical solution to the need for bridge replacement in several counties around the state of Iowa. Other advantages include the ease of construction and maintenance along with the flexibility of bridge length and abutment type. Careful RRFC selection along with proper design and construction procedures can result in RRFC bridges for LVRs that will successfully carry legal loads. The performance of these bridges has also been shown to be accurately represented using grillage modeling and analysis.

1.1.1 RRFC Selection

A RRFC may be decommissioned for various reasons including age, derailment, and economics. The main concern with aged cars is the remaining fatigue life; however, since LVR bridges see little traffic frequency, fatigue is not a concern. RRFCs derailed because of significant damage should be avoided due to the members' ineffective load carrying capabilities. As newer, more economically built and maintained cars are being used, older cars are often derailed and replaced with new cars because the cost of repairing items such as breaks, wheels, and bearings often cost more than the value of the car itself. Therefore, RRFCs out of service due to age or economics are ideal for RRFC bridges on LVRs. The structure of the RRFC must also be examined including location and size of longitudinal and transverse members. Redundancy within the members is essential in order to ensure proper load transfer throughout the bridge superstructure [2].

1.1.2 RRFC Bridges

Several Iowa counties have previously expressed interest in the RRFC bridge concept and have collaborated with ISU for construction and testing of some demonstration bridges. In the 1999 feasibility study [1], a bridge in Tama County, IA was tested, and for the 2003 demonstration project [2] bridges in Buchanan and Winnebago County, IA were designed, constructed, and tested in a collaborative effort between the counties and ISU.

1.1.2.1 Tama County Bridge, IA

A RRFC bridge in Tama County, IA spanning 42 ft from center to center of abutments was composed of two RRFCs placed side-by-side to create a 12 ft width. Metal gratings followed by transverse timber planks create the driving surface. Each RRFC had, as the primary longitudinal load bearing members, two exterior girders (C-sections) and two interior girders (I-sections). Multiple transverse members, including one exterior member and one interior member, had sustained significant damage prior to construction. Support conditions at the abutments were not uniform for each flatcar; hence, bridge symmetry and redundancy in load paths at the abutments was questionable [1].

Testing of the Tama County Bridge (TCB) was conducted both before and after connections between the two RRFC were established, and the differences in strains and deflections from the two tests varied only slightly. Therefore, it was shown that the longitudinal connections did very little to distribute the loads between the flatcars, but, instead, the timber planks alone could effectively transfer traffic loads across the bridge width [1].

A finite element model created using beam elements verified the results found through the field test conducted on the TCB. Maximum stresses found in the RRFC members were below the yield strength of the steel and the maximum deflections were also less than the American Association of State and Highway and Transportation Officials

(AASHTO) maximum recommendation of 'span'/800 for live load deflections. In conclusion, the analytical model and field tests conducted verified that the TCB could adequately carry Iowa legal loads despite the previous damage of the RRFC before construction [1].

1.1.2.2 Buchanan County Bridge, IA

Buchanan County, IA replaced an existing kingpost pony truss bridge with a single span 56-ft RRFC bridge (clear span: 51ft – 9 1/2 in.). Three 56-ft V-shaped RRFCs placed side-by-side created a 29 ft wide deck, which had a driving surface composed of pea gravel and asphalt millings. A guardrail system was also installed to provide traffic safety across the waterway. Each RRFC had a redundant cross-section consisting of an interior girder seated 6 in. below the two exterior girders, thus creating the V-shaped deck. Using visual inspection and string line, straightness of members was ensured and the cambers of all three RRFCs were found to vary by only 1/2 in. The RRFCs were placed upon concrete abutments using bearing plates [2].

A longitudinal reinforced concrete beam was used to connect the RRFCs. Formwork was clamped to the flanges of the adjacent RRFC exterior members, and midspan shoring was constructed. Longitudinal reinforcement was placed in the void region between the adjacent exterior girders and holes were drilled through the exterior members to insert transverse threaded rods, which were tightened. The void region was then filled with concrete and allowed to cure for two weeks before the formwork was removed [2].

Three separate field load test were performed on the Buchanan County Bridge 1 (BCB1). The first load test was conducted before the concrete beam connection was installed. The second load test was performed after the longitudinal connections between the RRFCs were constructed, and involved testing the bridge both before and after the driving surface was installed. One year after service on the BCB1, the third, final load test, was conducted. All of the load tests involved measuring deflections and strains at critical

locations in the bridge by instrumenting longitudinal and transverse members along with the bridge deck [2].

A grillage analysis of the RRFCs joined with the longitudinal concrete beam connections was performed. The results indicated that the 56-ft RRFCs could each support Iowa legal loads and that the concrete connection could sufficiently distribute the live loads to each of the three RRFCs, reducing both the maximum strains and deflections in the longitudinal girders. A laboratory connection specimen, similar to the longitudinal concrete beam connection used for the BCB1, was tested in both torsion and flexure. The results showed the connection had adequate strength for use in the BCB1. Field tests of the BCB1 verified the analytical and laboratory results: the RRFC structural members experienced stresses below the yield stress of the material and deflections were below the recommended AASHTO recommendations when exposed to traffic loads. Therefore, it was concluded that the BCB1 could sufficiently support Iowa legal traffic loads [2].

1.1.2.3 Winnebago County Bridge, IA

Due to deterioration of the substructure, a three-span, timber bridge crossing the North Fork Buffalo Creek in Winnebago County, IA was replaced with a three-span RRFC demonstration bridge. The two lane bridge had three 89-ft RRFCs side-by-side placed upon steel piles and caps at the abutments and piers. The roadway was 26 ft – 9 in. wide with a transverse timber deck, gravel driving surface, and guardrail system.

A longitudinal reinforced concrete beam was constructed to create the connection between the RRFCs. Holes were drilled through adjacent RRFC exterior girder webs and threaded rods were inserted and bolted. Steel plates were then welded to the bottom flanges of the adjoining exterior girders. Longitudinal reinforcement was placed on top of the transverse threaded rods and the void region between the exterior girders of adjacent

RRFCs was filled with concrete. After seven days of concrete curing, steel plates were welded to the adjacent RRFCs, above the concrete connection [2].

Field testing of the Winnebago County Bridge 1 (WCB1) involved instrumenting longitudinal and transverse members with strain and deflection transducers during four separate field tests. The first test was carried out before the concrete connection was built between the RRFCs and before any driving surface was installed. The following two tests were conducted immediately after completion of the bridge, and the last test was performed after approximately 9 months of traffic loading [2].

Both theoretical and field test data for the WCB1 had comparable results. Theoretical data was obtained for the WCB1 by constructing a grillage model of the bridge in which the structural members were modeled as prismatic, symmetrical beam elements. Results indicated that 99.9% of the bridge bending moment was resisted by the RRFCs' interior girders. This non-redundancy assumption of the 89-ft RRFC was verified from field tests performed on the WCB1 in which exterior girders experienced nearly zero strains while interior girders recorded strains over 400 $\mu\text{in/in}$ (11.6 ksi). Field tests show that the longitudinal concrete beam connections between the RRFCs, along with transverse timber planks on the bridge deck, adequately distribute the traffic loads to all RRFCs. Data from theoretical and field tests show that the RRFC stresses were well below the yield stress of the material, and deflections were below the maximum values specified by AASHTO [2].

1.2 Objective and Scope of Project

Additional research was recommended by the 2003 ISU demonstration project [2], namely including further field testing of RRFC bridges for the purpose of obtaining additional data on the structural behavior of these bridges. The objectives for this research include (1) investigate variables in RRFC bridge construction to improve performance, constructability, and cost; (2) design, construct, and test two RRFC bridges implementing variables from

objective (1); (3) refine the design methodology presented in TR-444. Tasks performed to accomplish these objectives include:

1. Examination and selection of available decommissioned RRFCs.
2. Analysis of design variables.
 - a. Steel sheet pile wall abutments
 - b. Abutment bearing supports for exterior and interior girders
 - c. Alternative longitudinal connection details
3. Data collection through field testing of two RRFC bridges containing different span lengths, longitudinal connection details, and abutment supports.

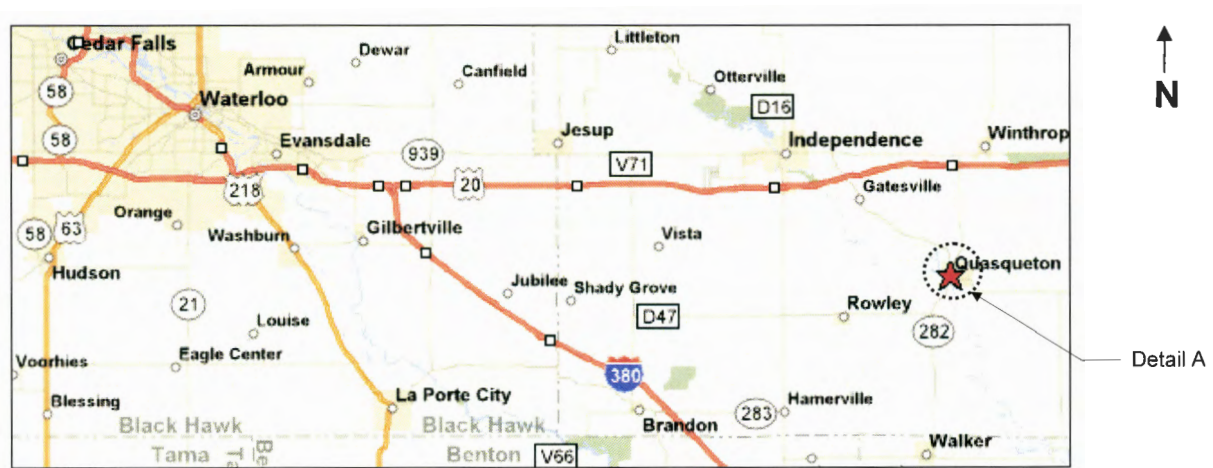
Bridges in Buchanan and Winnebago Counties in Iowa were replaced using the RRFC concept. This document will discuss the design, construction, testing, analysis and results for these RRFC bridges (BCB3 and WCB2). The BCB3 is a single span bridge with bolted longitudinal connections. Reinforced concrete connections were constructed for the WCB2, which was a simply supported bridge with a single, main span and small overhangs at each abutment. Other significant differences between the two bridges are the driving surface: timber planks and gravel were used on the WCB2 while only gravel was added on the BCB3.

Other design variables including sheet pile wall abutments and alternative bearing supports are include in Appendix A and B, respectively. Appendix A discusses the feasibility of using steel sheet pile abutments for RRFC bridges and also includes a design example utilizing site conditions at the WCB2 location. Abutment bearing supports for RRFC bridge lengths between 47 ft – 4 in. and 66 ft – 0 in. are detailed in Appendix B. The interior girders in this range have a depth transition, thus creating difficulties when bearing on constructed abutments.

2. BUCHANAN COUNTY BRIDGE 3 ON 270th St.

2.1 Introduction

In fall of 2004, construction of a RRFC bridge was completed on a LVR in Buchanan County, Iowa. This bridge will be referred to as Buchanan County Bridge 3 (BCB3) since it is the third RRFC bridge constructed in Buchanan County and tested by ISU. The BCB3 crosses Smith Creek 1.5 miles east of Quasqueton, Iowa, on 270th St. A map of the BCB3 location is presented in Figure 2.1.



b. Quasqueton, IA



b. Detail A

Figure 2.1. Location of the Buchanan County RRFC Bridge 3 [3].

The BCB3 replaced a two-span timber bridge (19 ft – 0 in. and 22 ft – 6 in. spans) with a 20 ft wide deck which was constructed in 1948 (FWHA No. 082160). A sketch of the previous structure can be seen in Figure 2.2. Five timber pilings at the abutments and pier were capped with a 12x12 timber section. Throughout the bridge length there were 11 equally spaced stringers; however, the west, smaller span was comprised of 6x16 timber stringers and the east, larger span had 4x16 timber stringers. Timber planks and gravel create the driving surface.

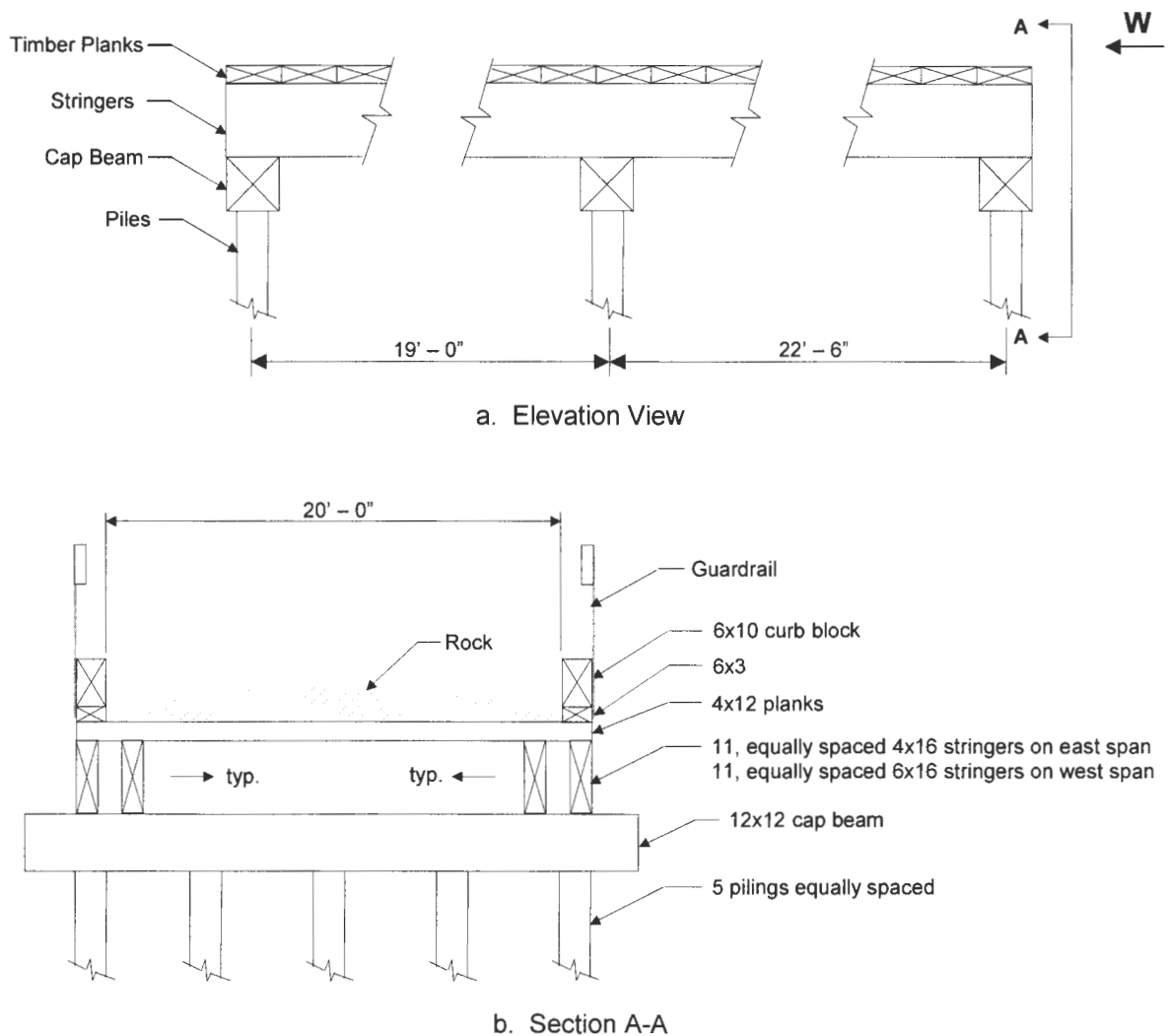


Figure 2.2. Original Buchanan County Bridge on 270th St.

2.2 Design and Construction

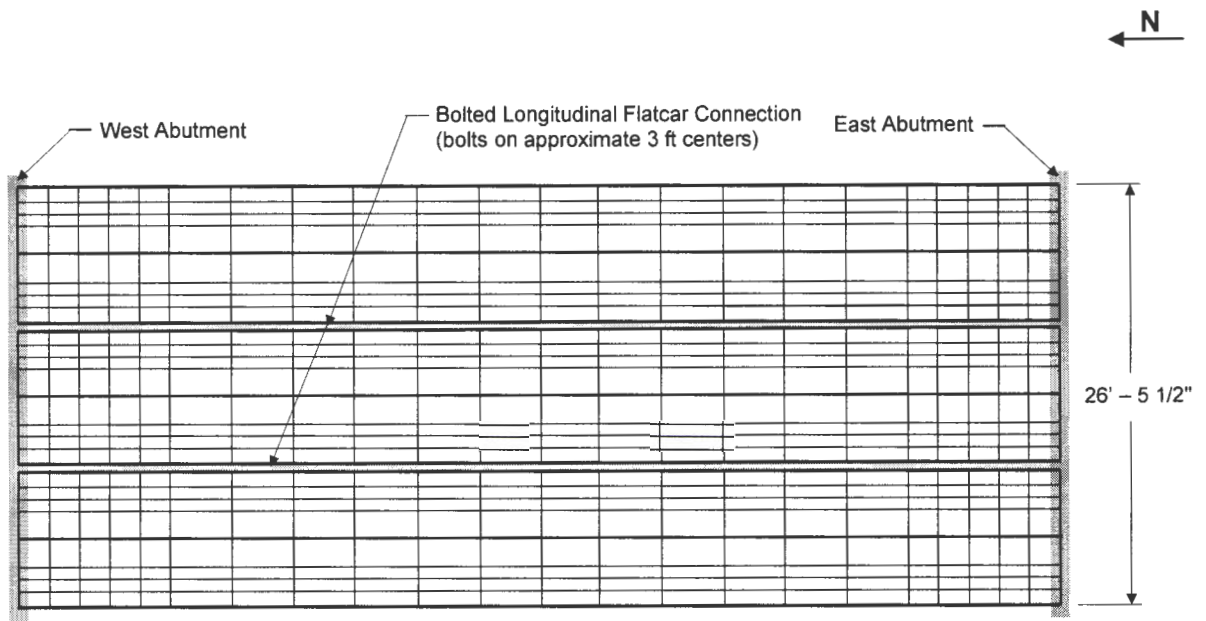
The BCB3 was constructed using the superstructure from three RRFCs that were positioned side-by-side and were connected using bolts between adjacent cars. As shown in Figure 2.3, the BCB3 spanned 66 ft – 2 in. from center-to-center of abutments and had a deck width of 26 ft – 5 1/2 in.

The abutment and backwall details for the BCB3 are presented in Figure 2.4. The abutment was a modification of the Iowa Department of Transportation (Iowa DOT) standard stub abutment with zero skew [4]. The constructed concrete abutment was 3 ft tall, 4 ft wide, and 30 ft long. Five HP 10x42 piles were extended 24 in. into the concrete cap and surrounded with spiral reinforcement within the cap. Cap beam reinforcement included #8 longitudinal bars for flexure and #5 stirrups for shear resistance. The backwall was connected to the cap using #6 reinforcement. A 1/4 in. thick, 12 in. wide, and 30 ft long plate (shown in Figure 2.4c) was welded to the top of the RRFCs to prevent foreign material from falling in the expansion joint between the backwall and the railcars.

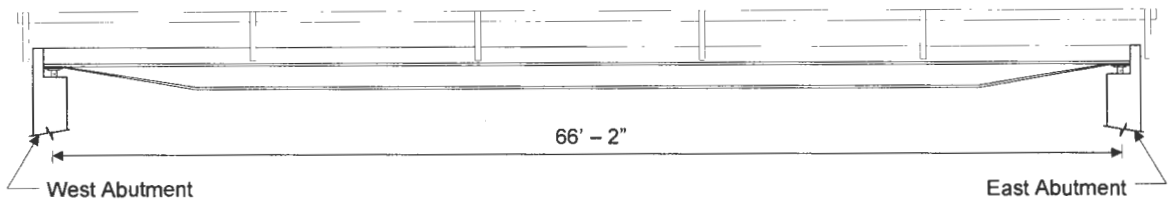


a. Photograph of the BCB3

Figure 2.3. Buchanan County RRFC Bridge 3.

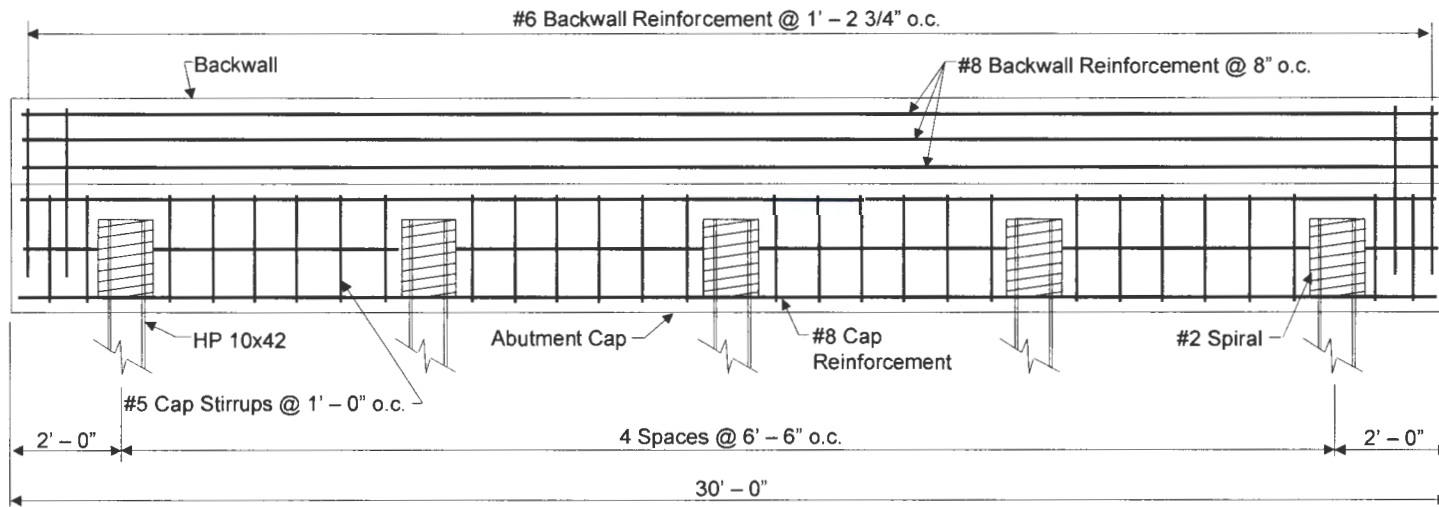


b. Plan View

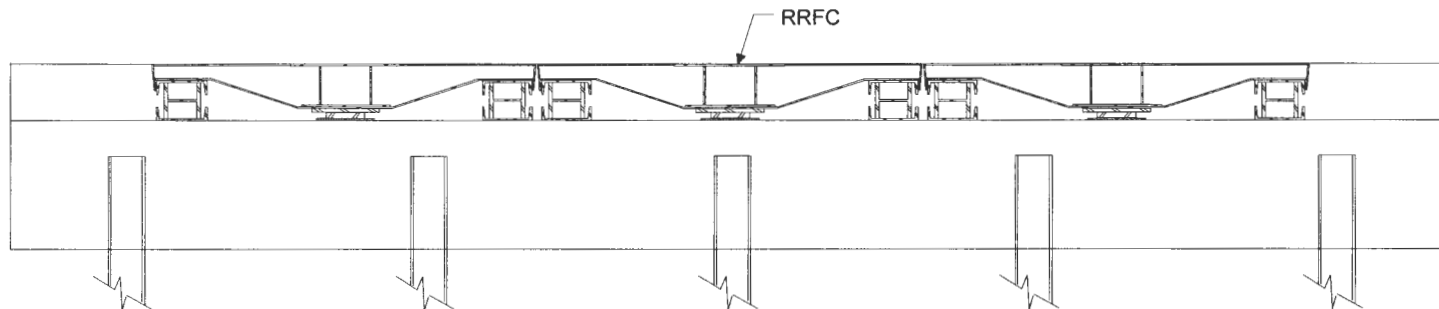


c. Elevation View

Figure 2.3. Continued.



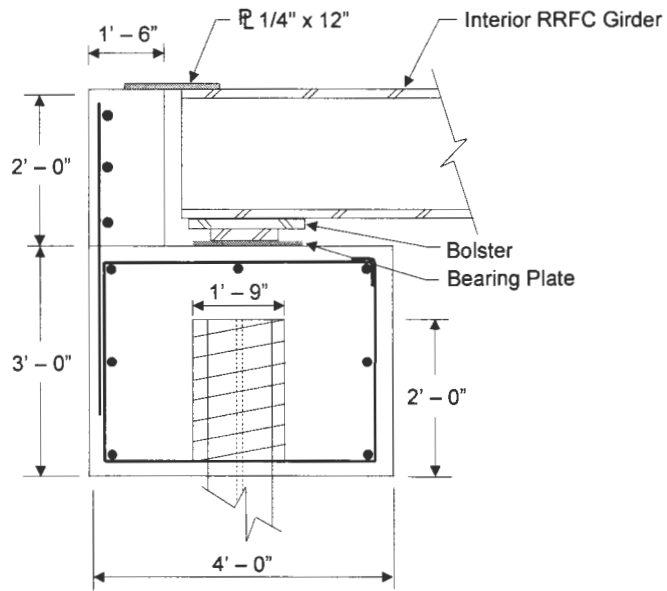
a. End view showing steel reinforcement



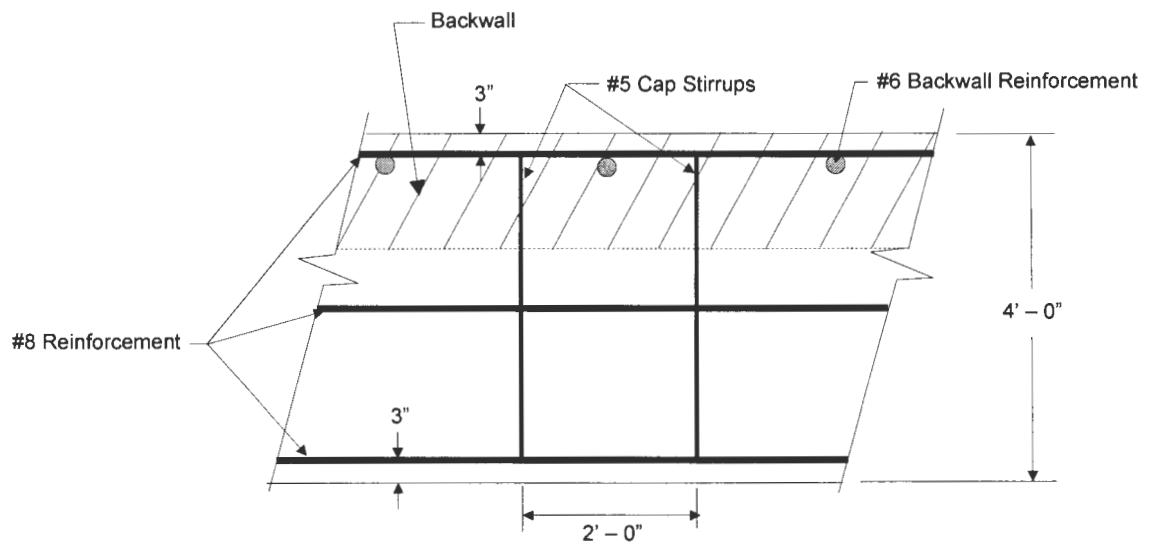
b. End view showing RRFC placement

Notes:
 All Reinforcing Steel is Grade 60.
 Structural Concrete is Class "C".

Figure 2.4. Details of the BCB3 concrete abutments.



c. Side view of abutment



d. Top view showing abutment reinforcement

Figure 2.4. Continued.

The RRFCs used for the bridge superstructure were 89-ft railcars, trimmed near the bolsters to create the 66 ft – 2 in. span. Details of the 89-ft RRFCs are presented in Figure 2.5. Each car has an identical, redundant cross-section consisting of three main longitudinal members; smaller, secondary longitudinal members; and transverse members. The main longitudinal members are one, large box (interior) girder and two exterior channel sections. In the central 47 ft – 4 in. of the RRFC, the interior box girder is 30 3/4 in. deep; it tapers to a 13 3/4 in. depth at the bolster. All exterior girders, except those located on the north and south exterior faces of the bridge, had the top portion of the girder trimmed flush with the top surface of the RRFC deck. To connect the adjacent exterior girders together at the bolted connections, the bottom flanges of the exterior girders were also trimmed. Secondary members in the RRFCs are T-shapes while the transverse members vary along the length and include U-shapes, S-shapes, and L-shapes. The U-shaped transverse members are located near the ends where the depth of the interior girder tapers. The L-shaped transverse members are located at the midspan and also where the interior girder starts to taper. The portion between the bolsters (other than those locations where the L-shaped and U-shaped transverse members are located) has the S-shaped transverse members. The longitudinal connection used to join the RRFCs (See Figure 2.6) was created with bolts (1 1/4 in. diameter), spaced approximately 3 ft on centers, inserted into the webs of the adjacent RRFCs' exterior girders. Approximately 22 bolts were required in each longitudinal connection.

Supports at the abutments for the exterior, longitudinal RRFC girders are shown in Figure 2.7. They were created from a W-section confined on top and bottom with inverted channel sections. A set of built-up bearing sections was located at the connection location, while bearing plates were placed under the interior girders.

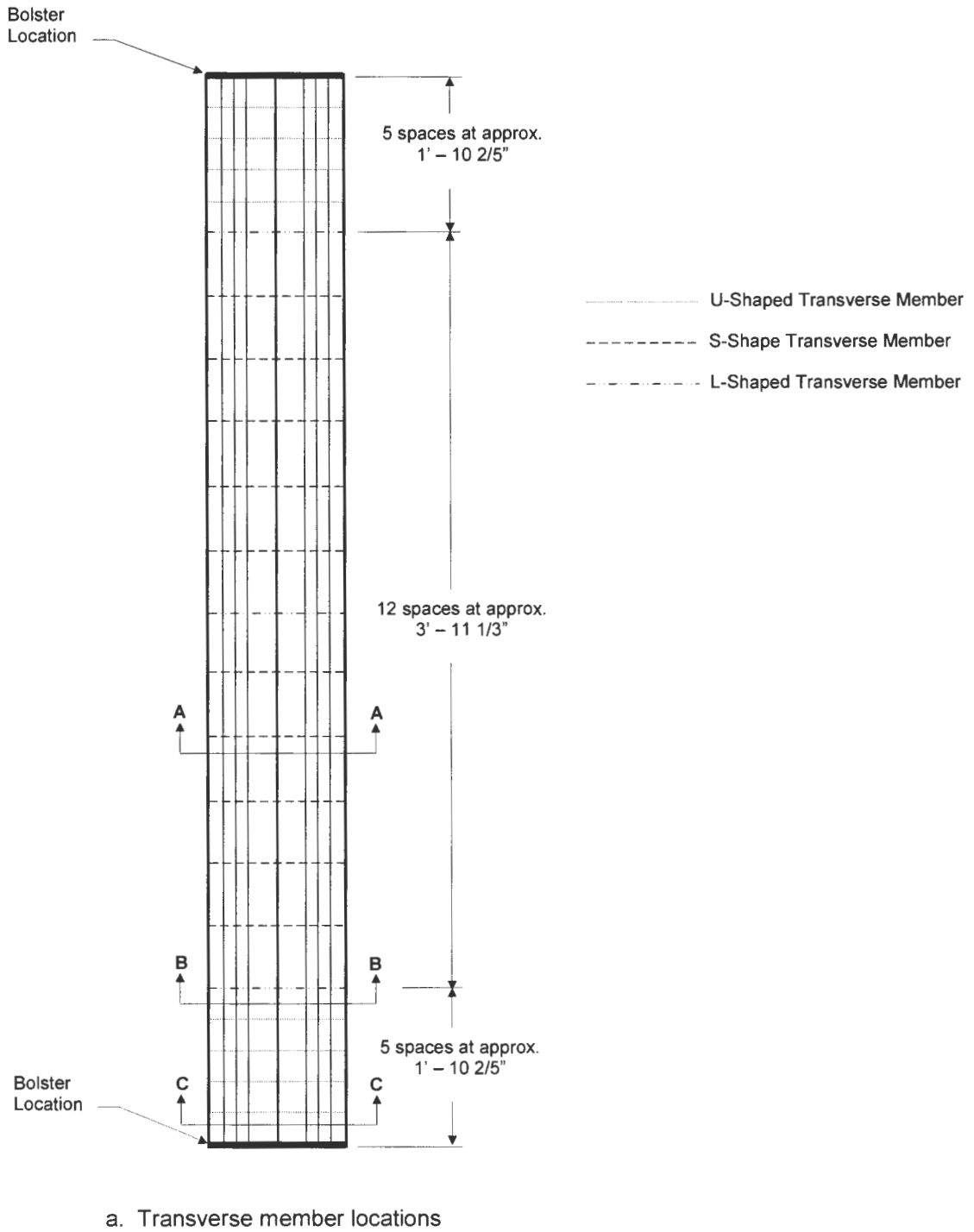
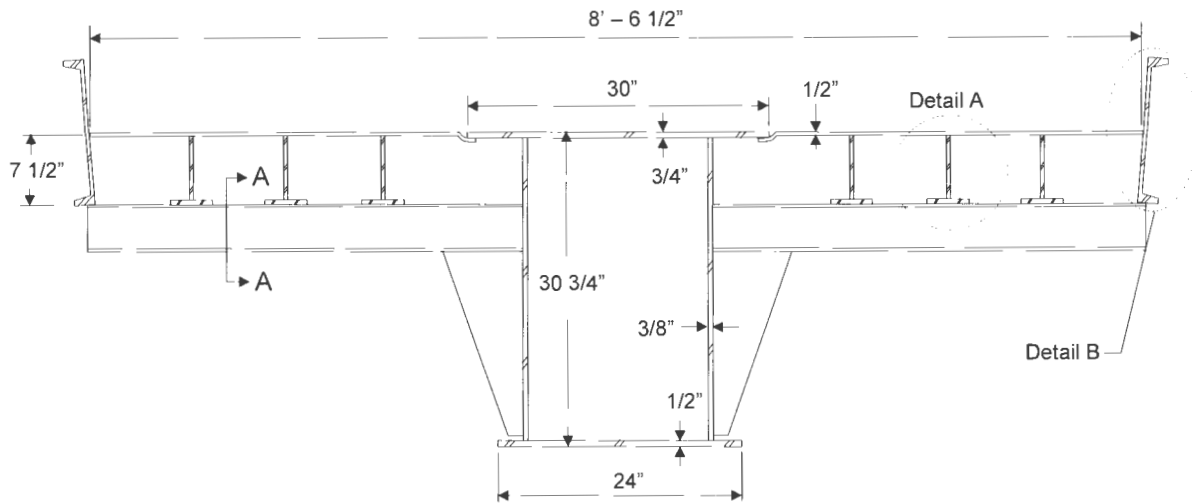


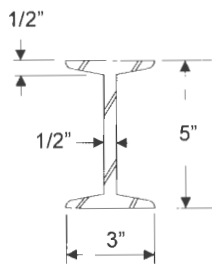
Figure 2.5. 66 ft - 2 in. RRFC cut from 89-ft RRFC.



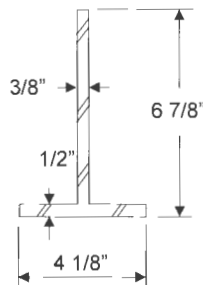
b. Photo of an 89-ft RRFC



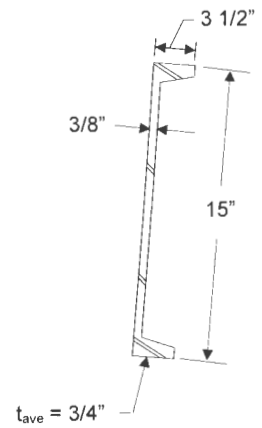
c. Section A-A: S-shape transverse member



d. Section A - A (S-shape)

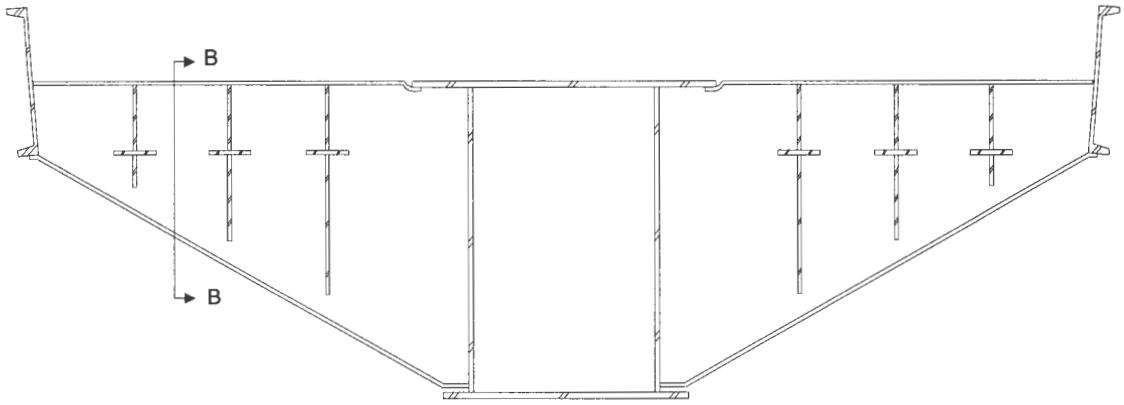


e. Detail A (T-shape)

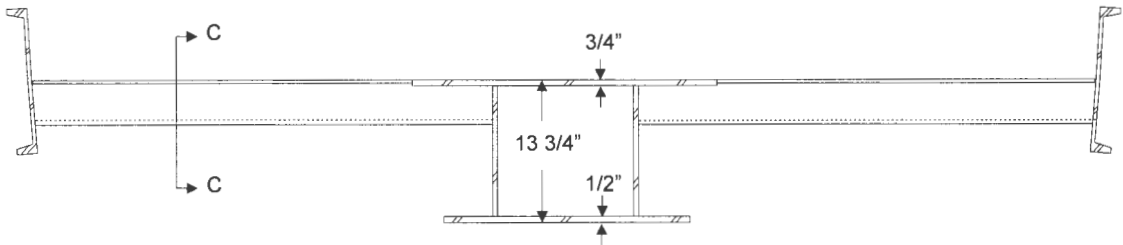


f. Detail B

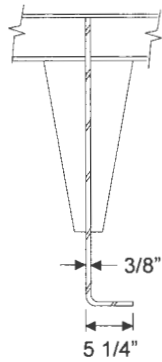
Figure 2.5. Continued.



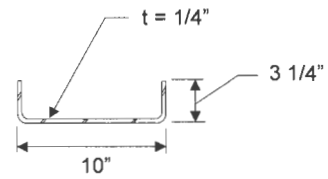
g. Section B-B: L-shaped transverse member



h. Section C-C: U-shaped transverse member



i. Section B - B (L-shape)

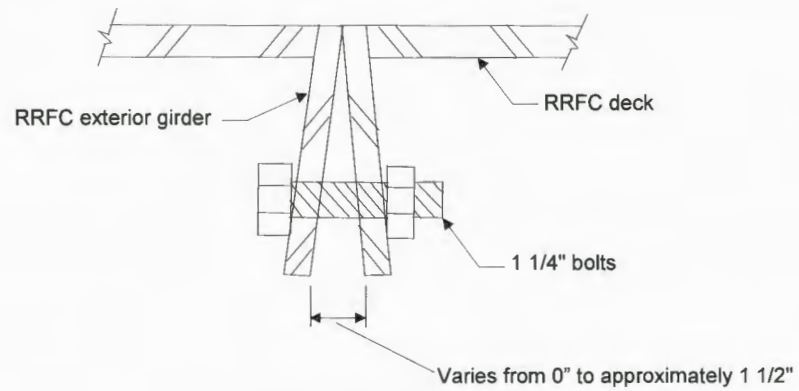


j. Section C - C (U-shape)

Figure 2.5. Continued.



a. Photograph of the bolted connection

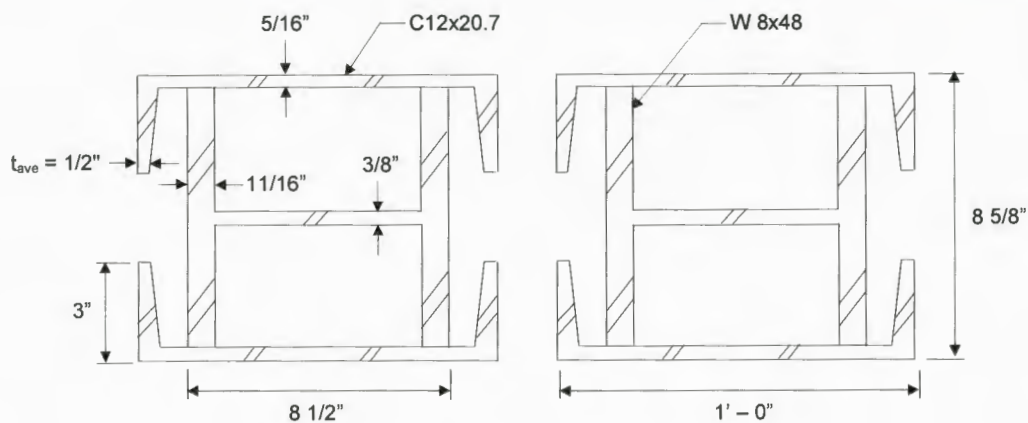


b. Bolted connection sketch

Figure 2.6. Bolted longitudinal connection.



a. Photograph of bearings at a longitudinal bolted connection

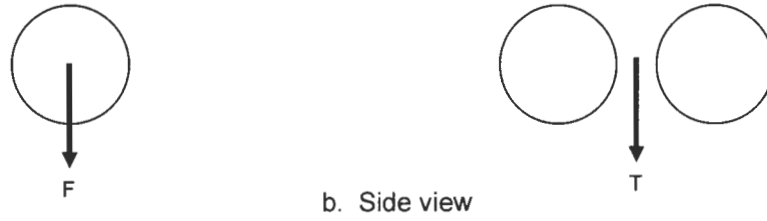
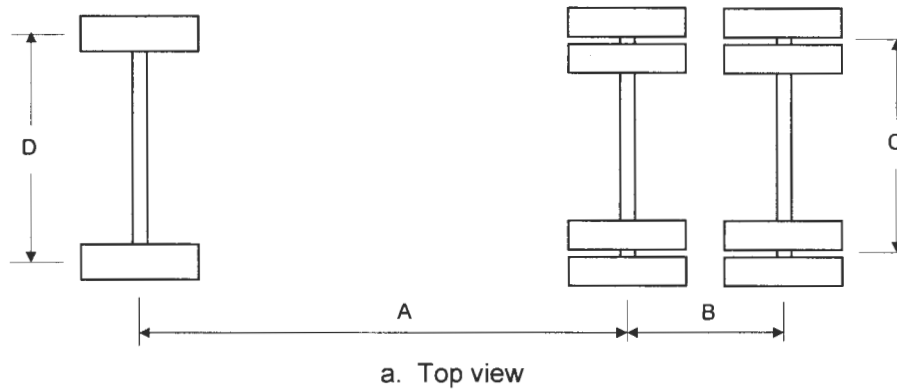


b. Bearing dimensions

Figure 2.7. Built-up bearing sections at the abutments of the BCB3.

2.3 BCB3 Field Testing

The field testing of the 270th St. BCB3 involved both dynamic and static testing using a tandem truck. Dimensions and weights of the tandem truck used in the field tests are presented in Figure 2.8, and a photograph of the truck is shown in Figure 2.9. The front tires were 1 ft – 2 in. wide, the individual rear tires were 10 in. wide, and a set of rear tandem tires had a width of 2 ft – 0 in. The truck had a gross weight of 48,200 lbs.



Dimensions				Load (lbs)		
A	B	C	D	F	T	Gross
13' - 6 1/2"	4' - 5"	6' - 0"	6' - 11"	11,940	36,260	48,200

Figure 2.8. Dimensions and weights of test truck used in BCB3 field tests.



Figure 2.9. Test truck used in BCB3 bridge field test.

The dynamic testing of the BCB3 was performed by driving the tandem test truck down the centerline of the bridge (See Figure 2.10). Five separate dynamic tests were completed; the first test was at a speed of 10 mph which was increased by 5 mph increments in subsequent tests until a maximum speed of 30 mph was reached for the final test. Through the dynamic tests, the dynamic amplification of the deflections and strains was determined.



Figure 2.10. Dynamic testing of the BCB3.

Static testing of the BCB3 included five different transverse positions of the tandem truck across the bridge which are illustrated in Figure 2.11 and photographs of the test truck on the bridge are presented in Figure 2.12.

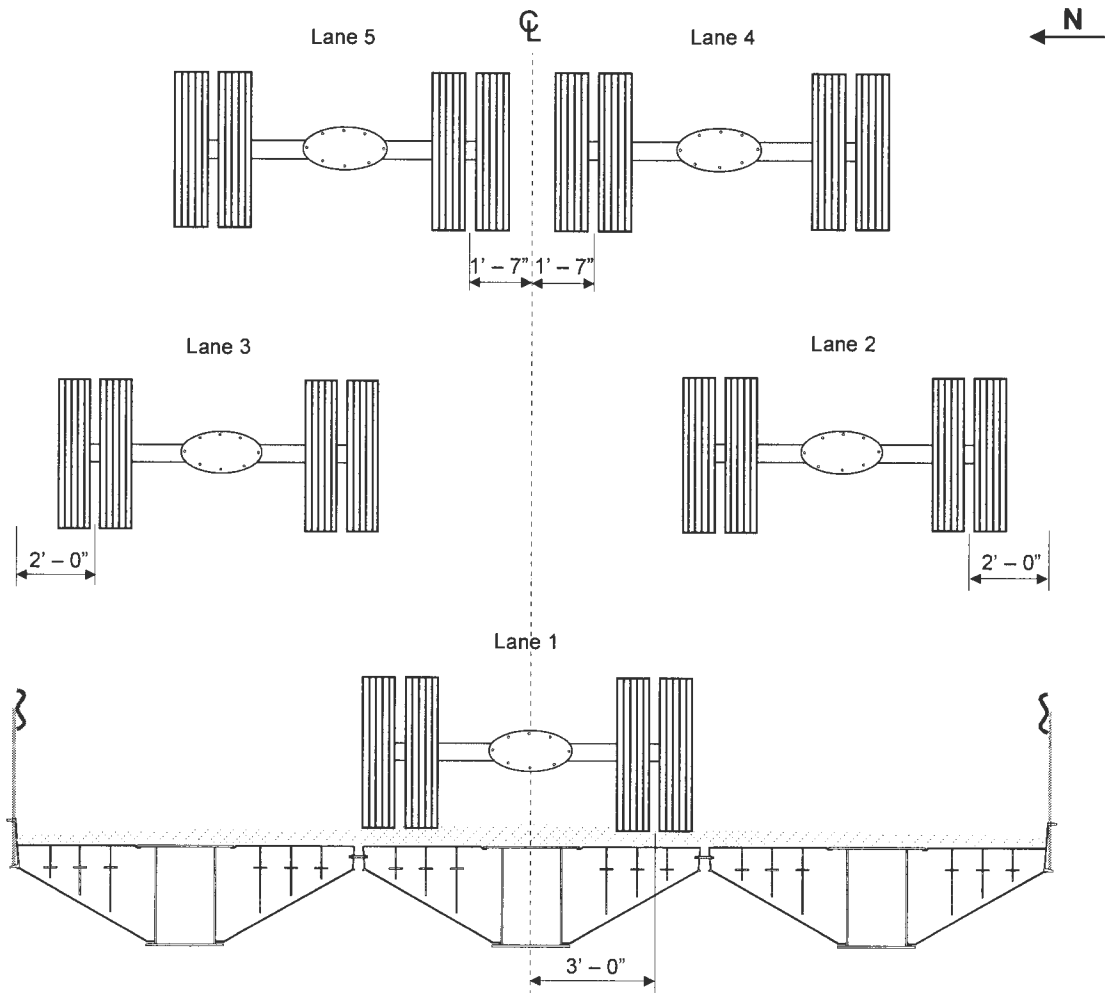


Figure 2.11. Transverse locations of the truck used in field tests.



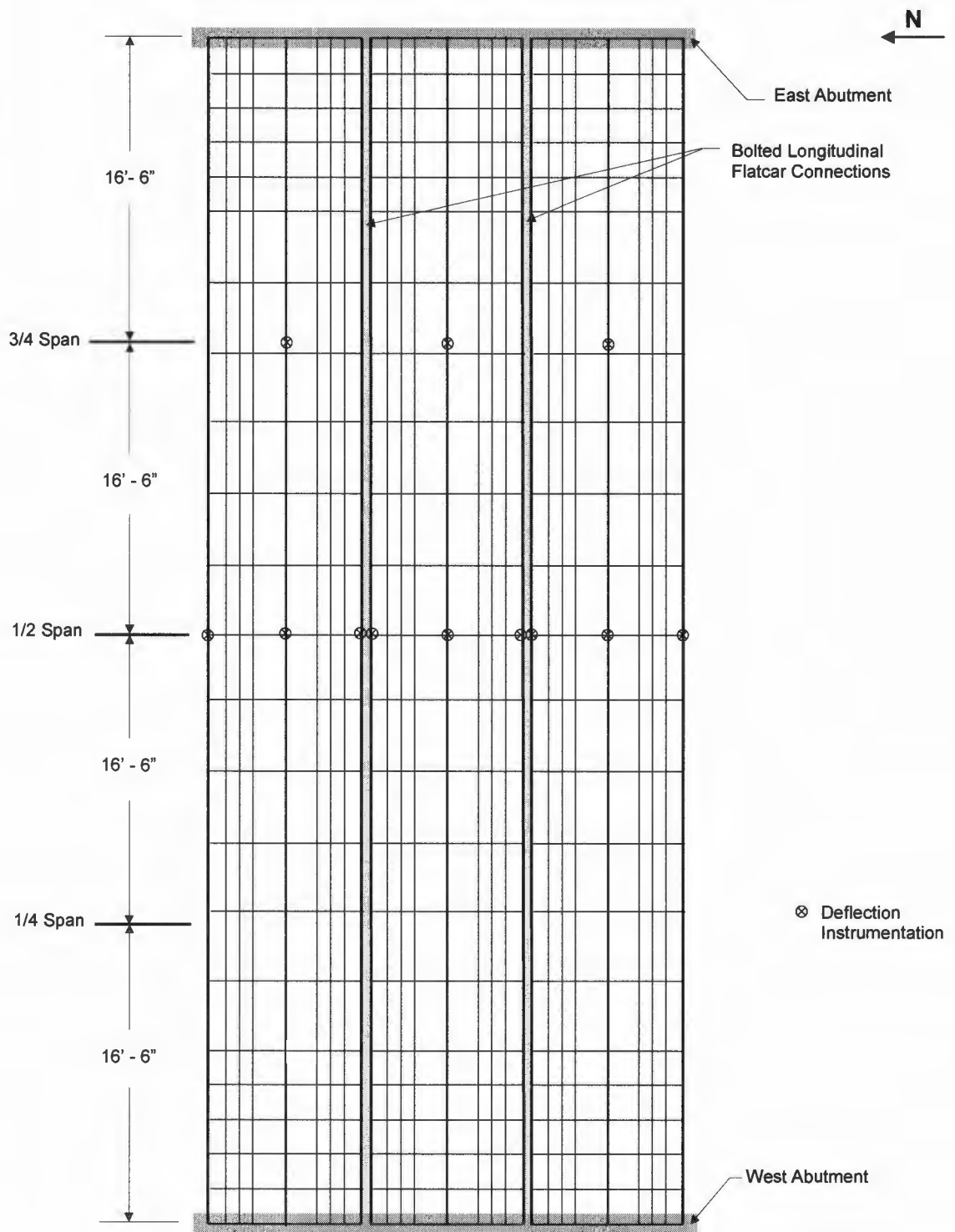
a. In Lane 1



b. In Lane 3

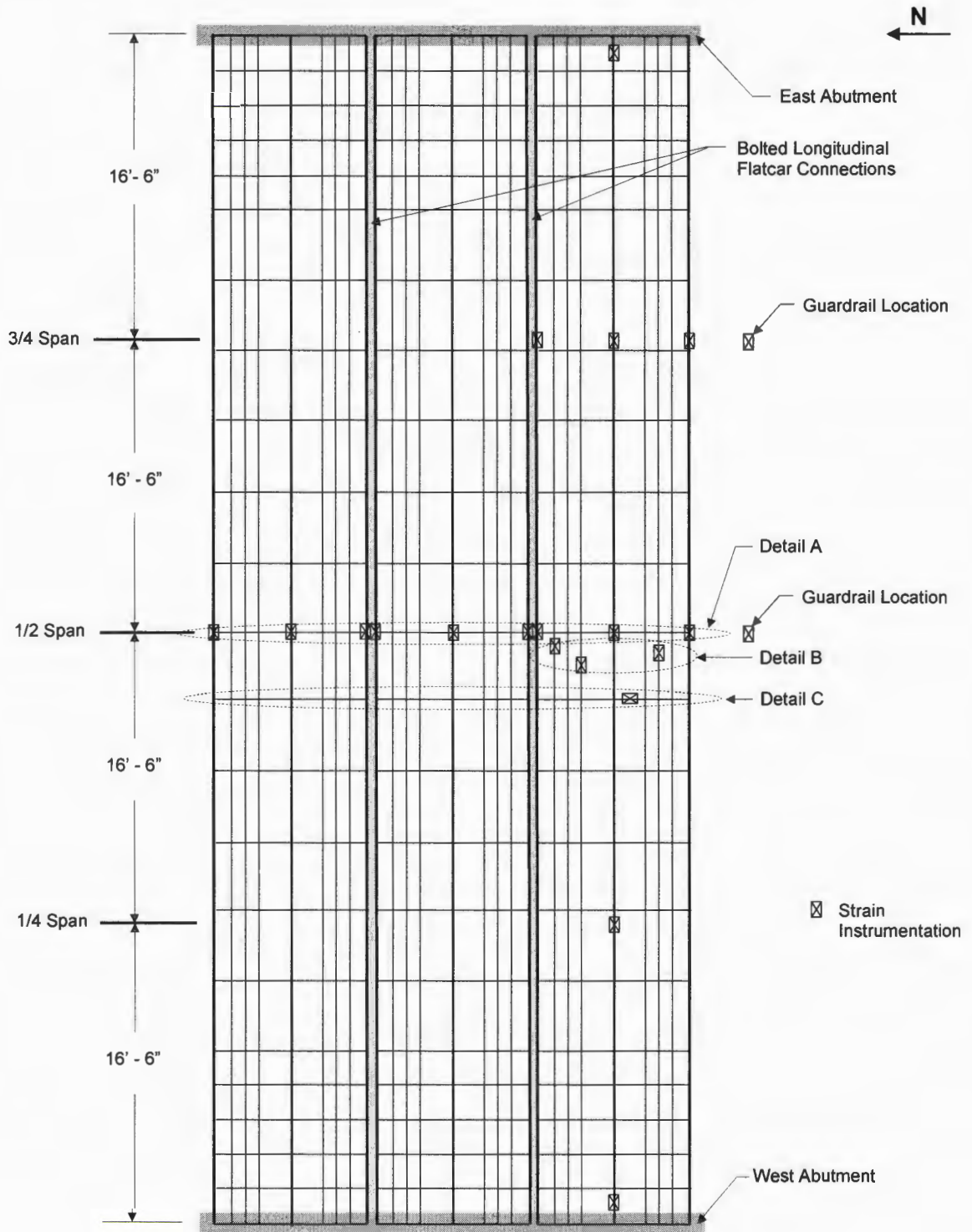
Figure 2.12. Photographs of the test truck on BCB3.

Instrumentation for the BCB3 test included both deflection and strain transducers placed on the various RRFC girders. The full instrumentation plan is presented in Figure 2.13. At the bridge midspan, deflection and strain instrumentation was placed on all interior box girders and exterior members of the three RRFCs. These data were used to perform a complete cross-sectional analysis of the member deflections and strains at the midspan, the location where maximum stresses and deflections occurred in the girder. The interior box girder of the South RRFC was instrumented with strain transducers near each abutment, at the midspan, and also at the 1/4 and 3/4 span locations. Information from instrumenting along the length of one of the RRFC enabled a time history analysis of the member when the tandem truck crossed the bridge. At the 3/4 span location, deflection instruments were placed on all three interior box girders to determine how the bridge behavior at this location differed from that at the midspan. Strain transducers were placed on the outer side of the guardrail system at the 3/4 span location of the South RRFC to determine if the guardrail system provided added stiffness to the structure. Lastly, secondary longitudinal members and a transverse member near the midspan were instrumented with strain transducers to determine the live load strains. A total of 12 deflections and 24 strains were measured in the bridge tests.



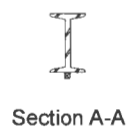
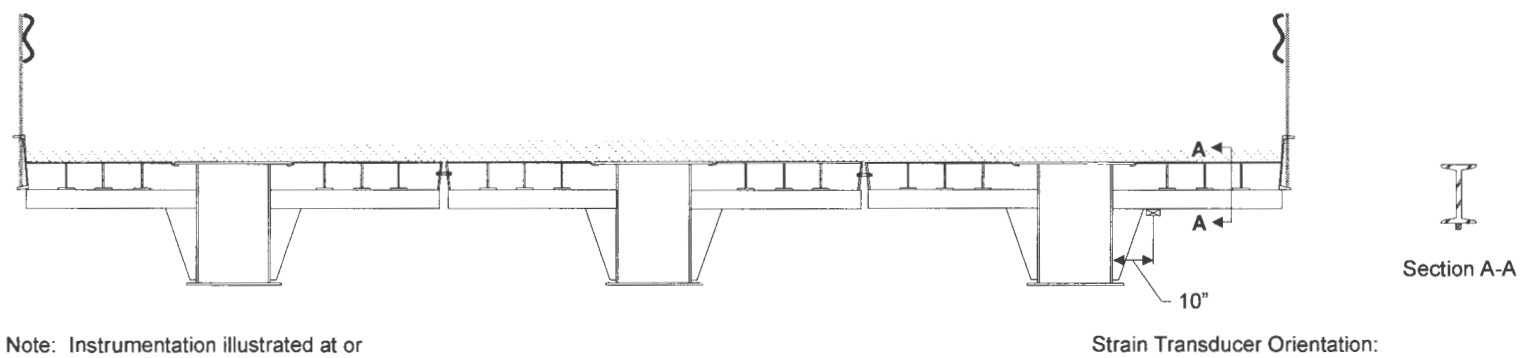
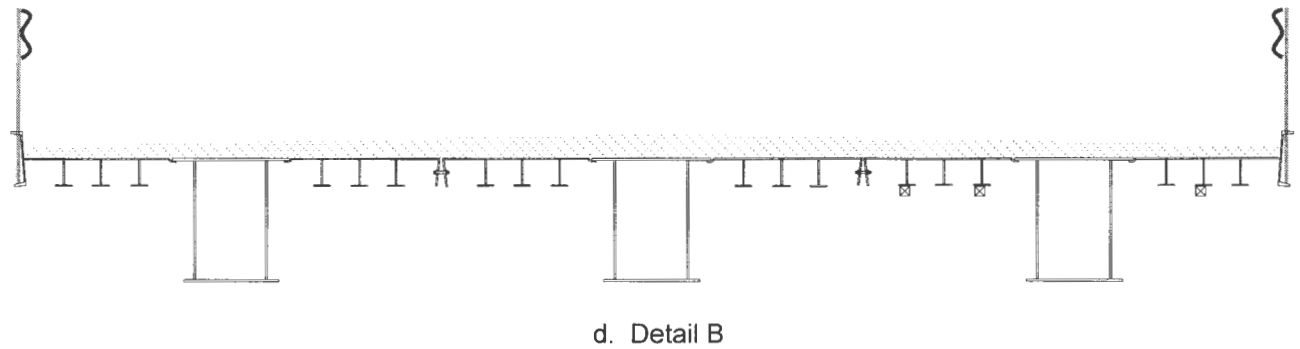
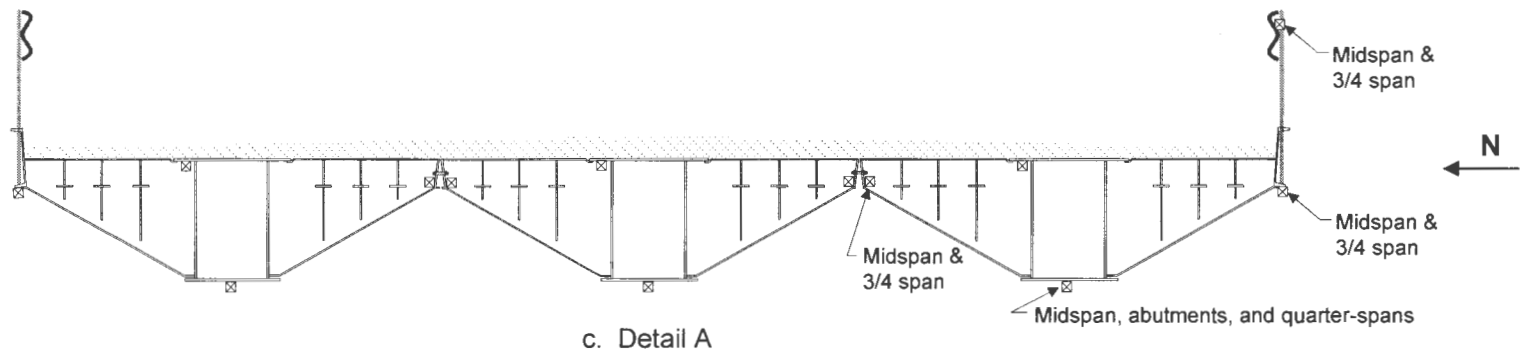
a. Deflection Instrumentation

Figure 2.13. Location of instrumentation used in BCB3 field test.



b. Strain Instrumentation

Figure 2.13. Continued.



Note: Instrumentation illustrated at or near midspan unless otherwise indicated.

Strain Transducer Orientation:
 ☒ Longitudinal axis transverse to the bridge span.
 ☒ Longitudinal axis parallel to the bridge span.

Figure 2.13. Continued.

2.4 BCB3 Dead Load Analysis

Total stresses in the RRFC members are obviously the combination of live and dead load stresses acting on the bridge. Live load stresses were determined from measured live load strains obtained in the field tests of the bridge previously described in Section 2.3. Dead load stresses, however, must be calculated using structural analysis procedures.

For the dead load analysis, it was necessary to make several assumptions. First, the bridge was assumed to be simply supported at the abutments. Secondly, the dead loads were assumed to be uniform across the width of the bridge and evenly distributed longitudinally along the bridge length; hence, each RRFC supported a uniform dead load force equal to 1/3 of the total distributed dead load. It was also assumed that although there were numerous smaller, secondary longitudinal members in each RRFC (See Figure 2.5), the three main longitudinal members (one interior box girder and the two exterior girders) support the entire bridge dead load. As stated previously, the exterior girders at the longitudinal connection were “trimmed” to accommodate the connection details. Both the “trimmed” and uncut exterior members were significantly smaller than the interior box girders, and thus were capable of supporting only a very small percentage of the dead loads. Therefore, the dead load on each RRFC was distributed to the main longitudinal girders based on their inertias.

Dead loads considered were the weight of the RRFCs, the guardrail system, and the rock driving surface. According to weight tickets provided, the weight of each flatcar was 33,000 lbs. The weight per unit length of the guardrail system was estimated to be 100 lb/ft. The rock driving surface was approximately 5 in. thick and was estimated to have a unit weight of 130 lb/ft³.

Following the noted assumptions and procedures, analysis of the BCB3 due to the described dead loads resulted in midspan tensile stresses of +12.4 ksi in the bottom flange

of the interior box girders, +1.9 ksi in the bottom flange of the “trimmed” exterior girders, and +5.15 ksi in the bottom flange of the uncut exterior girders.

2.5 BCB3 Field Testing Results

Deflection and strain data collected during the field testing were analyzed, and the RRFC bridge behavior was investigated. Maximum live load stresses determined from field testing data were combined with the calculated dead load stresses (presented in Section 2.4). The total stresses were then compared to the allowable stress limitations for the RRFC girders.

2.5.1 Static Testing

The measured midspan deflections and strains in the exterior and interior members of the three RRFCs are presented in Figures 2.14-2.17. Dashed lines have been added to show trends between data points. The midspan location was selected for presentation since the structure is simply supported and deflections and strains are maximum near this location. As can be seen in these figures, maximum deflections and strains occur in the respective RRFC when the test truck is positioned on that flatcar, and the live load is distributed transversely across the bridge through the longitudinal bolted connection between the adjacent flatcars. The adequacy of the bolted connection in distributing live load distribution is illustrated in Figure 2.17. During Lane 1 loading, the deflection and strain measurements appear symmetric to the two adjacent flatcars. However, when the truck is in Lane 2 the deflection of RRFC3 is significantly larger than that of RRFC1 when the truck is in Lane 3. Using the areas under the deflection curves, the moment distribution to an exterior RRFC when the truck was positioned on that side of the bridge was found to be 60%.

The maximum deflection (-0.88 in.) occurred in the South RRFC exterior girder when the test truck was located in Lane 2 (See Figure 2.17). The AASHTO LRFD Bridge Design Specifications [5] recommends a maximum deflection of ‘span’/800 for legal truck loads.

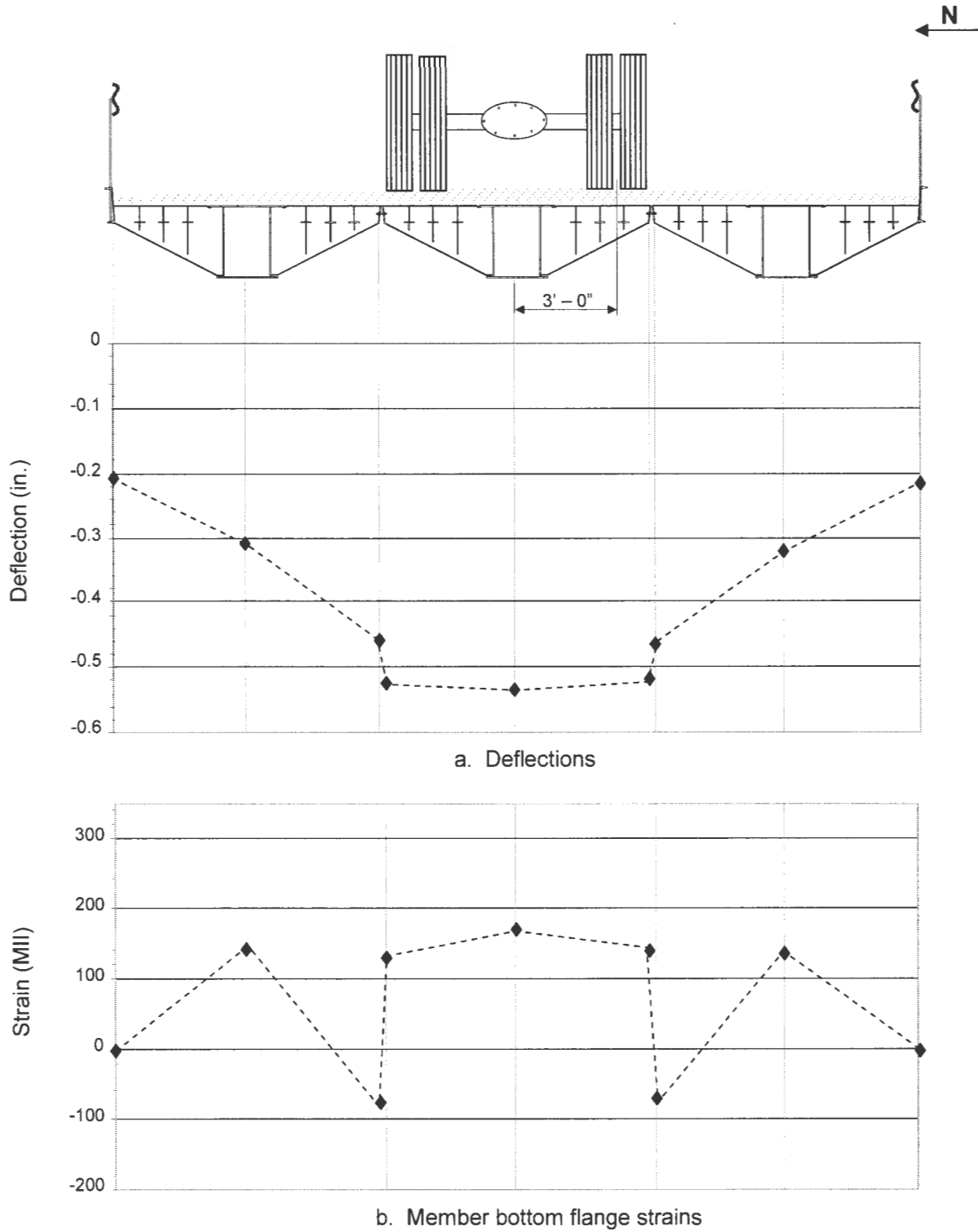


Figure 2.14. Midspan deflections and strains for tandem truck in Lane 1.

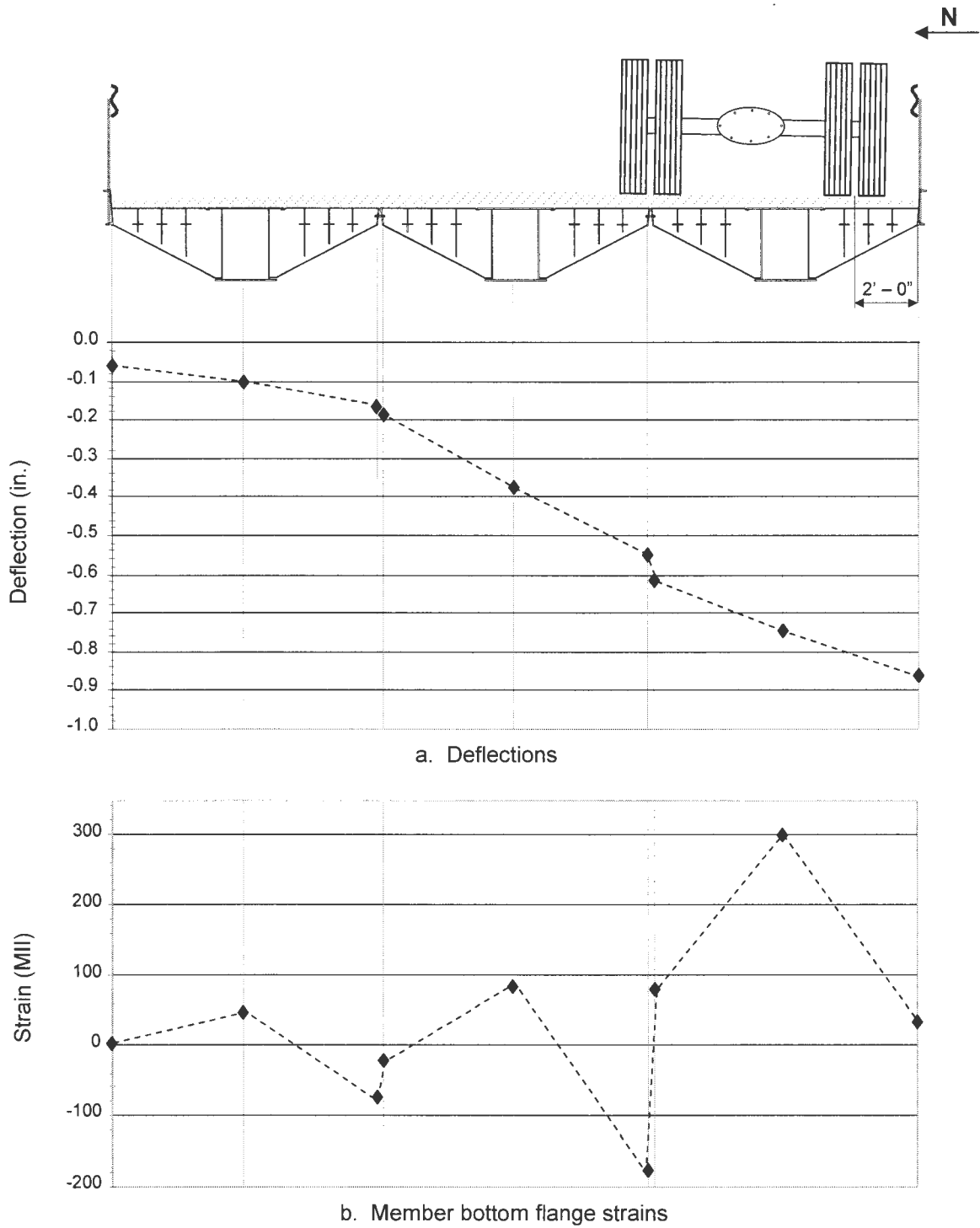


Figure 2.15. Midspan deflections and strains for tandem truck in Lane 2.

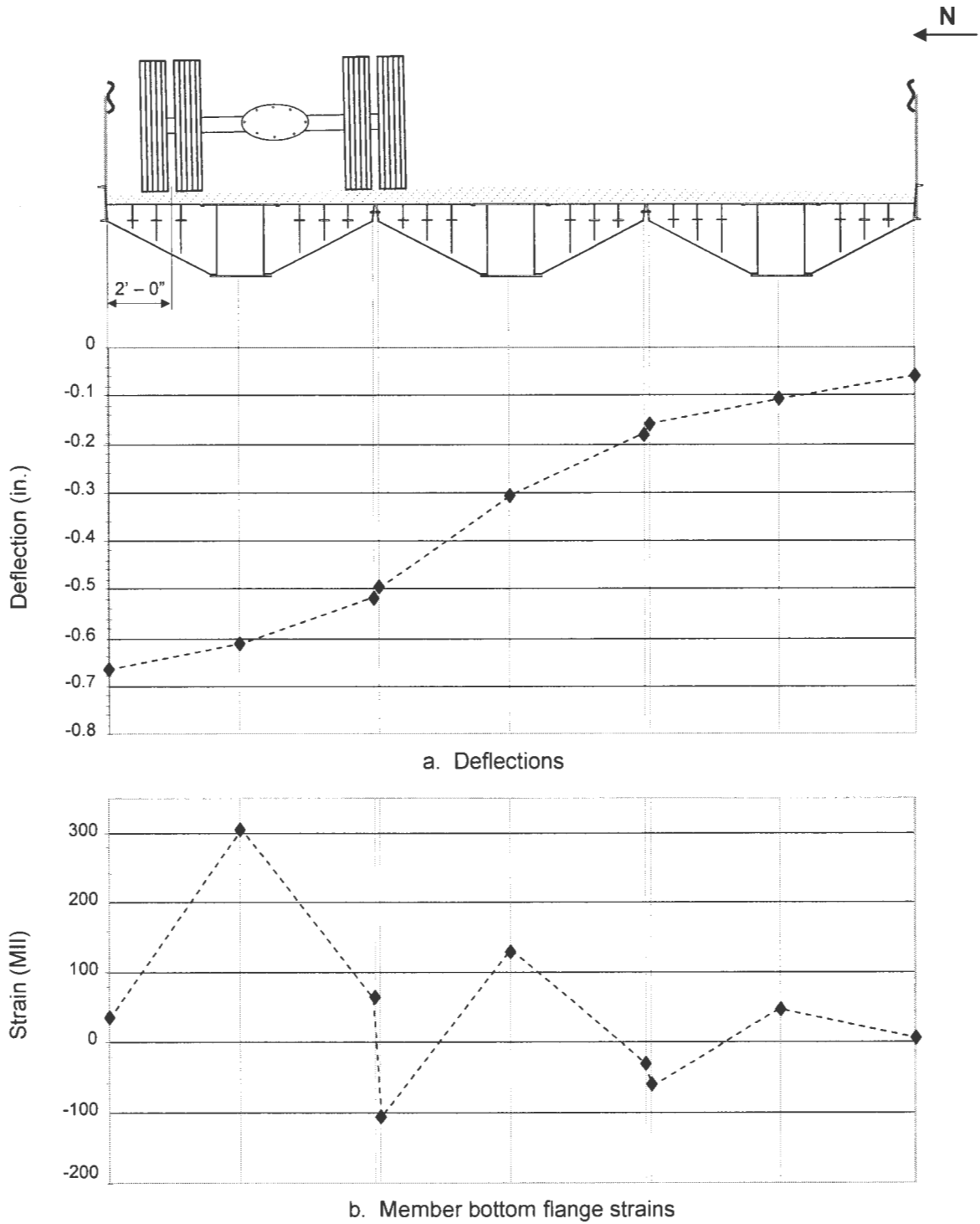


Figure 2.16. Midspan deflections and strains for tandem truck in Lane 3.

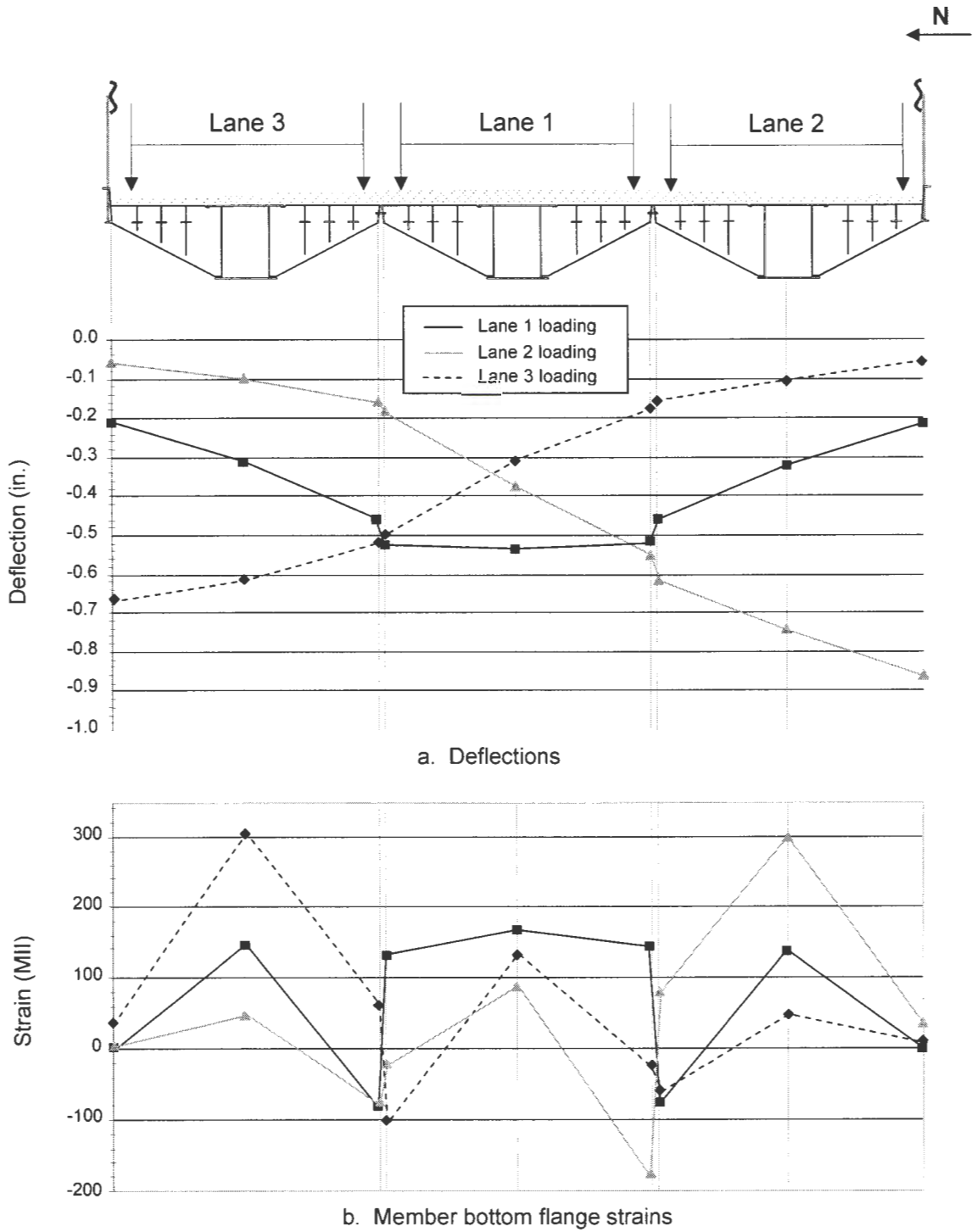


Figure 2.17. Comparison of midspan deflections and strains for Lanes 1, 2, and 3.

This limitation would be -0.99 in. for a clear span of 66 ft – 2 in.; hence, for this truck loading, the maximum measured deflection is below recommended values. If the measured deflection were increased in proportion of the test truck load to an HS-20 loading, the experimental deflection would be -1.31 in., which is significantly above AASHTO limits.

Since the 89-ft RRFCs used for the BCB3 were similar to those used in previous projects [1,2], it was assumed that the material properties in these RRFCs were the same as those previously determined; the proportional limit and modulus of elasticity were assumed to be 40 ksi and 29,000 ksi, respectively. In the project, a conservative yield strength of the steel was assumed to be 36 ksi [2]. Through analysis of the field data, it was determined that the interior box girders experienced the largest strains (stresses) since they are larger than the exterior girders, the secondary longitudinal members, and the transverse members. The relative size of the RRFC structural members can be described by comparing their inertias as seen in Table 2.1. The maximum live load tensile strain (stress) for the bottom flanges of the interior box girders was +322 MII (+9.3 ksi), while the bottom flanges of the uncut exterior members on the outer south and north edges of the bridge experienced maximum tensile strains (stresses) of +38 MII (+1.1 ksi). The exterior girders at the longitudinal connection had maximum strains (stresses) in their bottom flanges varying from -193 MII (-5.6 ksi) to +148 MII (+4.3 ksi). Secondary longitudinal members and the transverse member experienced maximum live load strains (stresses) in their bottom flanges of +161 MII (+4.7 ksi) and +86 MII (+2.5 ksi), respectively.

Table 2.1. Inertias of various RRFC members.

RRFC Structural Member	Inertia (in. ⁴)
Interior Box Girder	8999.2
Exterior Uncut Girder	345.1
Exterior "Trimmed" Girder	12
T-Shape Secondary Member	20.7
S-Shape Transverse Member	14.7

The total stresses for the girders were computed by combining the theoretical dead load stresses with the live load stresses calculated from the measured live load strains. The interior box girder had a maximum total stress in the bottom flange of +21.7 ksi, while a maximum total stress of +6.3 ksi was determined for the bottom flange of the exterior girder on the outer edge of the bridge.

Theoretical analysis with an HS-20 design truck loading (not including impact) was performed to determine maximum stresses. The theoretical live load stresses were calculated from design truck loading for the bottom flanges of the interior girders (+12.8 ksi), exterior (uncut) girder bottom flanges (+5.3 ksi), and bottom flanges of the exterior (cut) girders (+2.5 ksi). Combining these values with the theoretical dead load stresses in the girders of an exterior RRFC, the maximum total stress due to an HS-20 design truck loading would be +25.2 ksi for the interior girder bottom flanges, +10.5 ksi for the uncut exterior girder bottom flanges, and +4.4 ksi for the trimmed exterior girder bottom flanges. If the allowable stress is calculated at 55% of the proportional limit (40 ksi), the maximum total stress of the interior girder bottom flanges (+25.2 ksi) is larger than the allowable limit of 22 ksi but the stresses in the exterior girder bottom flanges are below the allowable stress.

2.5.2 BCB3 Longitudinal Connection Behavior

As stated previously, the longitudinal connection between adjacent RRFCs is created by joining adjacent exterior girders with 1 1/4 in. diameter bolts spaced on approximately 36 in. centers. A cross-section of the BCB3 at midspan is illustrated in Figure 2.18. The RRFCs are referenced as follows: FC1 is the North RRFC, FC2 is the middle RRFC, and FC3 is the South RRFC. Joints A and B, near midspan of the bridge, are the North and South bolted connections between FC1 and FC2 and between FC2 and FC3, respectively. The exterior girder of FC1 at Joint A is Girder 3; the exterior girders of FC2 are Girders 4 and 6 at Joints A and B, respectively; and the FC3 exterior girder at Joint B is

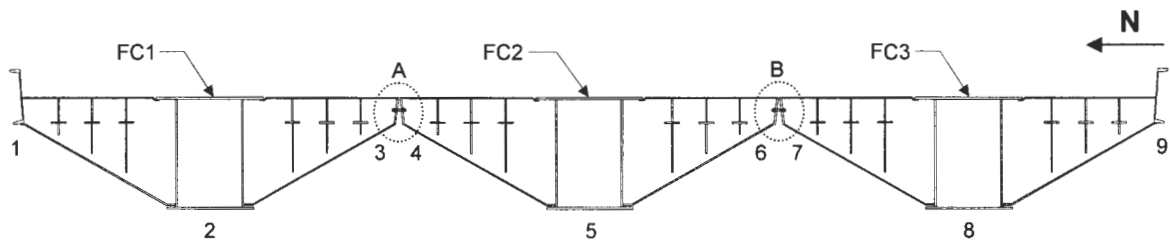


Figure 2.18. Midspan cross-section of BCB3.

Girder 7. Strain transducers (located 6 in. below the bridge deck) were placed near the midspan on the connected exterior girders of both longitudinal joints (Joints A and B in Figure 2.18). The theoretical neutral axis of the BCB3 was determined to be 10.37 in. below the deck. Since the exterior girders, and consequently also the strain transducers, are above this neutral axis, compressive strains should be measured when the girders are subjected to bending about the horizontal axis (See Figure 2.19). However, this is not always the case as shown in Figures 2.14b – 2.17b where some of the exterior girders experience tension when the truck is positioned at certain transverse locations on the bridge. A review of these three figures reveals that the tensile strains always occur in the exterior member of a longitudinal joint when the test vehicle is positioned on that RRFC. For example, in Figure 2.14b when the test vehicle is on FC2, tensile strains are recorded in Girders 4 (+131 MII) and 6 (+143 MII). In Figure 2.16b, when the test vehicle is on FC1, a strain of +61 MII is measured in Girder 3. The strain transducers at these exterior girder locations are measuring the combination of the bending about the bridge's neutral axis (i.e. the horizontal axis) and bending about the vertical axis (See Figure 2.19). In the cases previously discussed, tensile strains due to bending about the vertical axis were larger than the compressive strains resulting from bending about the bridge's neutral axis; the net effect (i.e. tensile strains) at these locations were thus measured by the strain transducers.

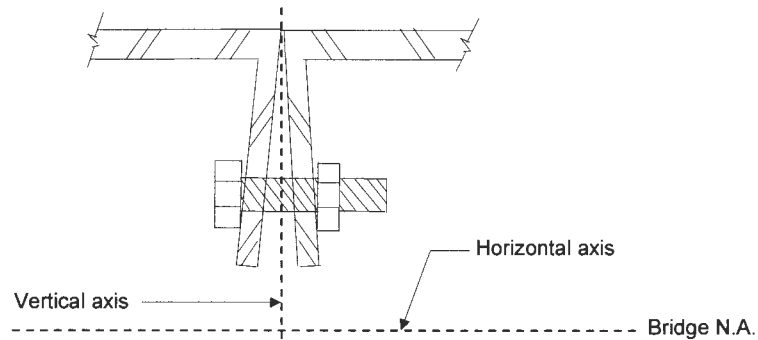


Figure 2.19. Horizontal and vertical axes of bending.

The bending of the exterior girders about the vertical axis is influenced by three factors: differential displacements between adjacent RRFCs at a longitudinal joint, differences in rotations of the girders at the longitudinal joint, and the presence of transverse stiffeners. Differential displacement and rotation at the joint are illustrated in Figure 2.20 where the differential rotation is defined as the algebraic sum of the change in rotation of the two RRFCs. The effect of the transverse stiffeners is illustrated in Figure 2.21; the strain transducer on the loaded RRFC has a net tensile strain while the unloaded RRFC has a net compressive strain since the loaded RRFC experiences larger bending about the vertical axis. As can be seen, the fact that the strain transducers were in close proximity to the transverse stiffeners obviously also influenced the measured strains.

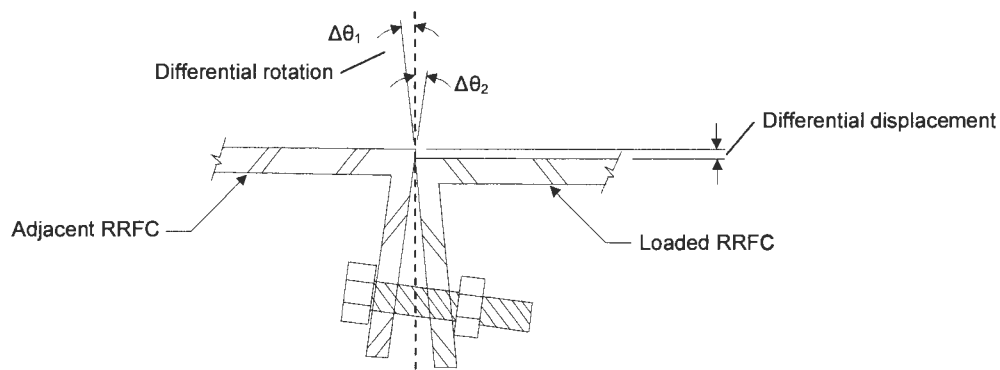


Figure 2.20. End view of the longitudinal connection joint during loading.

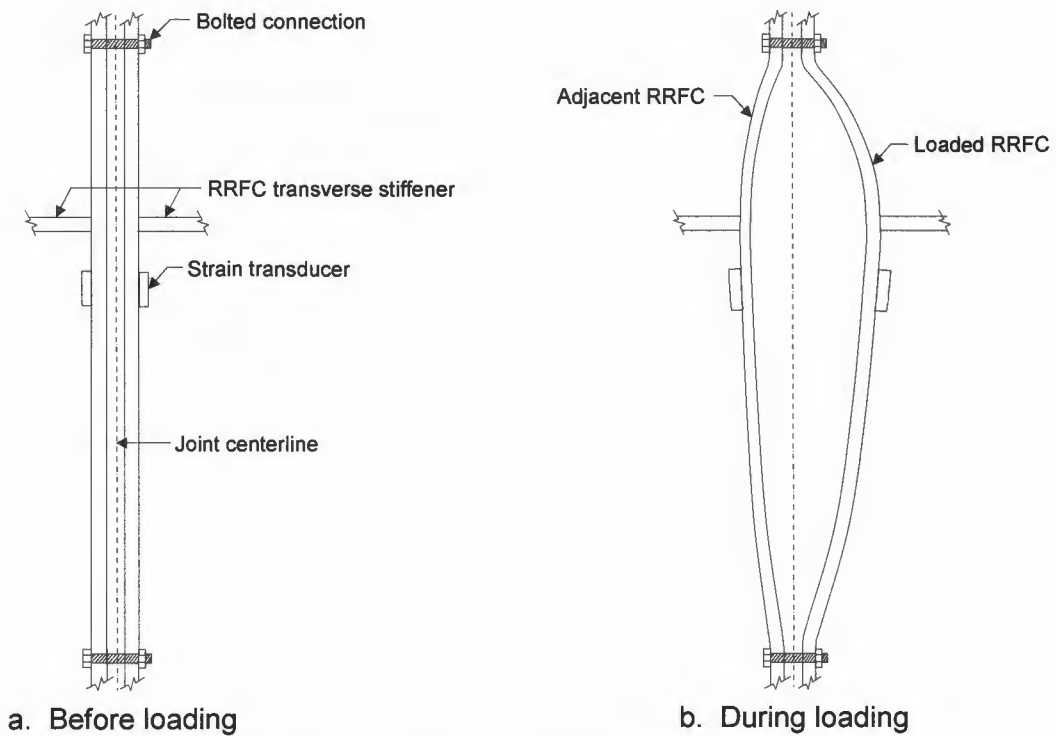


Figure 2.21. Plan view of the longitudinal connection joint.

2.5.3 Time History Analysis

As stated previously in Section 2.3, strain transducers were installed at 5 locations on the bottom flange of the South RRFC interior girder. These locations shown in Figure 2.22 were 12 in. from the west abutment, at the 1/4 span, 1/2 span, 3/4 span, and 12 in. from the east abutment.

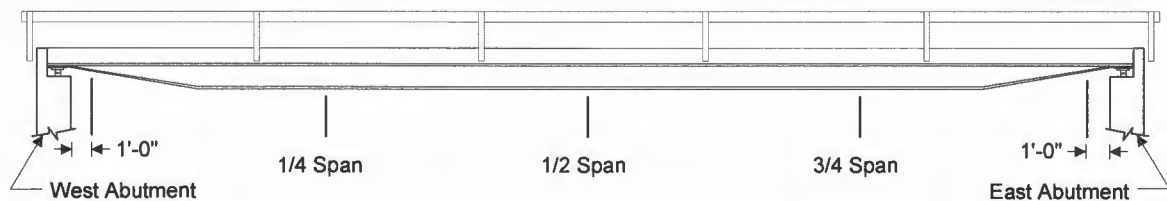


Figure 2.22. Strain instrumentation locations for BCB3 time history analysis.

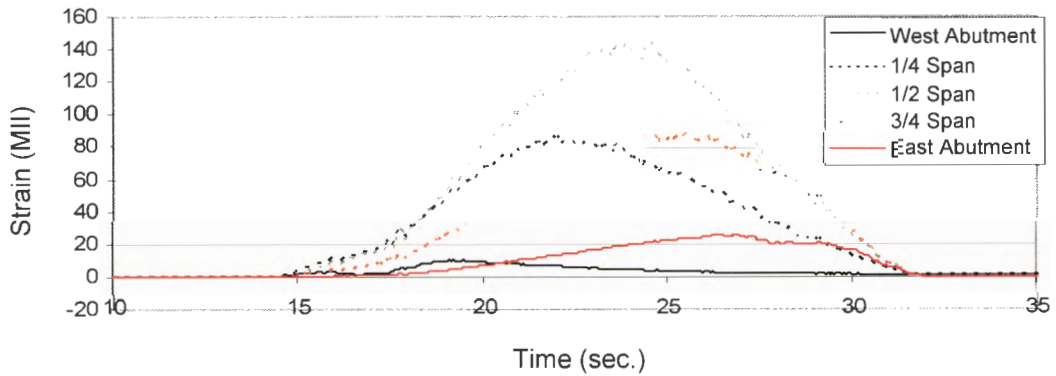
Time history plots of the strains from the South RRFC's interior girder are shown in Figure 2.23. The maximum strains were measured at the midspan location which was expected since the maximum moment for a simply supported structure occurs near midspan. Strains measured at the abutment locations should be essentially zero in an idealized situation. However, the strain instrumentation was placed 1ft – 0 in. from the abutment face due to inaccessibility, so strains were measured at these locations.

Maximum strains of +69 MII were measured at both abutments when the truck was in Lane 2. The largest strains measured at the quarter points also occurred during Lane 2 loading: +224 MII at the 1/4 span and +220 MII at the 3/4 span location. The maximum strain when the truck is on the South RRFC is +306 MII, and when the truck is in Lanes 1 and 3, these maximum strains are +145 MII and +53 MII respectively.

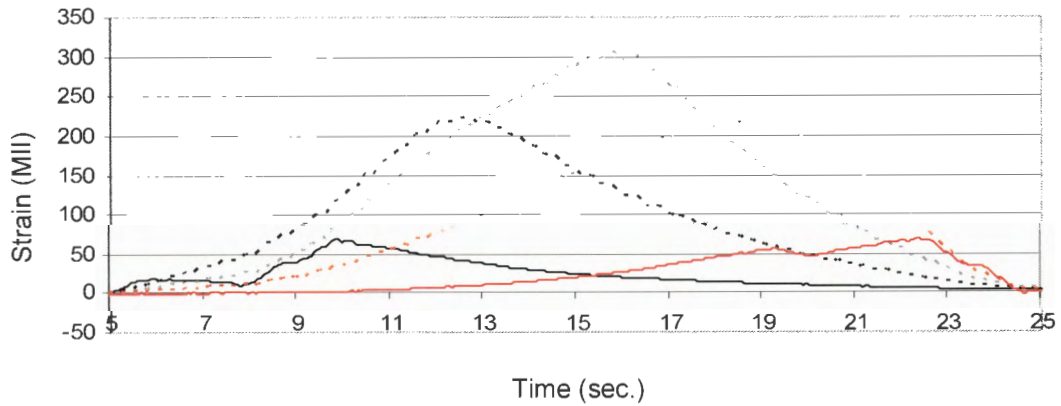
2.5.4 Dynamic Testing

Dynamic testing of the BCB3 was also performed during the field testing; this enabled the structural dynamic properties of the bridge to be determined along with the dynamic amplification of deflections and strains in the girders. The free vibration of the interior girders can be seen from the oscillating strains when the tandem truck has exited the bridge. Based on this free vibrational response, the period, frequency, and damping of the interior girders were determined. The period was found to be 1.3 seconds, resulting in a member frequency of 0.77 Hz, and the damping of the interior girders was approximately 4%.

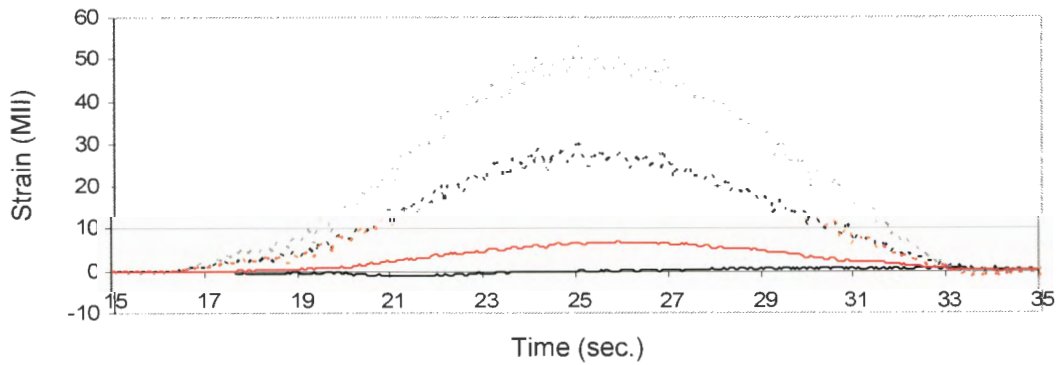
Of the five dynamic test runs that were performed, it was found that the maximum dynamic amplification occurred at a truck speed of 25 mph. A plot of the time history comparison of the deflections and strains during the static and dynamic field testing are presented in Figures 2.24 and 2.25, respectively. These graphs illustrate the dynamic amplification that occurred in the interior box girders of the North, Middle, and South RRFCs.



a. Truck in Lane 1

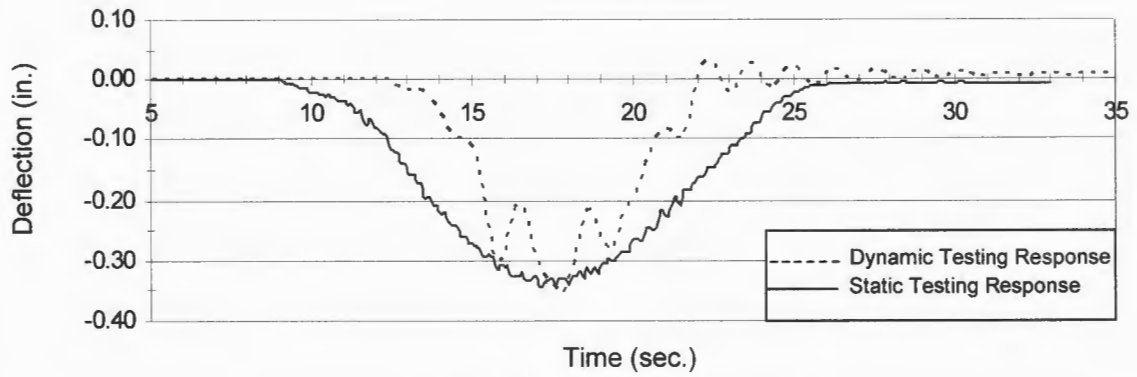


b. Truck in Lane 2

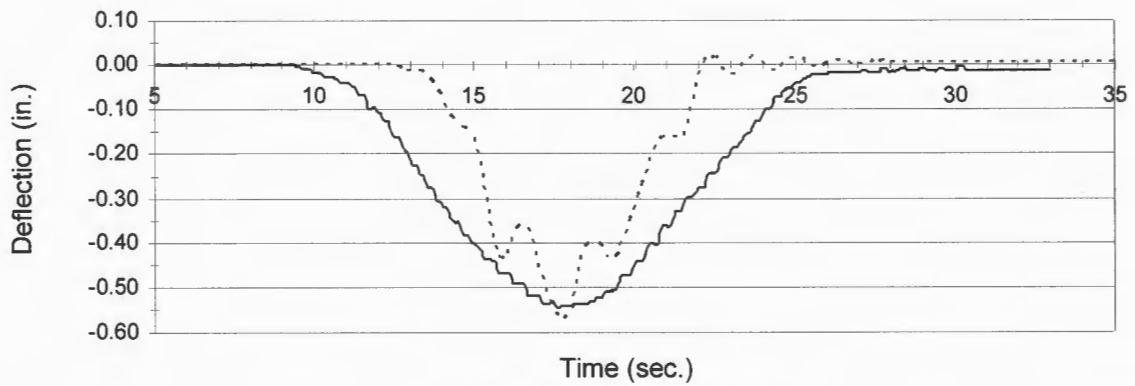


c. Truck in Lane 3

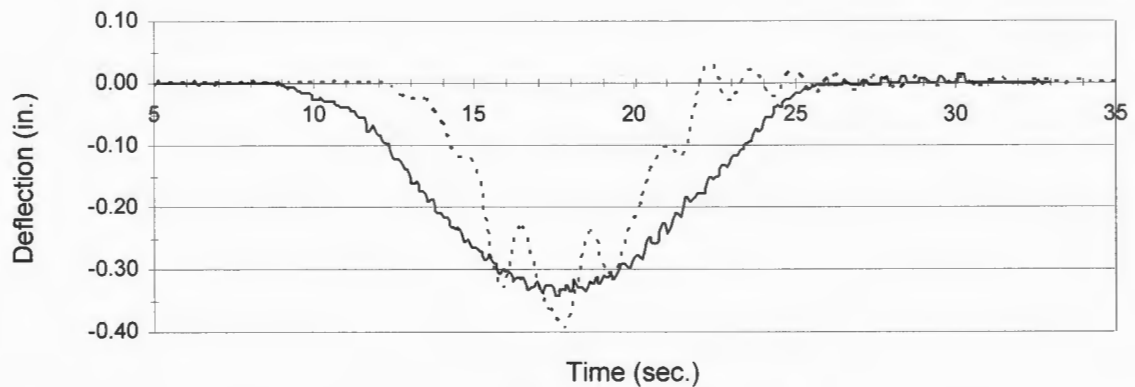
Figure 2.23. Time history of bottom flange strains in the South RRFC interior girder.



a. North RRFC interior girder

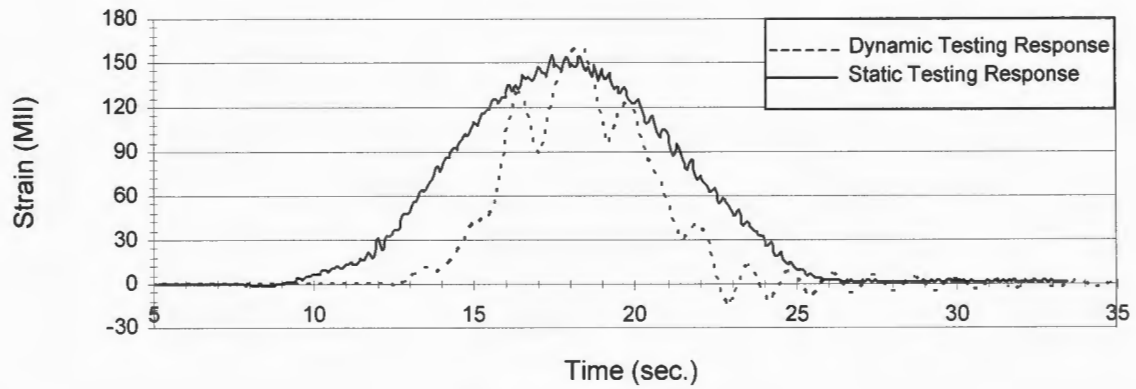


b. Middle RRFC interior girder

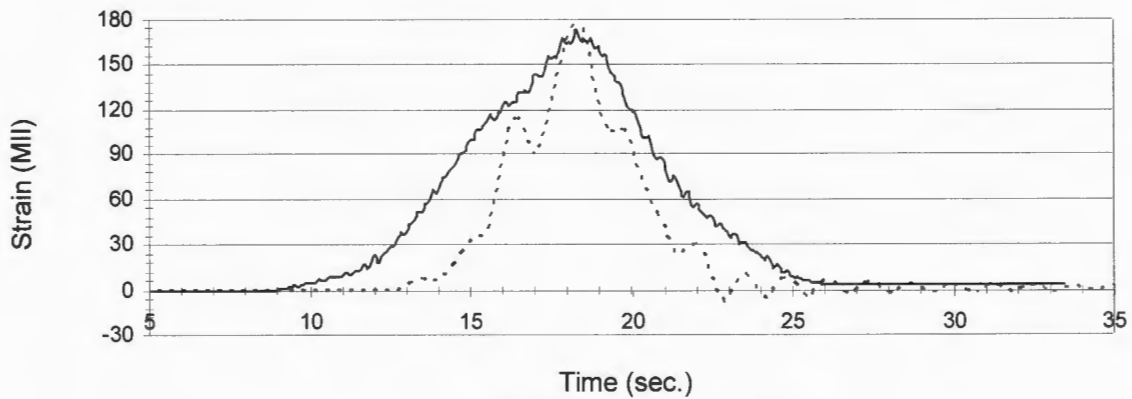


c. South RRFC interior girder

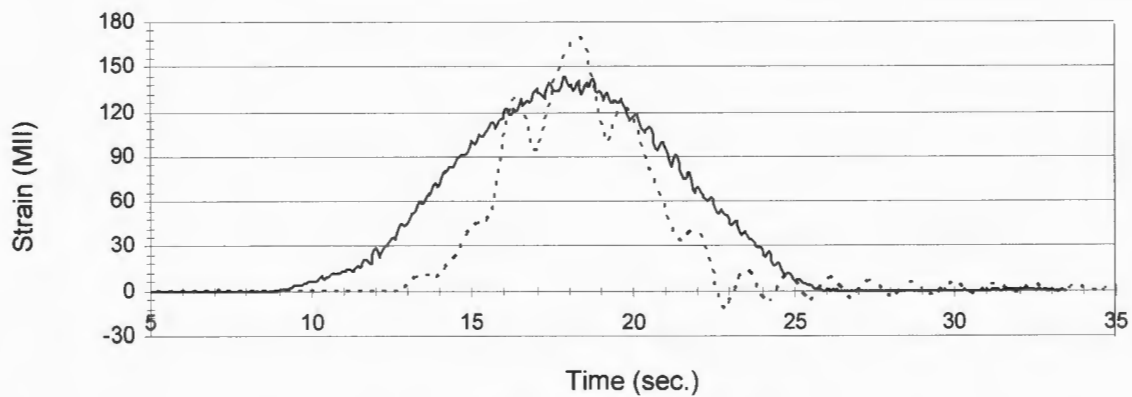
Figure 2.24. Comparison of the measured interior girder deflections of the North, Middle, and South RRFCs from static and dynamic field tests (Lane 1 loading).



a. North RRFC interior girder



b. Middle RRFC interior girder



c. South RRFC interior girder

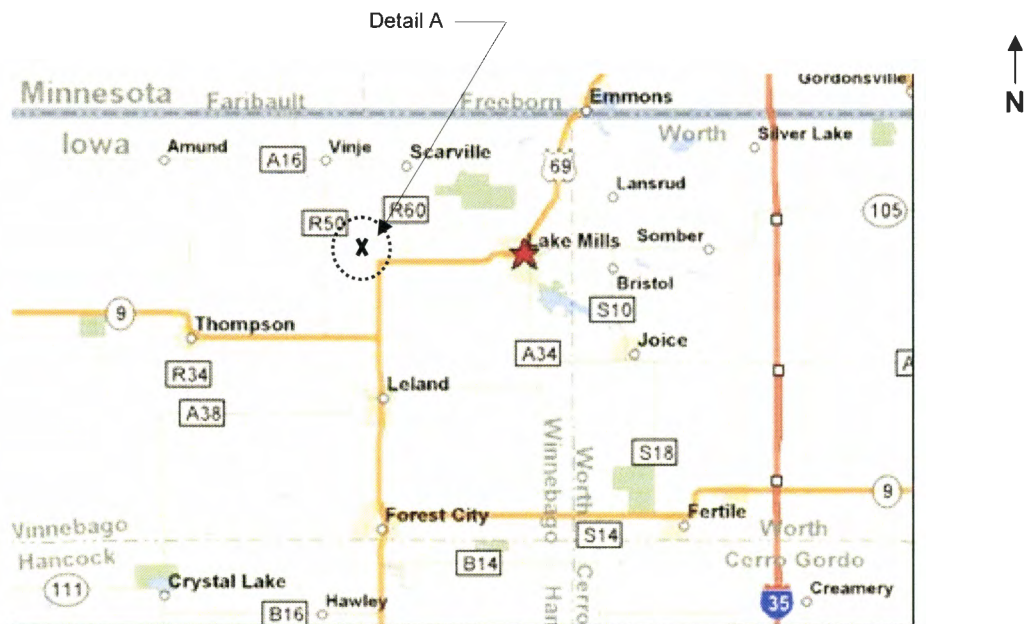
Figure 2.25. Comparison of the measured interior girder bottom flange strains of the North, Middle, and South RRFCs from static and dynamic field tests (Lane 1 loading).

The largest amplification of both deflection (17%) and strain (17%) was experienced in the South RRFC. This likely occurred due to the tandem truck not positioned precisely in Lane 1 (centered on the roadway). Assuming the truck is positioned slightly south of the centerline during the dynamic testing, this misalignment would have placed more load on the South RRFC and thus increasing both the strains and deflections measured in the interior girder.

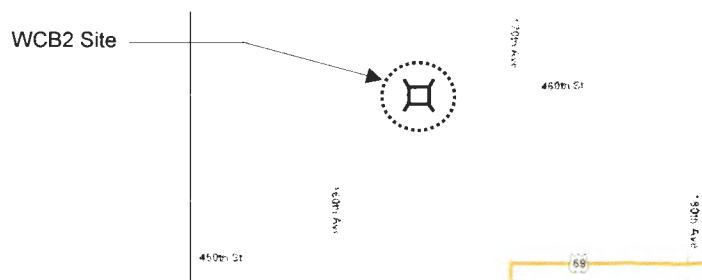
3. WINNEBAGO COUNTY BRIDGE 2 ON 460th St.

3.1 Introduction

In the summer of 2005, a RRFC bridge was constructed in Winnebago County. This is the second RRFC bridge in Winnebago County tested by ISU and will be referred to as Winnebago County Bridge 2 (WCB2). Maps showing the location of the WCB2 are presented in Figure 3.1; the bridge is located approximately 5.5 miles west and 1 mile north of Lake Mills, Iowa, on 460th St.



a. Lake Mills, IA



b. Detail A

Figure 3.1. Location of the Winnebago County RRFC Bridge 2 [6].

The previous three-span timber bridge (FWHA No. 344890) at the WBC2 site (See Figure 3.2) had a total length of 62 ft from center to center of the abutments and a central span length of 23 ft. The timber substructure consisted of 6 timber piles at each abutment and pier, and 12x12 creosoted timbers were used for the abutment caps. The stringers were 6x16 creosoted timber and the deck was constructed with 3x12 creosoted timber plank.



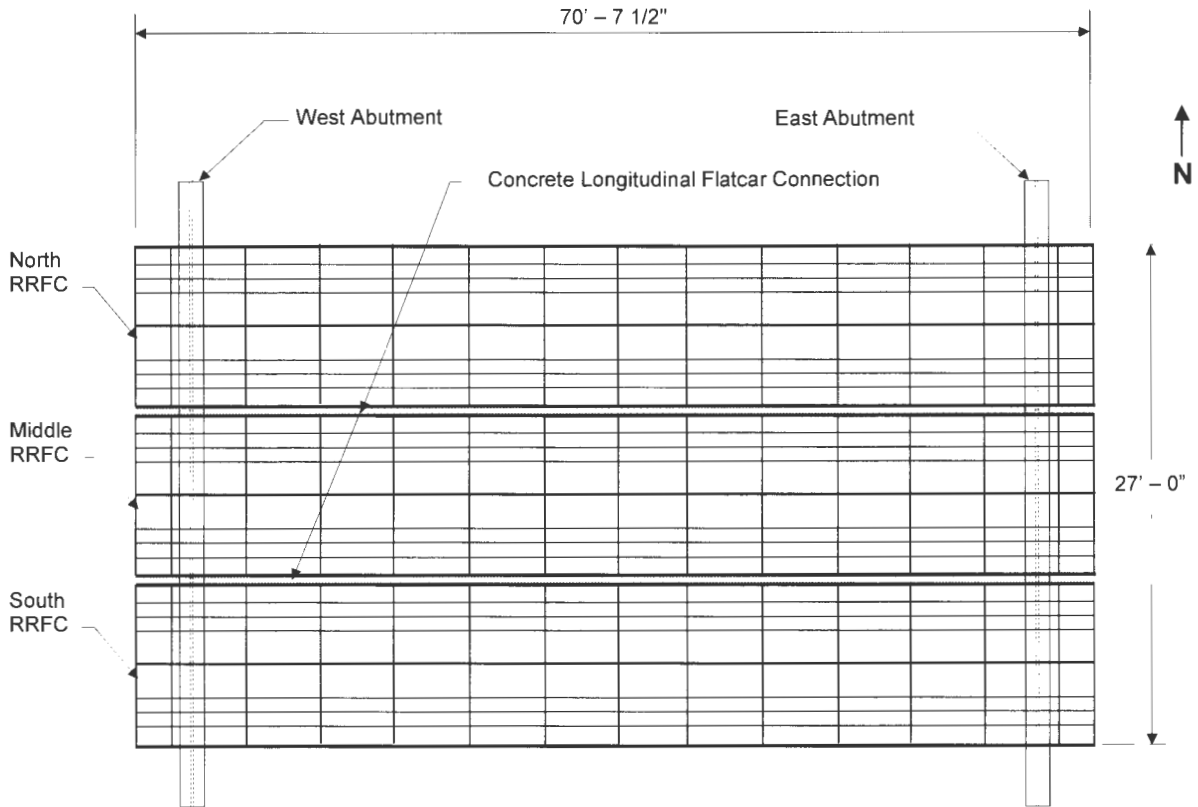
Figure 3.2. Original three-span, timber bridge at the WBC2 site.

3.2 Design and Construction

The WCB2 shown in Figure 3.3 was constructed using the superstructure from three RRFCs that were positioned side-by-side and connected with a reinforced concrete beam. The span length is 66 ft – 4 in. from center to center of abutments with 2 ft – 1 3/4 in. overhangs at each end; the bridge width is 27 ft (26 ft – 5 in. driving surface). End abutments consist of 6 steel HP12x53 piles and HP12x53 steel caps (See Figure 3.3c) with sheetpile backwalls at the end of the overhangs for soil retainment. The 70 ft – 7 1/2 in. lengths of RRFCs, cut from 89-ft RRFCs, used in the WCB2 were the same as those for the BCB3 as described in Chapter 2 (Figure 2.5).



a. Photograph of the WCB2



b. Plan View

Figure 3.3. Winnebago County RRFC Bridge 2.

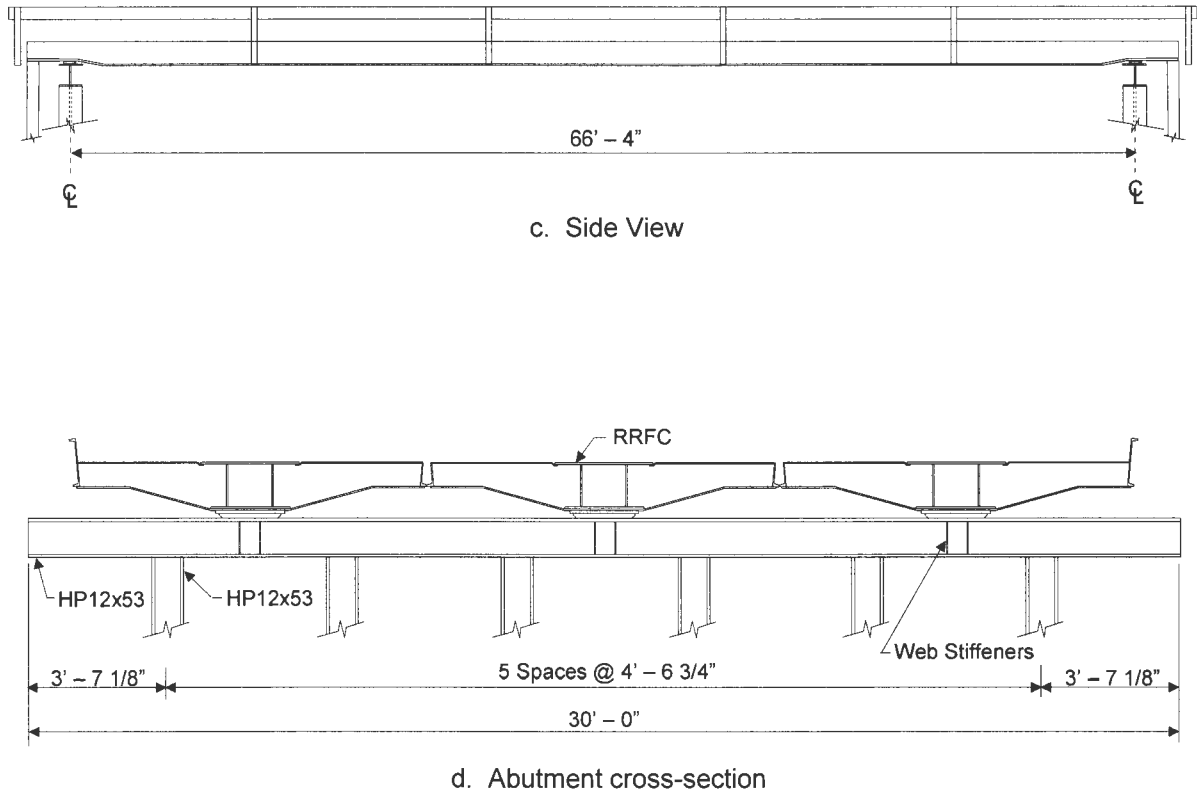
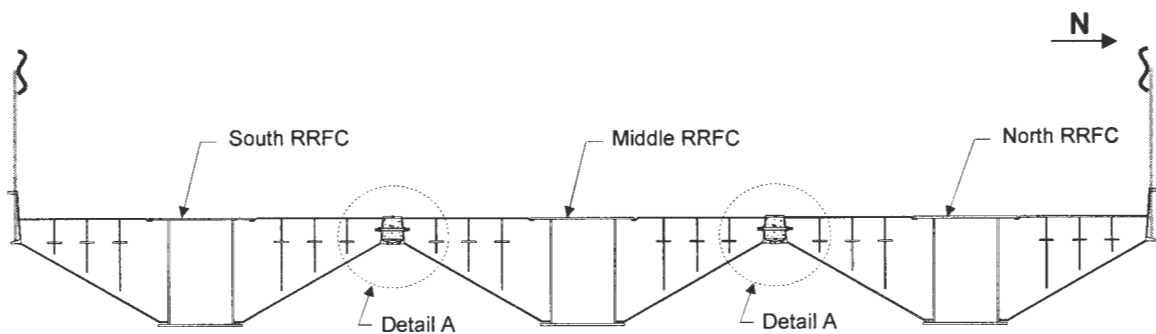


Figure 3.3. Continued.

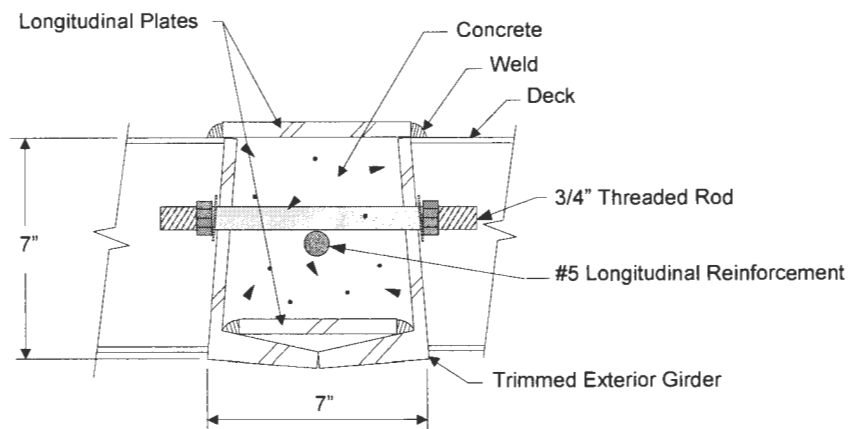
The driving surface was constructed using timber planks with gravel. The north half of the bridge had 3x12 timber planks butted against one another while the south side had 4x12 tongue-and-groove timber planks. The depth of the gravel driving surface varied randomly across the bridge from a minimum of 1 1/4 in. to a maximum of 5 1/2 in.

Exterior girders of adjacent flatcars were joined using 3/4 in. diameter threaded rods located 2 1/2 in. below the deck on approximately two foot centers. Details of the reinforced

concrete beam connection between adjacent RRFCs are presented in Figure 3.4. The void between the adjacent exterior girders was framed with 24 in. steel plates and filled with reinforced concrete and a #5 reinforcement bar to complete the connection between the flatcars. The bottom plates begin at the end of the RRFCs and are spaced on 24 in. centers. The top plates are also on 24 in. centers, and are staggered from the bottom plates. This connection is similar to that of the WCB1 with the exception of the location of the reinforcement bar and the plate details [2].



a. Cross-section



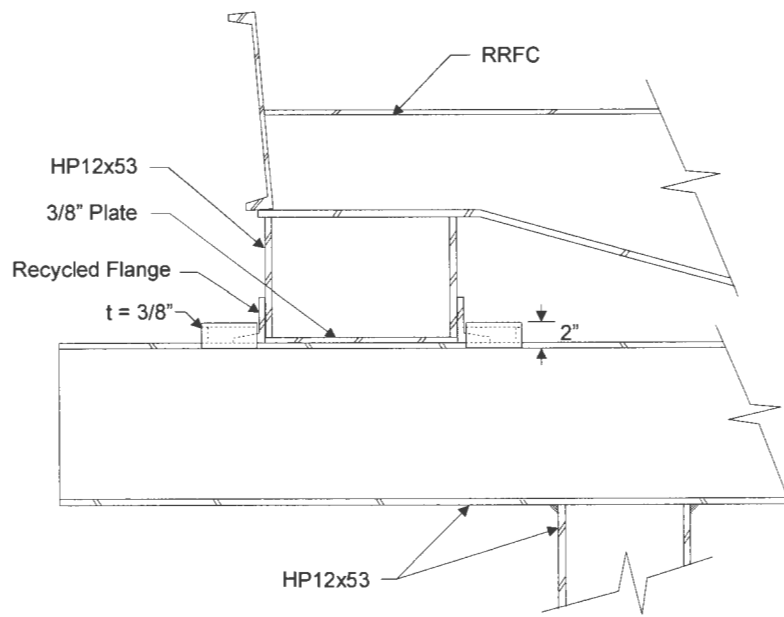
b. Detail A

Figure 3.4. Longitudinal concrete beam connection used in the WCB2.

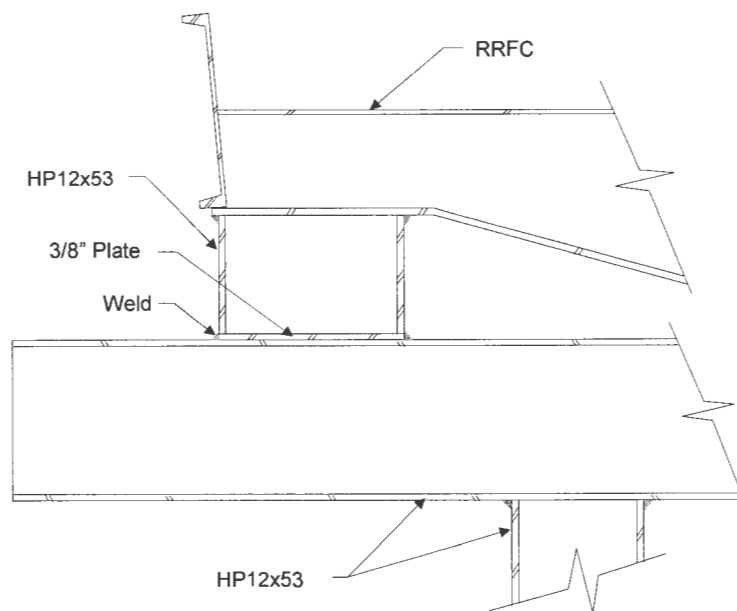
Supports for the exterior girders were necessary at the abutments because the elevation of the bottom of these girders was higher than rest of the RRFC. Recycled HP12x53 sections from the abutments and piles, which are shown in Figure 3.5, were used to create the needed supports. The supports at the east abutment were welded to the steel cap beam. At the west abutment, a roller condition was created to allow for expansion and contraction of the bridge. Recycled flanges from the trimmed portions of the exterior girders were welded on to either side of the west support. A “box” fabricated out of 3/8 in plates allows the recycled RRFC flange on either side of the support to move horizontally (parallel to the bridge length) and restricts movement vertically and horizontally (perpendicular to the bridge length).

3.3 WCB2 Field Testing

On July 6, 2005, a week after completion of the bridge construction, a field test of the WCB2 was conducted by loading the bridge with a tandem truck. Truck dimensions and axle weights are presented in Figure 3.6. The front tires on the test truck were 12 in. wide while each set of tandem tires was 22 in. wide. Spacing between the centers of the front tires was 7 ft – 3 in. and the spacing between centers of the tandem tire pairs was 6 ft – 0 in. The gross weight of the truck was 52,020 lbs, with 17,100 lbs distributed to the front axle. It was noted during testing that the gravel was not uniformly distributed in the truck’s box. A larger portion of the gravel was positioned on the south side of the truck, thus increasing the weight of the truck on its south side and consequently increasing loading applied to the bridge on that side of the truck. Therefore, in all load tests, a larger portion of the truck’s load was on the south side of the truck.

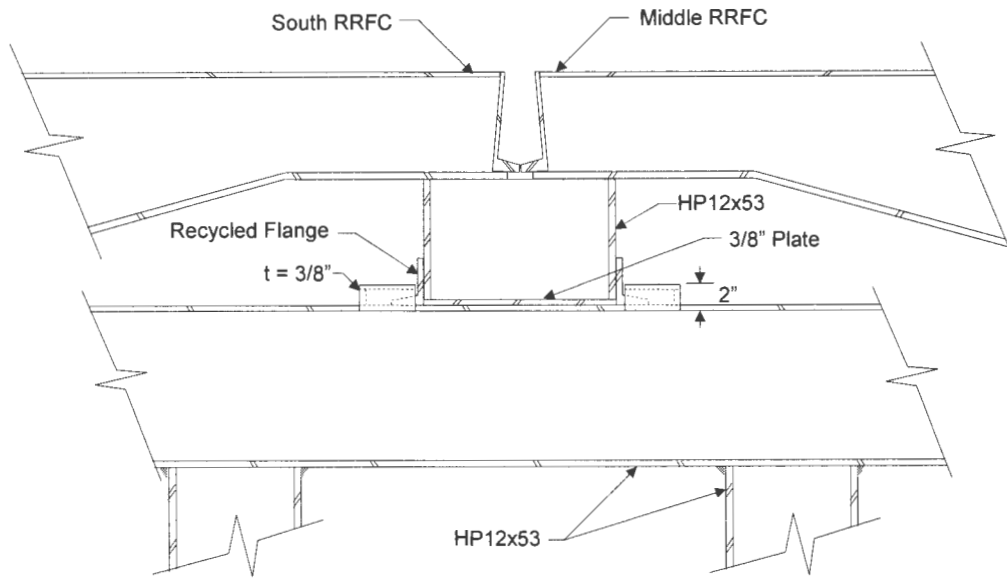


a. Exterior girder support at the west abutment

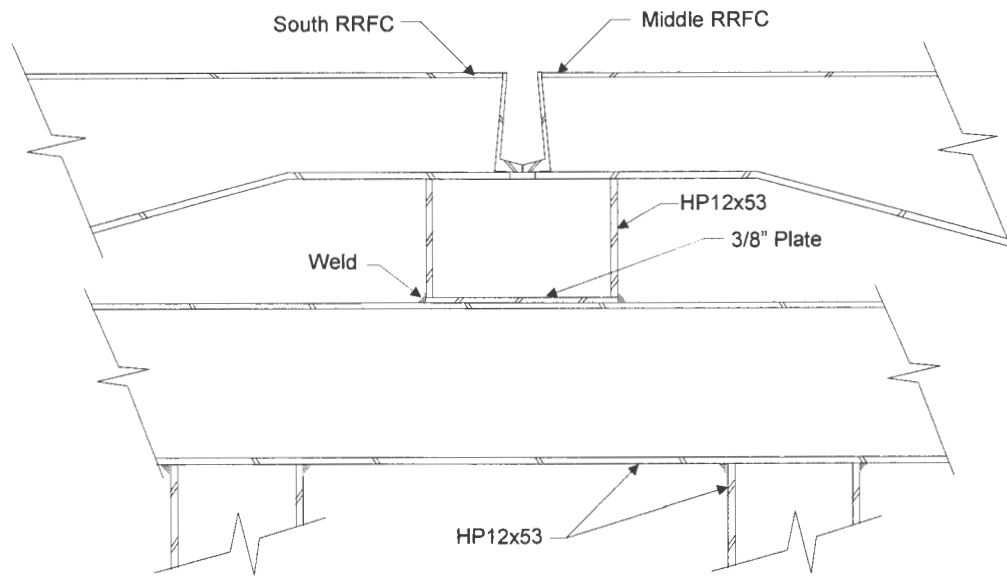


b. Exterior girder support at the east abutment

Figure 3.5. Exterior girder supports for the WCB2.



c. Connection support at the west abutment



d. Connection support at the east abutment

Figure 3.5. Continued.

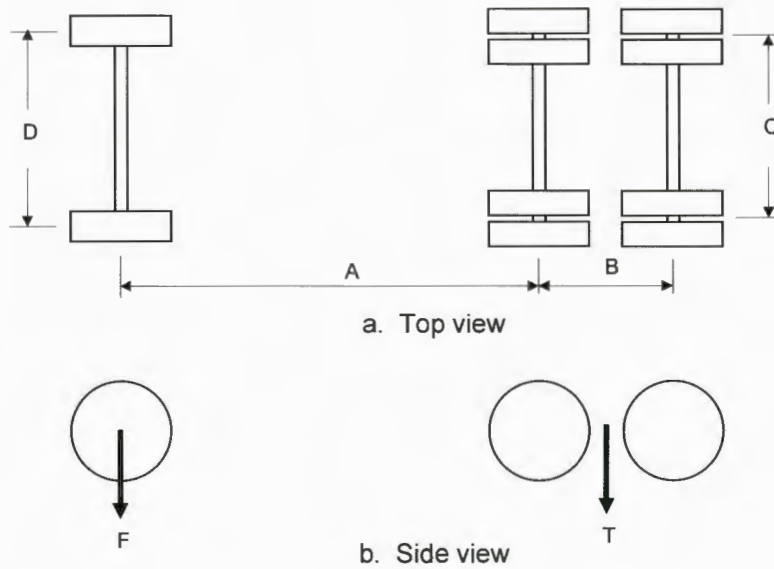


e. East abutment edge support



f. West abutment connection support

Figure 3.5. Continued.

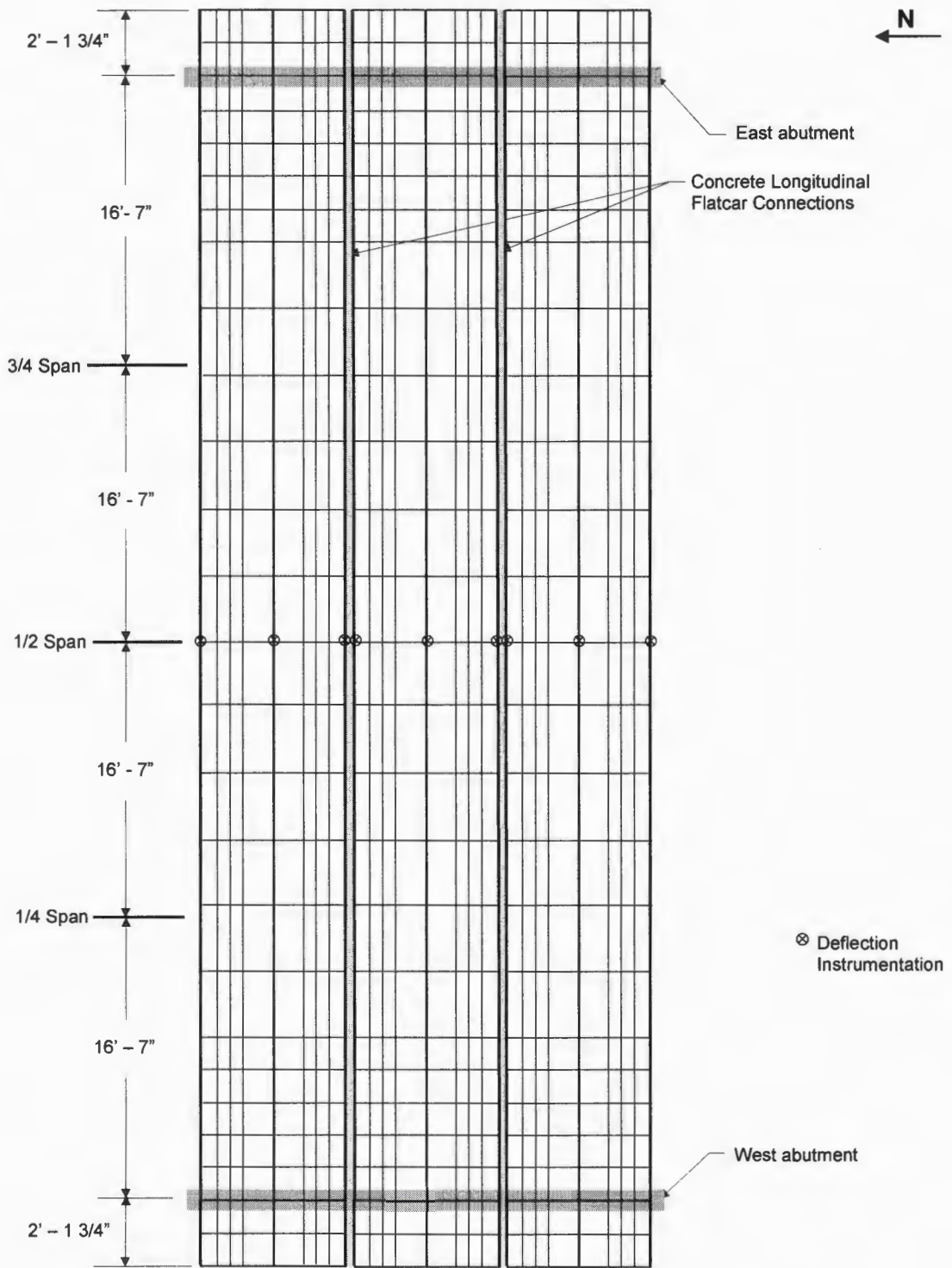


Dimensions				Load (lbs)		
A	B	C	D	F	T	Gross
14' - 1"	4' - 7"	6' - 0"	7' - 3"	17,100	34,920	52,020

Figure 3.6. Dimensions and weights of truck used in WCB2 field test.

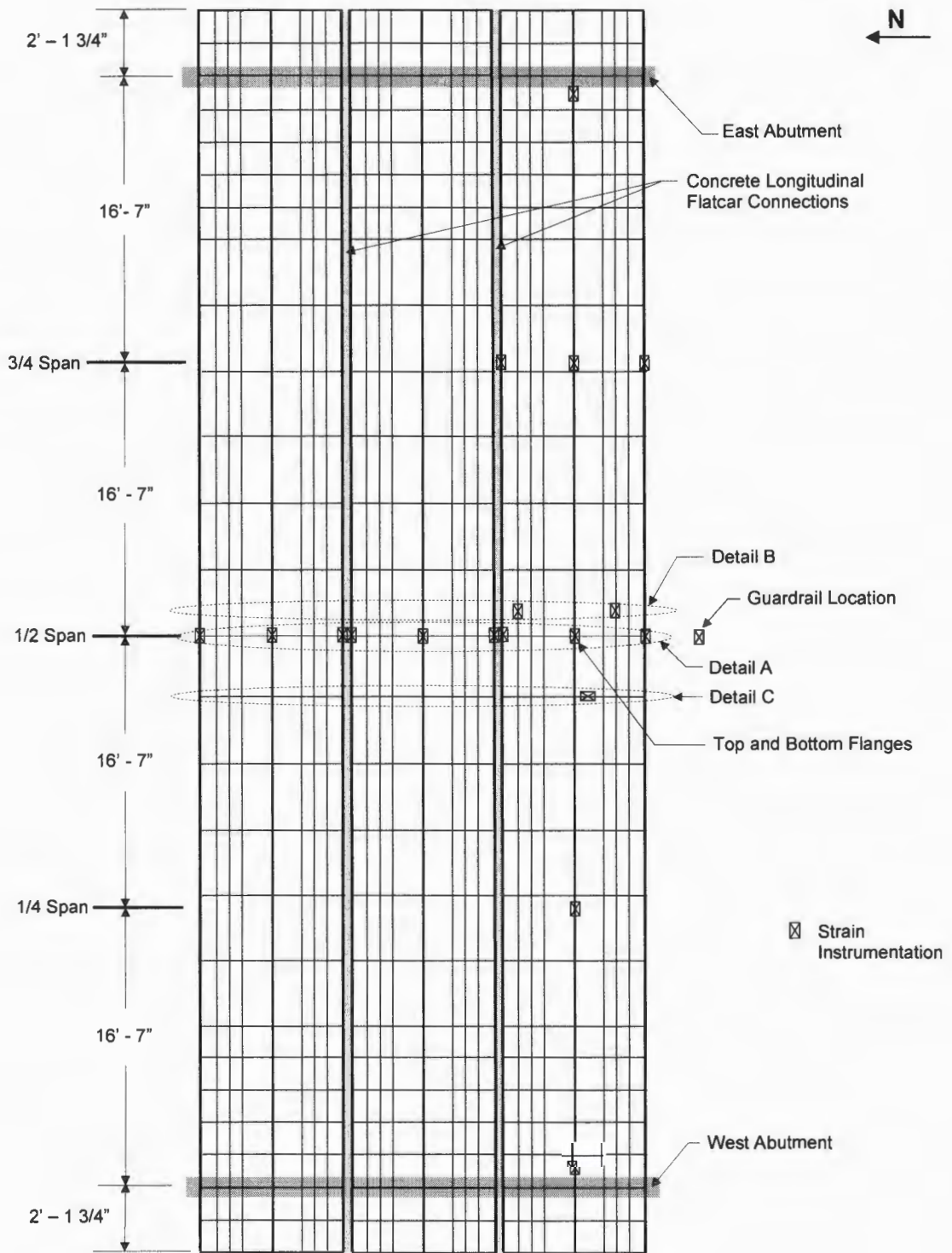
Instrumentation for the WCB2 field test involved both strain and deflection transducers placed on the RRFC girders. Strains and deflections were measured at 20 and 9 locations on the bridge, respectively. Specific locations of the deflection and instrumentation on the respective girders, along with photographs of some of the instrumentation are presented in Figures 3.7 and 3.8, respectively. Deflection transducers were placed along the midspan cross-section at all the interior and exterior girders of the three flatcars. Strain data were collected on the interior girder of the South RRFC near the abutments and at the 1/4, mid, and 3/4 spans. At the 3/4 span location, strain instrumentation was also placed on the exterior girders of the South RRCC. Strain transducers at midspan were placed on all the interior and exterior members of the three RRFCs and near the top of the south guardrail. Also, strain transducers were placed on two secondary longitudinal members located 12 in. east of midspan and on a transverse member located approximately 4 ft west of the midspan. Data (deflections and strains) were collected across the width of the bridge at the midspan so that the load distribution among the flatcars could be determined.

Continuous data were measured and recorded as the tandem truck traveled across the bridge during each test run. Data were recorded as the truck's tandem crossed each abutment and at 1/4, 1/2, and 3/4 span locations. To determine the bridge's behavior at different transverse loading locations, four transverse truck positions across the width of the bridge were used as illustrated in Figures 3.9 and 3.10.



a. Deflection Instrumentation

Figure 3.7. Location of instrumentation used on the WCB2.



b. Strain Instrumentation

Figure 3.7. Continued.

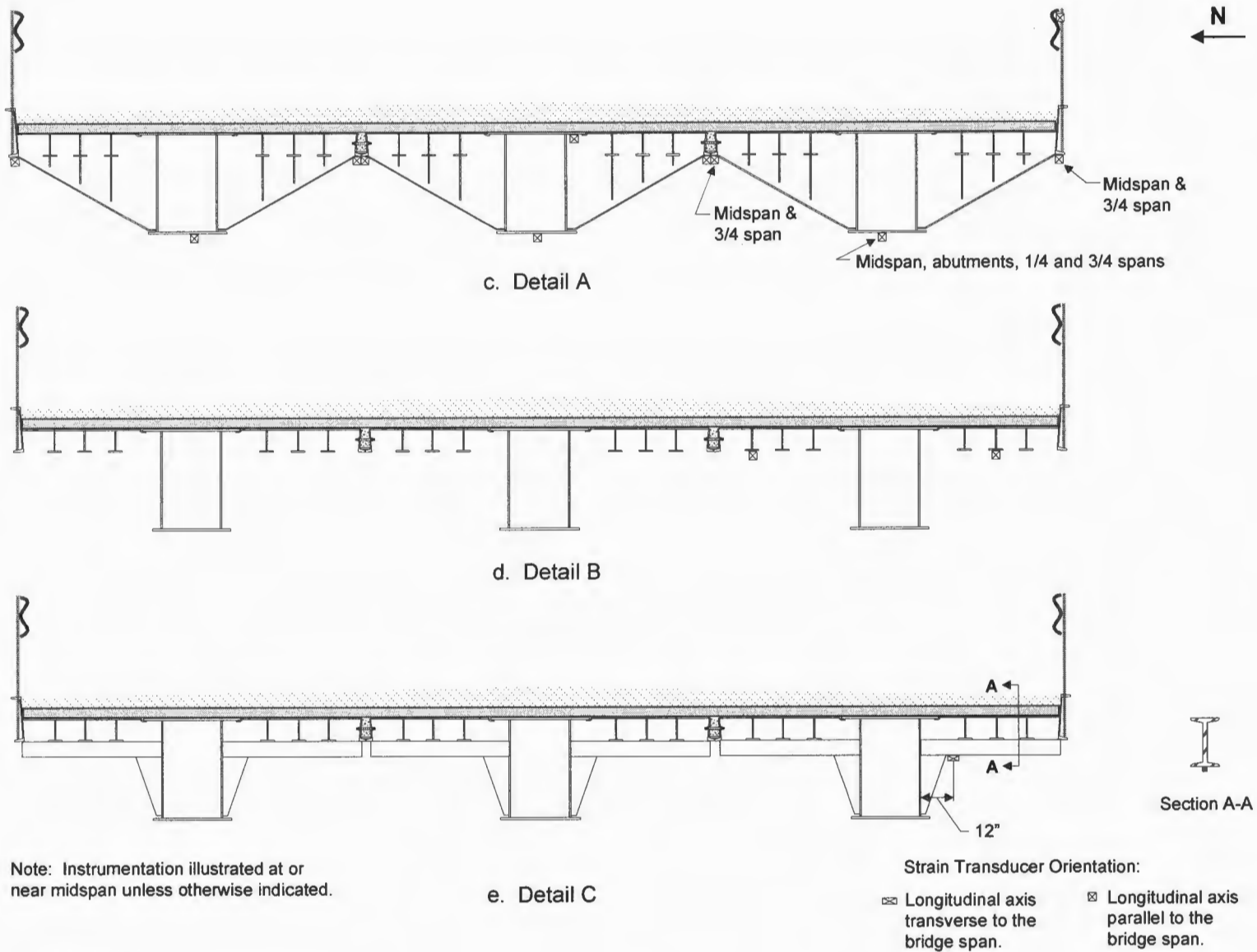
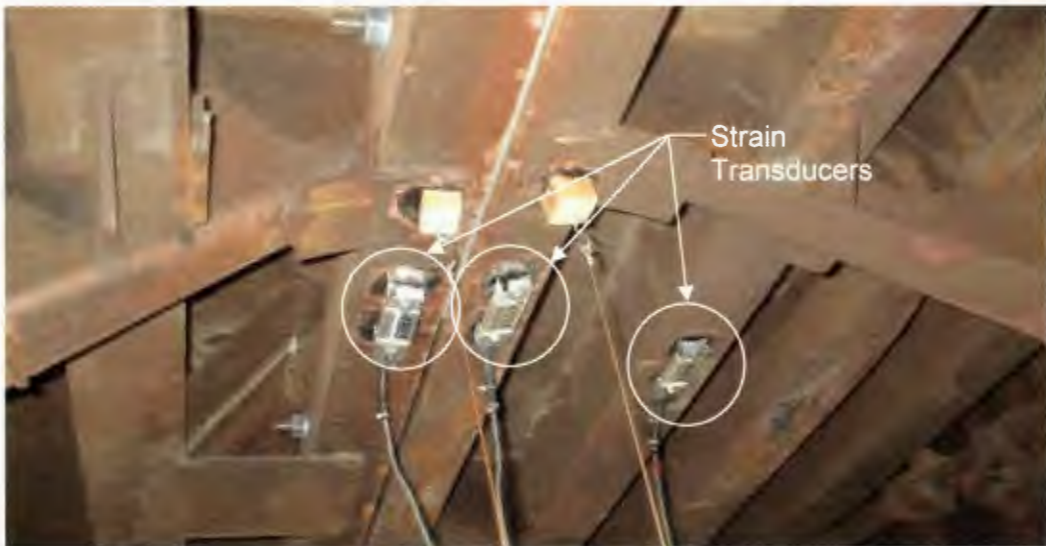


Figure 3.7. Continued.



a. Installed deflection instrumentation on the WCB2



b. Instrumentation at the south longitudinal concrete connection

Figure 3.8. Deflection and strain instrumentation on the WCB2.

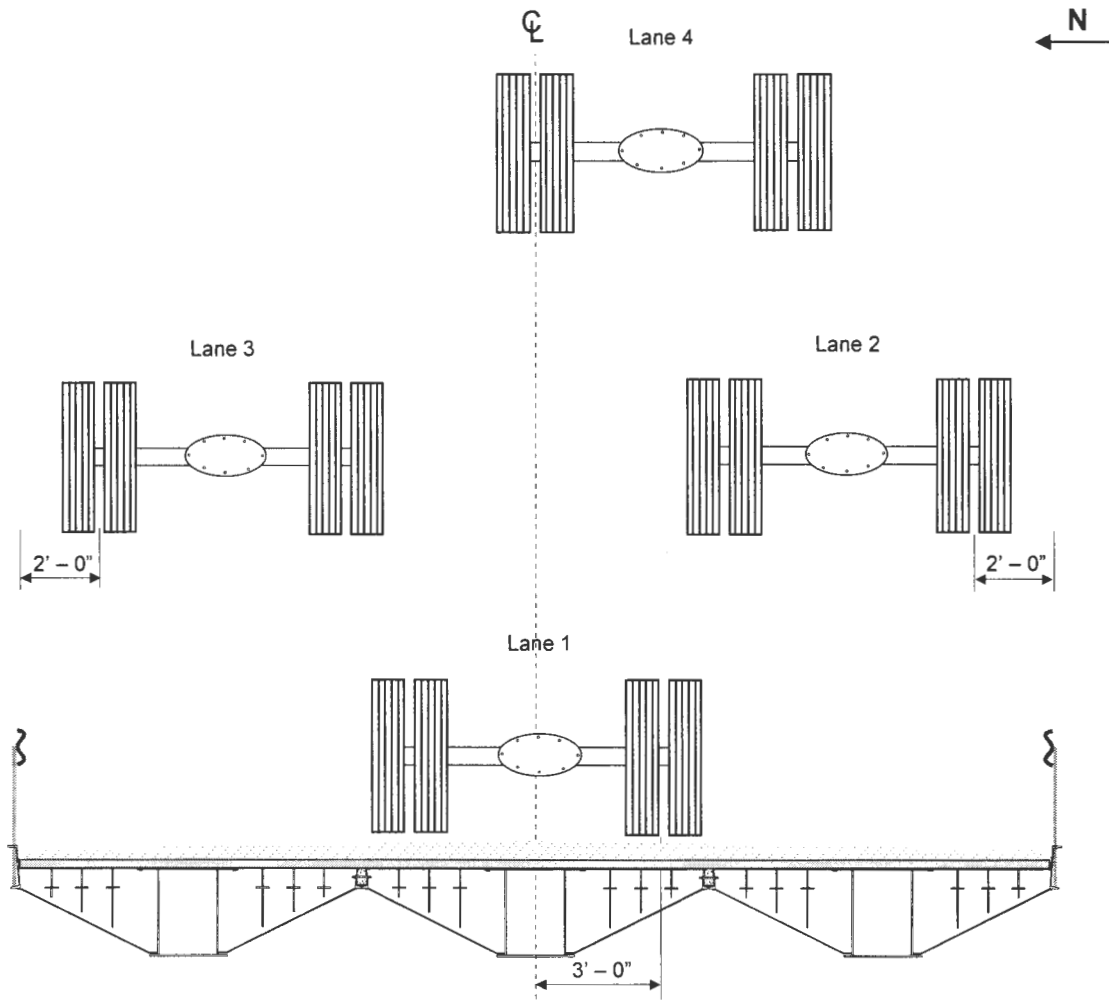


Figure 3.9. Transverse truck locations during the WCB2 load testing.



a. Test truck in Lane 1



b. Test truck in Lane 3



c. Test truck in Lane 2

Figure 3.10. Photographs of WCB2 field testing.

3.4 WCB2 Dead Load Analysis

Dead load analysis for the primary girders (interior box girders and exterior girders) was performed using various assumptions. The WCB2 was assumed to be simply supported at the abutments with a 66 ft – 4 in. clear span and 2 ft – 1 3/4 in. overhangs. Since the timber planks on the north and south halves of the bridge were different (3x12 timber planks were used on the north side and 4x12 tongue-and-groove planks were used on the south side), it was assumed that the dead loads on the each side were evenly distributed transversely only along that half of the bridge. However, all dead loads were assumed to be evenly distributed along the length of the bridge on each side. As discussed in Section 2.4 with the BCB3, the three main longitudinal members were assumed to support the entire bridge dead load, and their inertia ratios were used to distribute these loads to the girders. The girder inertias are similar to those in Table 2.1 with the exception of the exterior “trimmed” girder’s inertia being 24.5 in⁴ for the WCB2.

Conventional bridge design methods include analysis of a continuous, rigid structure across the width of the bridge. Hence, for the WCB2, it was assumed that the concrete connection between the flatcars was rigid and thus the dead load across the connection was uniformly distributed to the adjacent flatcars. After trimming excess material from the RRFCs and installation of guardrail posts, the weight of each railcar was 33,120 lbs. The guardrail system was assumed to be 100 lbs/ft while the gravel driving surface was estimated have a unit weight of 110 lbs/ft³ and the timber planks were approximated at 36.3 lbs/ft³. Field measurements estimated the gravel thickness to be 3.6 in. thick on the north half of the bridge and 4.2 in. thick on the south side. As stated previously, the timber planks on the north and south sides were 3 in. thick and were 4 in. thick, respectively.

Because the bridge is simply supported, and the dead load was assumed to be evenly distributed along the bridge length, the maximum dead load stresses for the exterior

Table 3.1. WCB2 bottom flange dead load stresses.

North RRFC			Middle RRFC			South RRFC		
Exterior Girder (uncut)	Interior Girder	Exterior Girder (trimmed)	Exterior Girder (trimmed)	Interior Girder	Exterior Girder (trimmed)	Exterior Girder (trimmed)	Interior Girder	Exterior Girder (uncut)
+4.8 ksi	+11.4 ksi	+3.6 ksi	+3 ksi	+12.6 ksi	+3.3 ksi	+3.8 ksi	+12.3 ksi	+5.1 ksi

and interior girders of each flatcar occurred at the bridge midspan. Maximum dead load stresses for the North, Middle, and South RRFCs are given in Table 3.1.

3.5 WCB2 Field Testing Results

As stated previously, the WCB2 was instrumented with deflection transducers across the midspan on interior and exterior girders, and strain transducers were placed on numerous interior and exterior girders, the south guardrail near midspan, and on two secondary longitudinal members and one transverse member of the South RRFC. Data collected from the field testing were reviewed and it was determined that the maximum deflections and strains occurred near midspan of the major members when the test truck tandem was at the midspan. Therefore, all analyses of live load deflections and strains are based on the data collected in the members at the bridge midspan when the truck tandem was also at midspan.

3.5.1 Static Testing

The midspan deflections and strains that were measured on the interior and exterior girders across the width of the bridge are presented in Figures 3.11-3.14. In these figures, trend lines are used to connect deflection and strain data points measured during the field testing. The maximum midspan deflection (-0.86 in.) occurred at the exterior girder of the

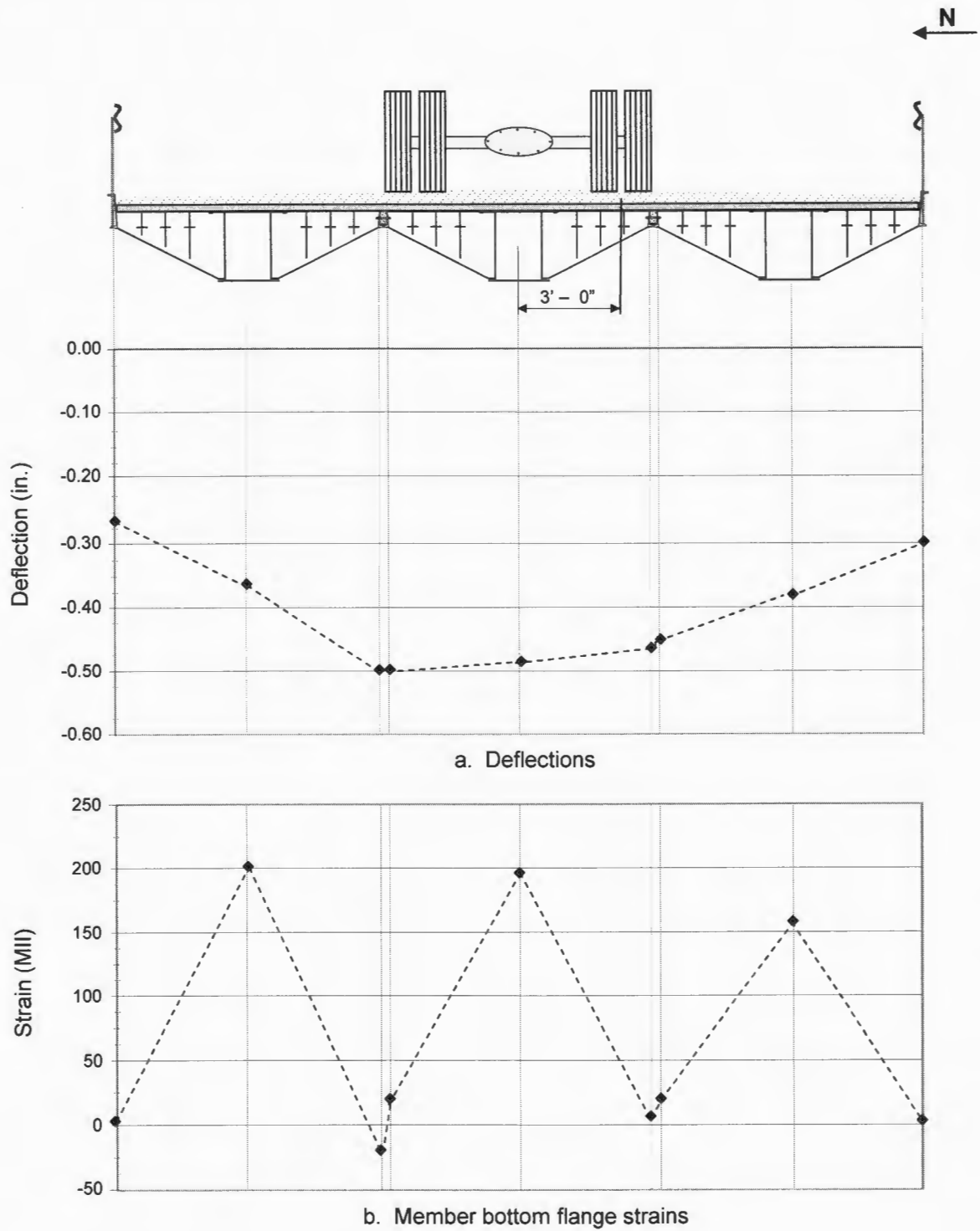


Figure 3.11. WCB2 midspan deflections and strains when the truck was in Lane 1.

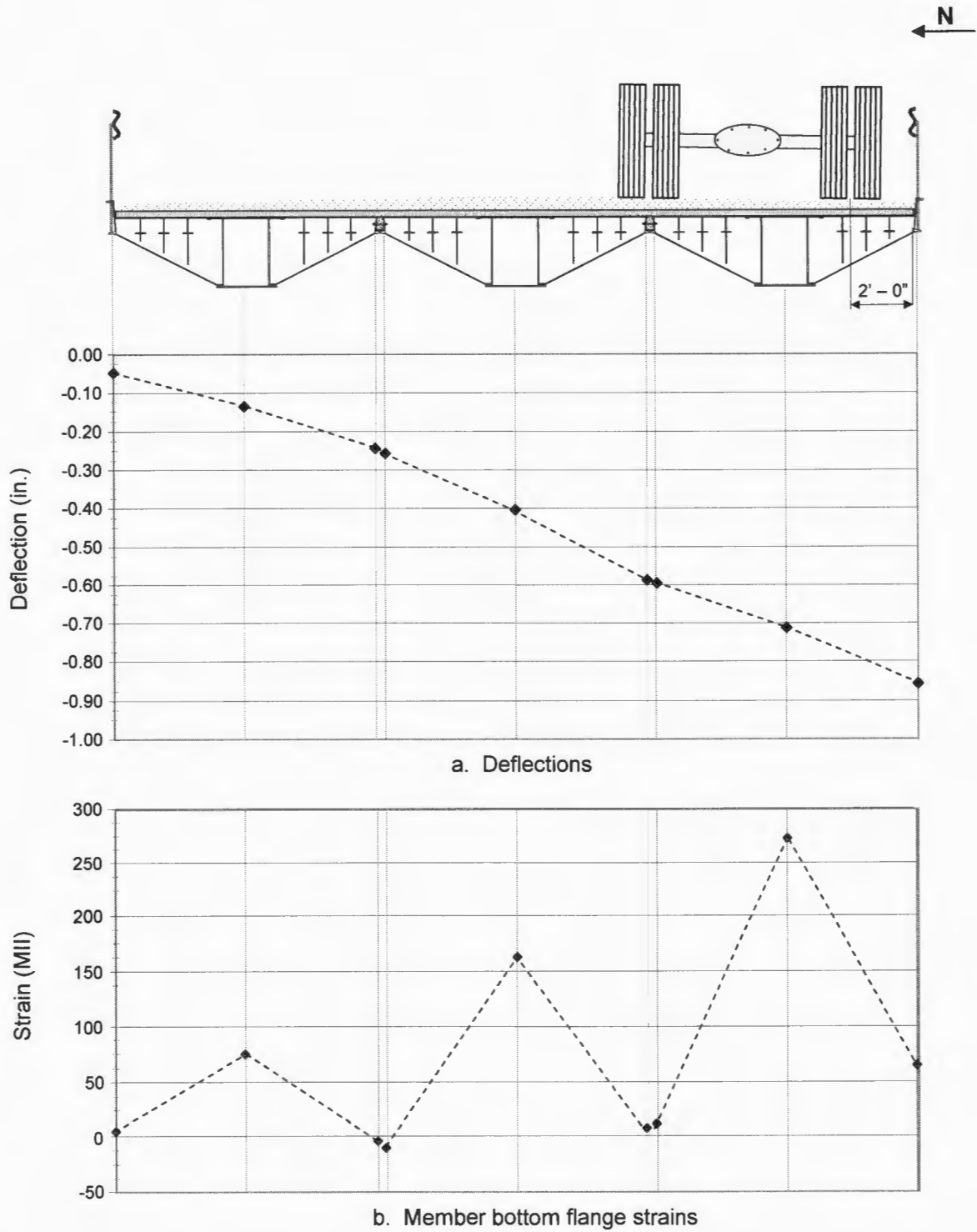


Figure 3.12. WCB2 midspan deflections and strains when the truck was in Lane 2.

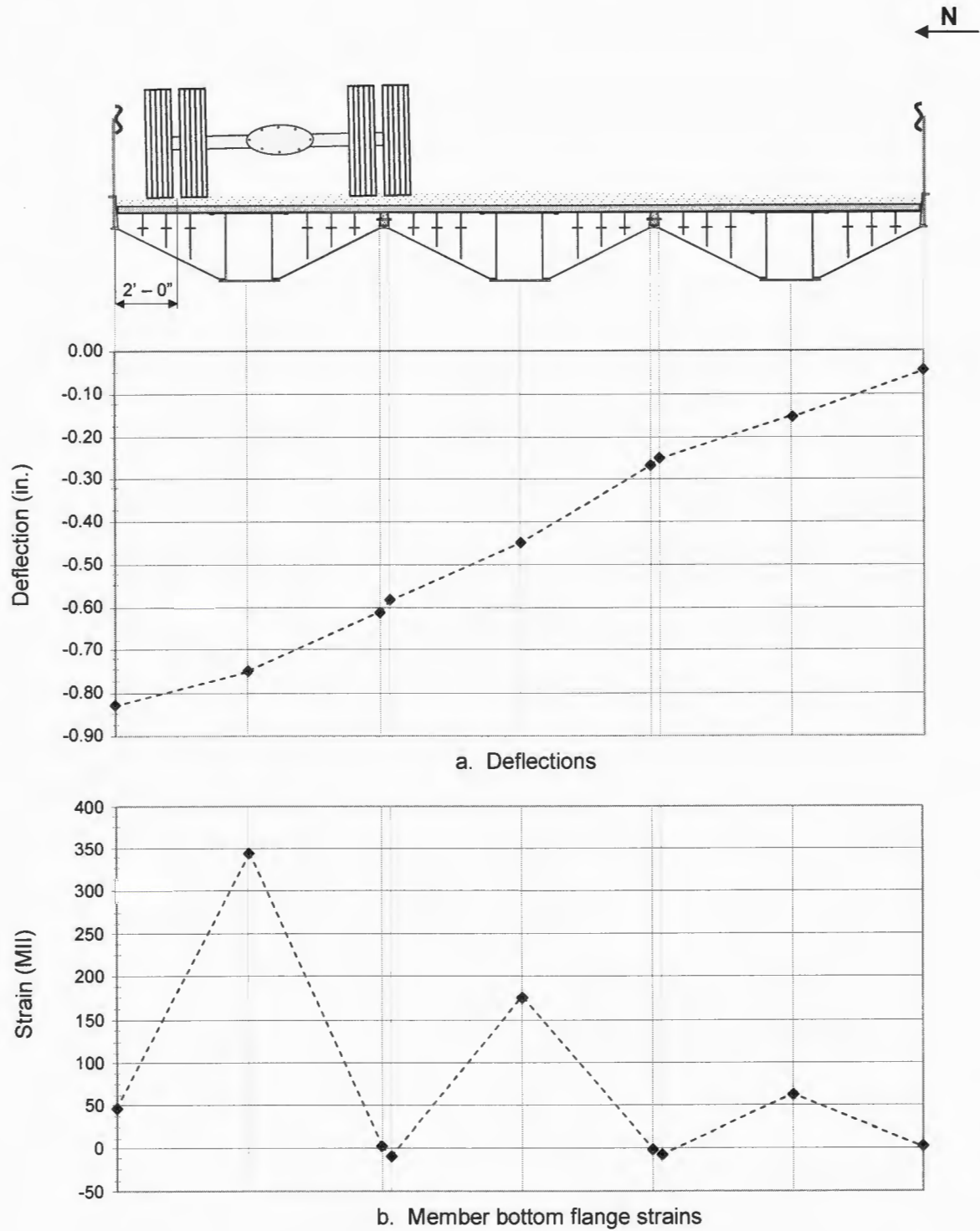


Figure 3.13. WCB2 midspan deflections and strains when the truck was in Lane 3.

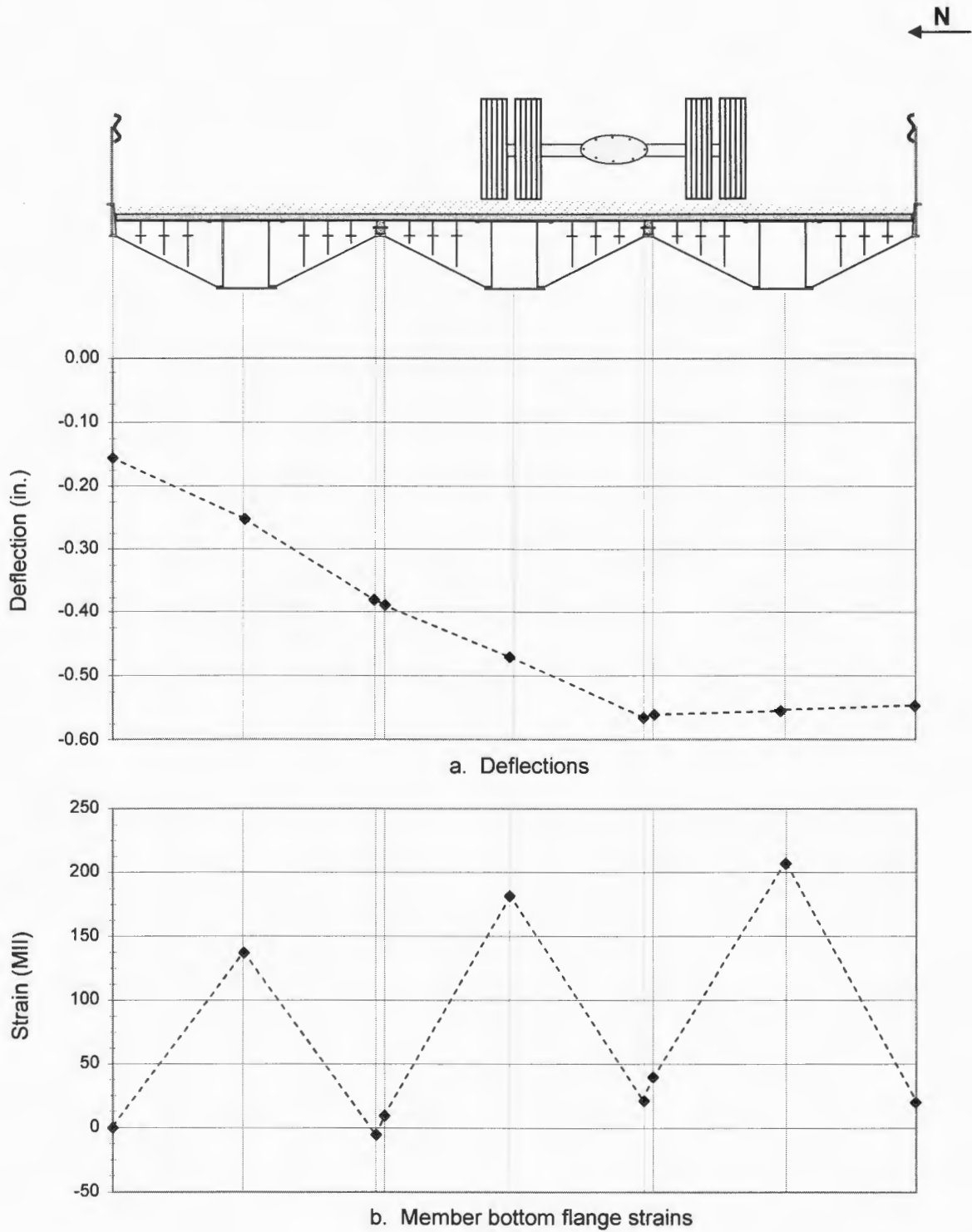
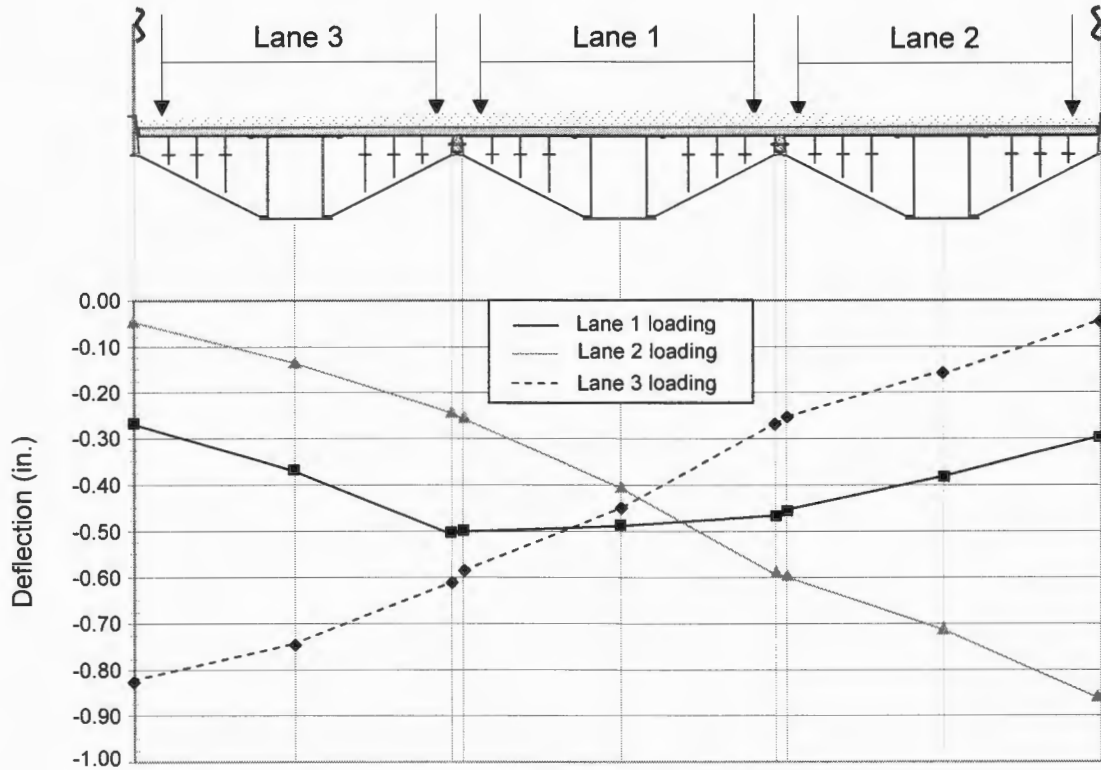


Figure 3.14. WCB2 midspan deflections and strains when the truck was in Lane 4.

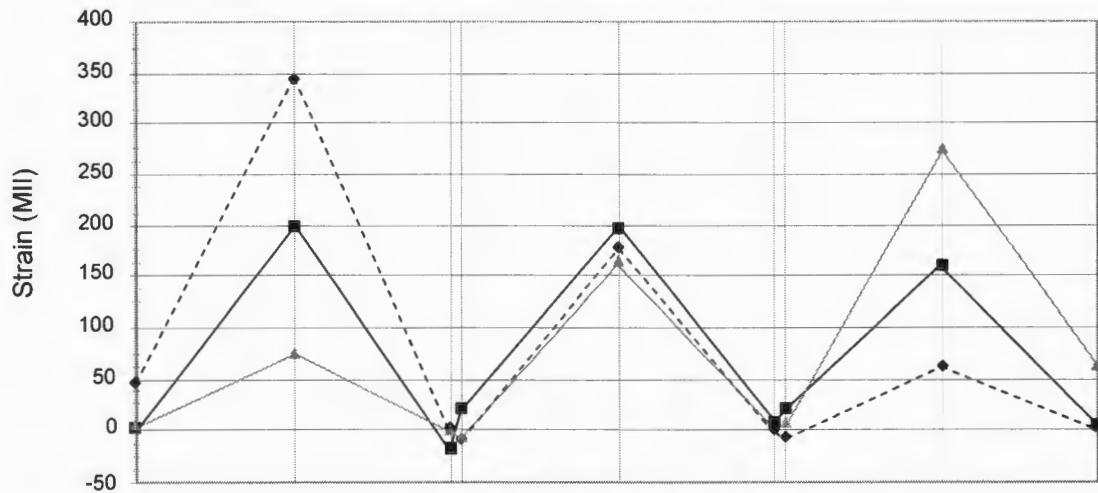
South RRFC when the truck was in Lane 2 (See Figure 3.12), and the maximum midspan strain (+343.7 MII) occurred during the Lane 3 loading at the interior girder of the North RRFC (See Figure 3.13). As can be seen in Figures 3.11-3.14, measured midspan strain and deflection values that occurred when the truck load was in Lanes 1-4 (truck rear tandem at midspan) for all other members are below the maximum midspan values previously noted.

As can be seen from Figures 3.11-3.14, the location of maximum deflection in each case occurred directly below the wheel position. The deflection decreased as the transverse distance between the girder and the truck wheel increased. In general, the same can be said for the strains, where the greatest strains occurred at the wheel location. An exception is the interior girder of the North RRFC during Lane 1 loading which had a slightly higher strain value (4 MII) than the interior girder of the middle RRFC. This may be the result of the lower rigidity of the north portion of the bridge due to the timber planking on that side of the bridge and/or the truck being positioned slightly to the north of the bridge's centerline.

Lateral load distribution as shown in Figure 3.15 was different on the north and south sides of the WCB2 because of the different timber planking used on each side of the centerline of the bridge. The south side, which had tongue-and-groove plank, distributed loads better than the north side planks. When the truck was positioned in Lane 1, larger deflections and strains were measured in the North RRFC than the South RRFC due to the better distribution on the south side. The tongue-and-groove timber planks could also distribute loads longitudinally to other secondary members, thus decreasing the deflections and strains on the bridge's south side. When the truck was in Lane 3, the distribution of loads was less, thus the interior girder of the North RRFC resisted more of the load and little was transferred to other members. This distribution can also be seen in the South RRFC's interior girder during Lane 2 loading in which there was better distribution and the load was



a. Deflections



b. Member bottom flange strains

Figure 3.15. Comparison of midspan deflections and strains for Lanes 1, 2, and 3.

transferred to other members, thus reducing the strains measured in the interior girder of the South RRFC. The live load distribution factor needed for design was found from analyses of the deflection data from the various loading positions. The maximum live load strains (stresses) and deflections occurred on the interior and exterior girders of an exterior RRFC when the truck was positioned on that side of the bridge. The live load moments in each girder, resulting in the maximum strains (stresses) was a function of the live load distribution factor. Using the areas under the deflection curves during loading in these truck positions, the moment distribution was found to be 55%.

The maximum deflection measured (-0.92 in.) occurred near the midspan and was measured in the South RRFC exterior girder when the test truck was located in Lane 2. Following the AASHTO LRFD Bridge Design Specifications [5], a recommended maximum deflection was 'span'/800 for legal truck loads. For the WCB2 with a clear span of 66 ft – 4 in., this legal load deflection limitation would be -1.00 in. Hence, for this truck loading, the maximum measured deflection was below recommended values. If the measured deflection were increased in proportion of the test truck load to an HS-20 loading, the experimental deflection would be -1.27 in., which is significantly above AASHTO limits.

It was assumed that the material properties for these RRFCs are similar to those of the railroad flatcars used in previous projects [1,2]. The proportional limit and modulus of elasticity for these railcars used in previous research were determined from coupon tests to be 40 ksi and 29,000 ksi, respectively. A conservative yield strength of the material was assumed to be 36 ksi [2]. The maximum live load strains in the exterior and interior girders were +360 MII (+10.4 ksi) in the North RRFC interior girder near midspan (Lane 3 loading), and +83.4 MII (+2.4 ksi) in the South RRFC exterior girder at the longitudinal connection at the 3/4 span location (Lane 1 loading). The maximum exterior girder strain occurred at the south longitudinal connection because, as previously noted, the truck load was concentrated

more towards the south side of the truck's box. The maximum strain occurred at the 3/4 span because it was near the location of the timber plank transition from 3x12 timber planks to 4x12 tongue-and-groove timber planks. Thus, the stiffness near this location was less, resulting in higher strains. The maximum strain in the transverse member instrumented near midspan was +42 MII (+1.2 ksi) and occurred when the truck was in Lane 4. The secondary members, also near midspan, had a maximum strain of +38 MII (+1.1 ksi) when the loading was in Lane 2. Maximum strains measured in other RRFC members were below those mentioned, and thus are not presented.

Combining the calculated dead load stresses with the live load stress values determined from the measured live load strains, the total member stresses were determined and are presented in Table 3.2.

Table 3.2. WCB2 bottom flange total stresses.

North RRFC			Middle RRFC			South RRFC		
Exterior Girder (uncut)	Interior Girder	Exterior Girder (trimmed)	Exterior Girder (trimmed)	Interior Girder	Exterior Girder (trimmed)	Exterior Girder (trimmed)	Interior Girder	Exterior Girder (uncut)
+6.3 ksi	+21.8 ksi	+4.5 ksi	+4.8 ksi	+18.6 ksi	+4.1 ksi	+5.3 ksi	+20.5 ksi	+7.1 ksi

The maximum total stresses in the North RRFC girders all occurred when the truck was positioned in Lane 3. The maximum stresses in the interior and north exterior girders of the Middle RRFC occurred during Lane 1 loading. The exterior girders at the south longitudinal connection between the Middle and South RRFCs had maximum stresses when the truck was in Lane 4. Lane 2 loading produced the maximum total stresses in the interior girder and exterior (uncut) girder of the South RRFC. The overall maximum stress of +21.8 ksi occurred in the interior girder of a side RRFC when the truck was positioned on that side

of the bridge. This is the same condition which resulted in a maximum stress of +16.7 ksi in the interior girder of a side RRFC of the 3-span WCB1 bridge described in Section 1.1.2.3.

Theoretical analysis of an HS-20 design truck loading (not including impact) was performed to determine maximum stresses of an exterior RRFC near the midspan. The design live load stress (+11.7 ksi) was calculated for the interior girder using the distribution factor determined using field test results. Combining this with the theoretical dead load stress in the interior girder, the maximum total stress due to an HS-20 design truck loading would be +24.0 ksi in the bottom flange of the interior girder of the South RRFC. As stated previously, the allowable stress was computed to be 22 ksi; therefore, the stress of +24 ksi for the interior girder's bottom flange exceeds this limit by approximately 9%.

3.5.2 Time History Analysis

With continuous data collected during a truck crawl speed (approximately 4 mph test), a time history analysis of the interior girder of the South RRFC was performed from strain transducers placed 1 ft from both abutments, at the 1/4 span, midspan, and 3/4 span locations (See Figure 3.16). It should be noted that the test truck traveled westward; hence peak values in the girders occurred first near the east abutment and lastly near the west abutment.

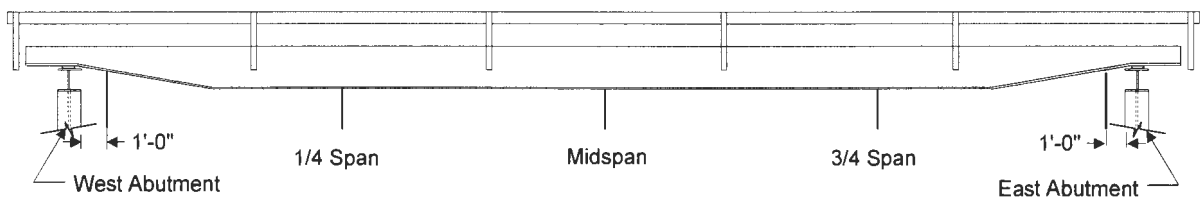


Figure 3.16. Strain instrumentation locations for WCB2 time history analysis.

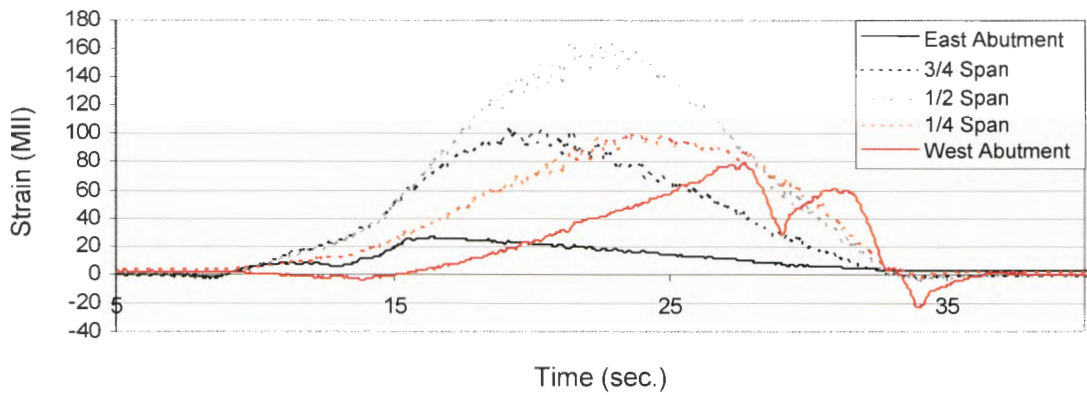
The time history strain data recorded during field testing is plotted in Figure 3.17. It can be seen that the maximum bottom flange strain was measured at the interior girder's midspan, since the structure is simply supported and maximum moments would occur near this location. Also, the fixity at the two abutments can be analyzed from the time history data. The east abutment is welded (restraining translations and rotations) while the west abutment allows for horizontal movement parallel to the bridge and some rotation. Strain instrumentation placed 12 in. from the supports at both abutments measured small strains signifying some restraint at the abutments.

3.5.3 Dynamic Analysis

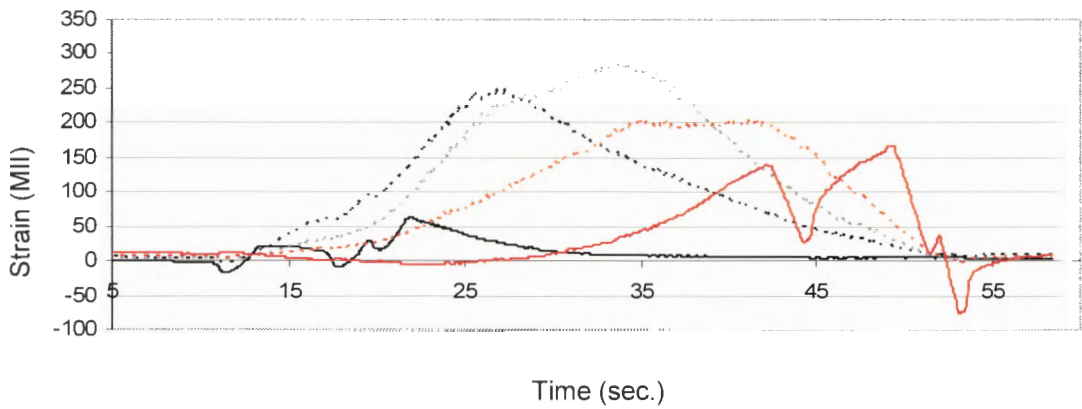
The structural dynamic properties of the WCB2 were determined through the dynamic testing performed during the field testing. Four dynamic tests were conducted at 10, 15, 20, and 25 mph truck speeds. Because of the flexibility of the WCB2, the 10 mph truck speed created the greatest dynamic amplification in the girders' deflections and strains.

The free vibration of the interior girders was used to determine their period, frequency, and damping. The oscillating strains when the tandem truck had exited the bridge indicated the free vibration of the bridge. Based on this data the period was found to be 1.4 seconds, resulting in a member frequency of 0.70 Hz, and the damping of the interior girders was approximately 1.5%.

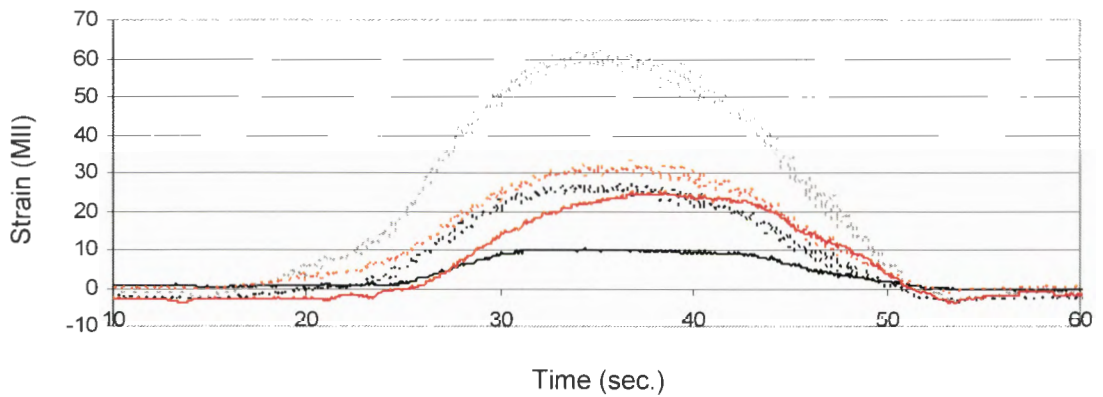
As previously noted, the maximum dynamic deflections and strains occurred at a truck speed of 10 mph. A plot of the time history comparison of the deflections and strains during the static and dynamic field testing are presented in Figures 3.18 and 3.19, respectively. The dynamic testing was performed in Lane 1; therefore, the data from static load testing is also from Lane 1 loading. The largest amplification occurred in the North RRFC interior box girder: the deflection was increased by 41% while the strain was amplified



a. Truck in Lane 1

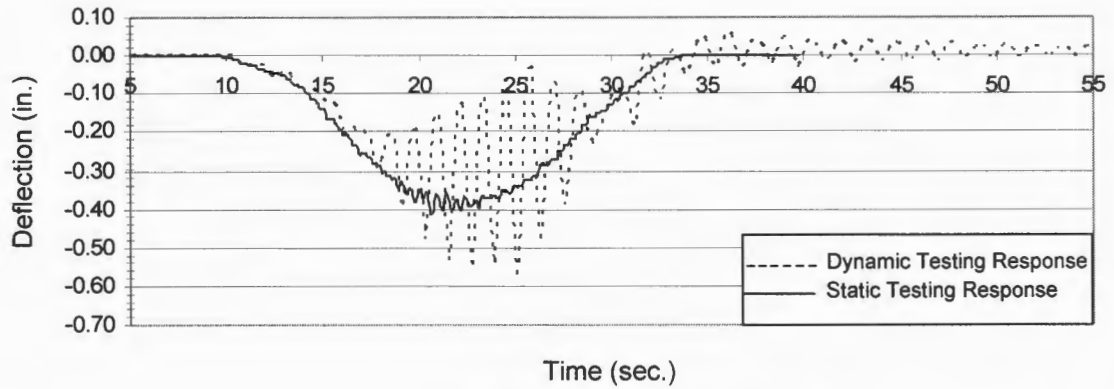


b. Truck in Lane 2

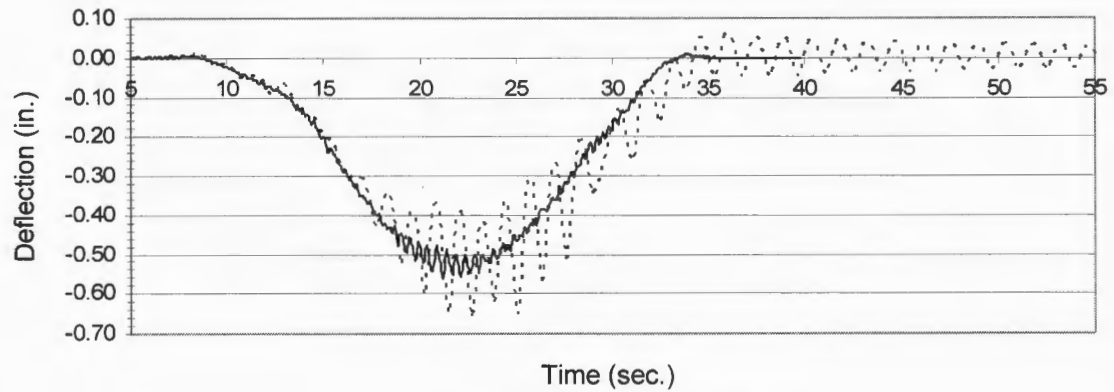


c. Truck in Lane 3

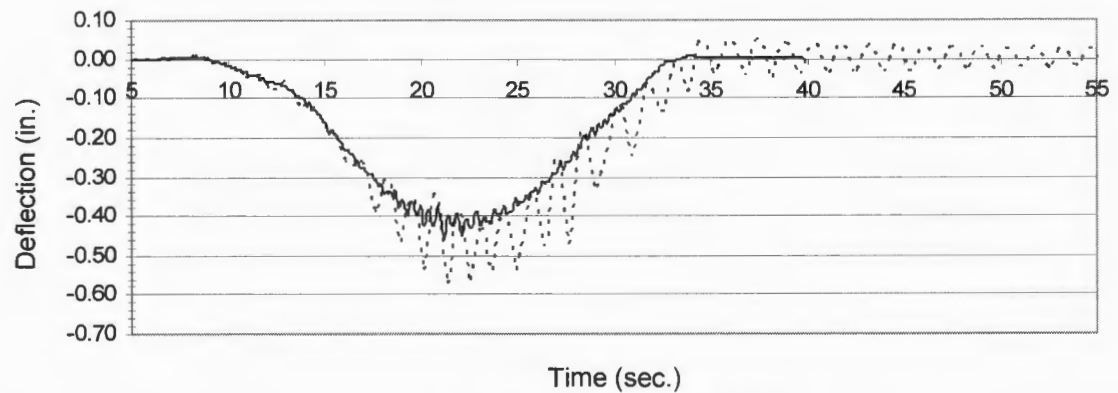
Figure 3.17. WCB2 strain vs. time for the South RRFC's interior girder bottom flange.



a. North RRFC interior girder

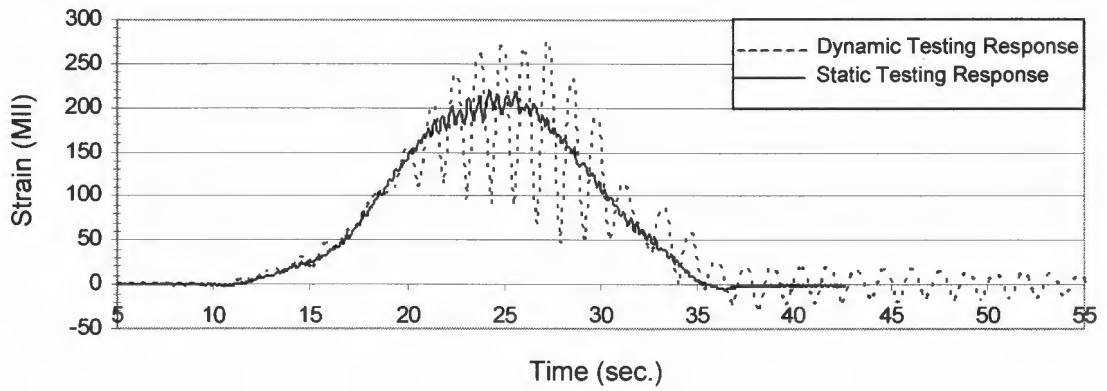


b. Middle RRFC interior girder

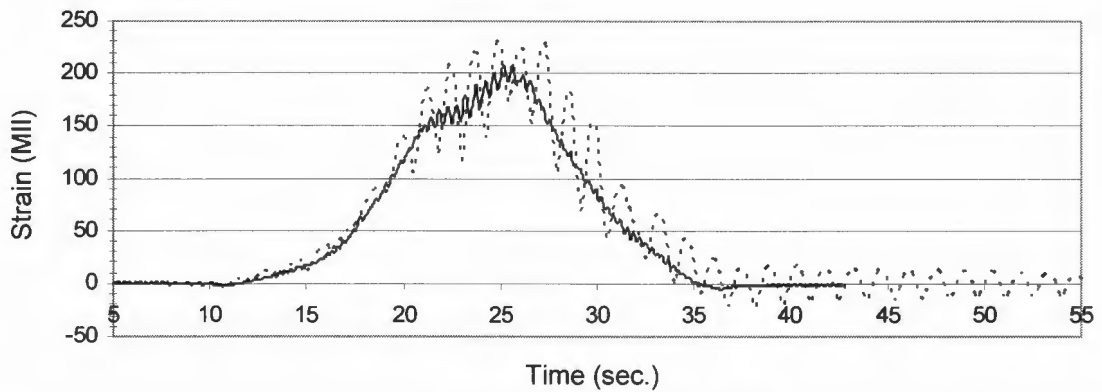


c. South RRFC interior girder

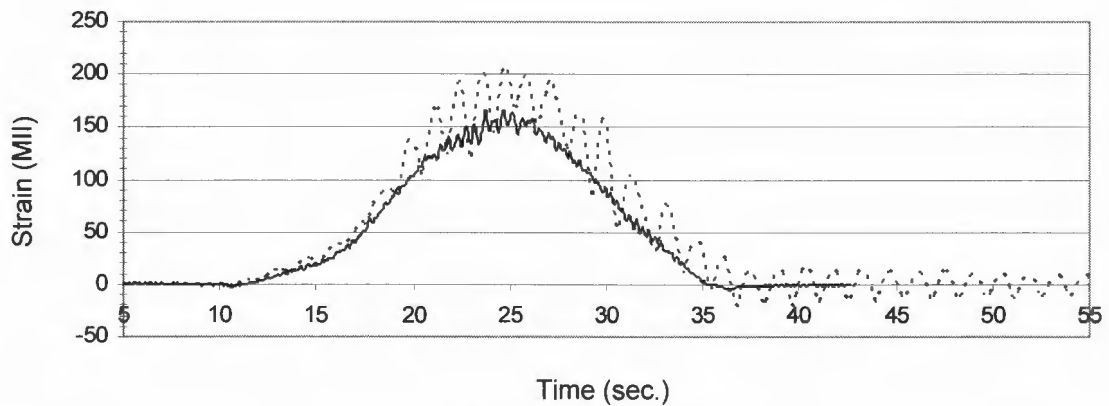
Figure 3.18. Comparison of the measured interior girder deflections of the North, Middle, and South RRFCs from static and dynamic field tests (Lane 1 loading).



a. North RRFC interior girder



b. Middle RRFC interior girder



c. South RRFC interior girder

Figure 3.19. Comparison of the measured interior girder bottom flange strains of the North, Middle, and South RRFCs from static and dynamic field tests (Lane 1 loading).

by 27%. As seen in Figures 3.18 and 3.19, the dynamic effects on the North RRFC are significantly more apparent with the large sinusoidal fluctuation of deflections and strains as the truck crosses the bridge. This is because the bridge's north side is less stiff than the south due to the tongue-and-groove timber planks positioned on the south side of the bridge. The increased flexibility of the north side of the bridge makes it more susceptible to dynamic amplification at the 10 mph truck speed.

A comparison of midspan field data collected from WCB1 and WCB2 during load testing is presented in Figures 3.20 - 3.22. The WCB1 and WCB2 bridges both have reinforced concrete longitudinal connections between adjacent railcars and are composed of three 89-ft RRFC superstructures; the length of the WCB2 railcars were "trimmed" to satisfy site specifications while the WCB1 utilized the entire railcars' lengths. The WCB2 bridge construction resulted in simply supported conditions while the WCB1 bridge was a three span continuous bridge. The difference in structural behavior of these two bridges was representative of these different support conditions, although the trends tended to be similar. The smaller deflections and strains measured in the WCB1 were expected due to the continuity of the bridge. Since the field truck weights varied little between the bridges (WCB1 = 51.1 k, WCB2 = 52.0 k), the increase in bridge length and support conditions were the controlling factors in the deflection and strain values. During Lane 1 loading, the deflection from WCB1 field test was, on average, 71% of that measured in the WCB2 test, while the strains measured in WCB1 were approximately 64% of WCB2 strains.

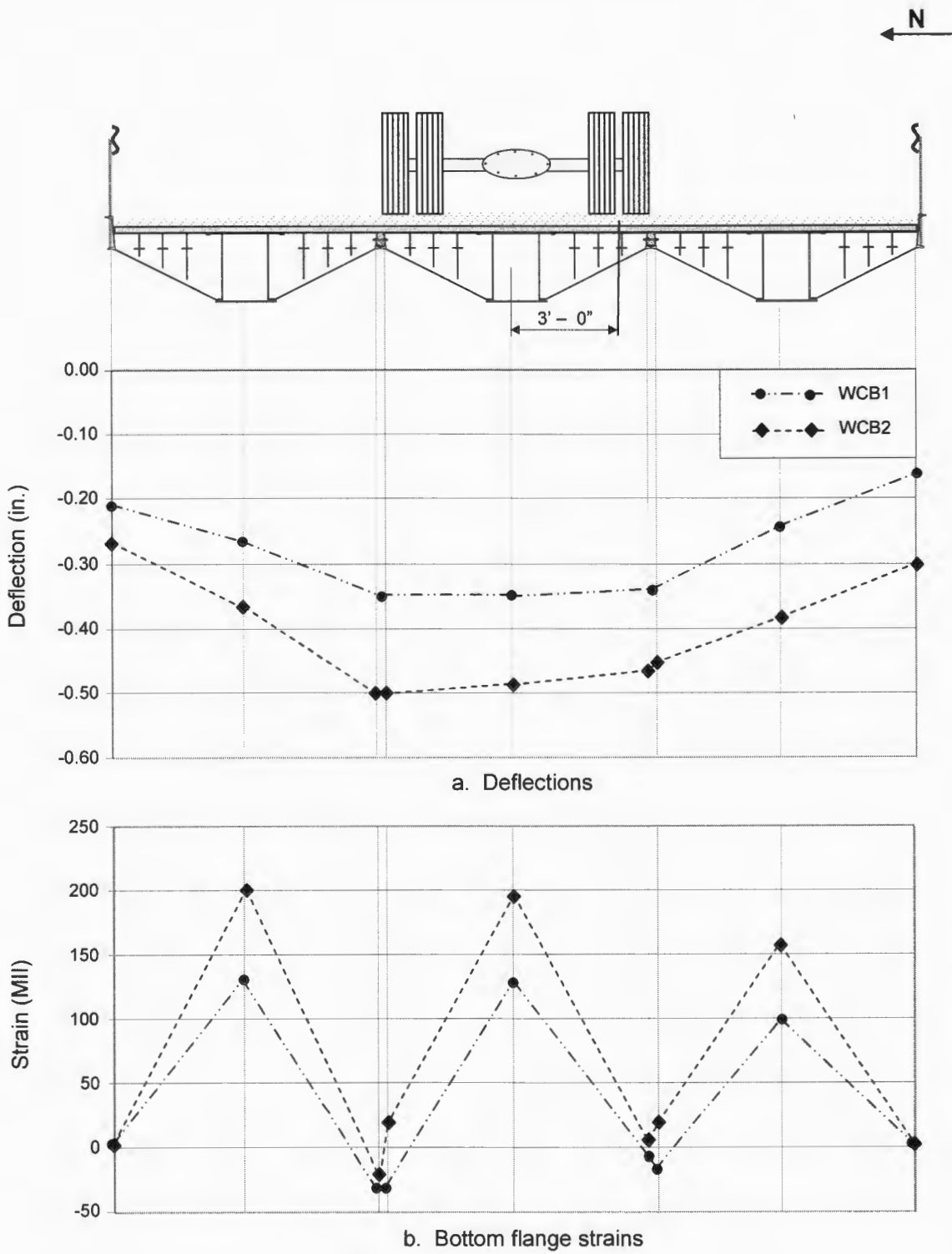


Figure 3.20. Comparison of field data from WCB1 and WCB2 (Lane 1).

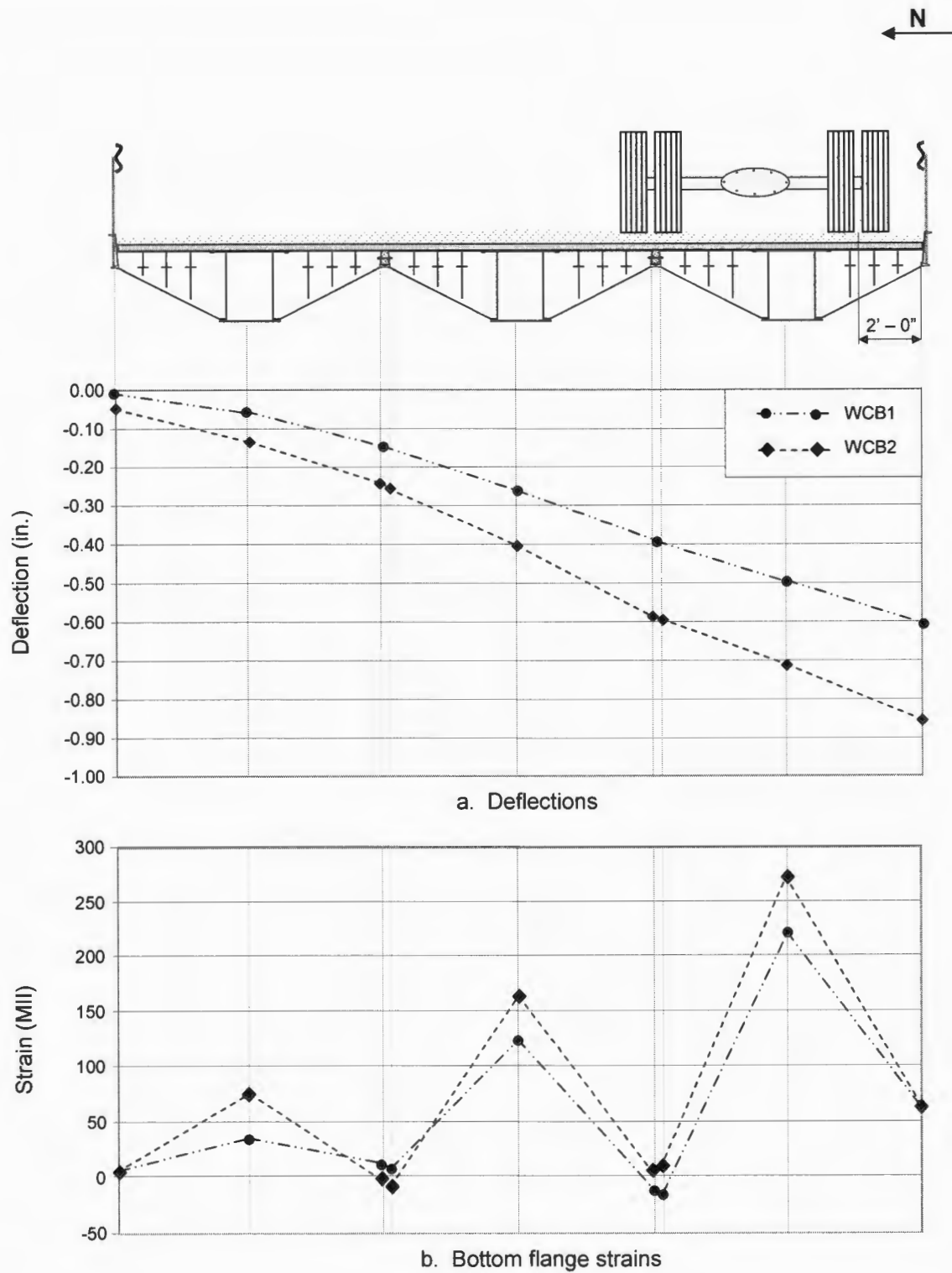
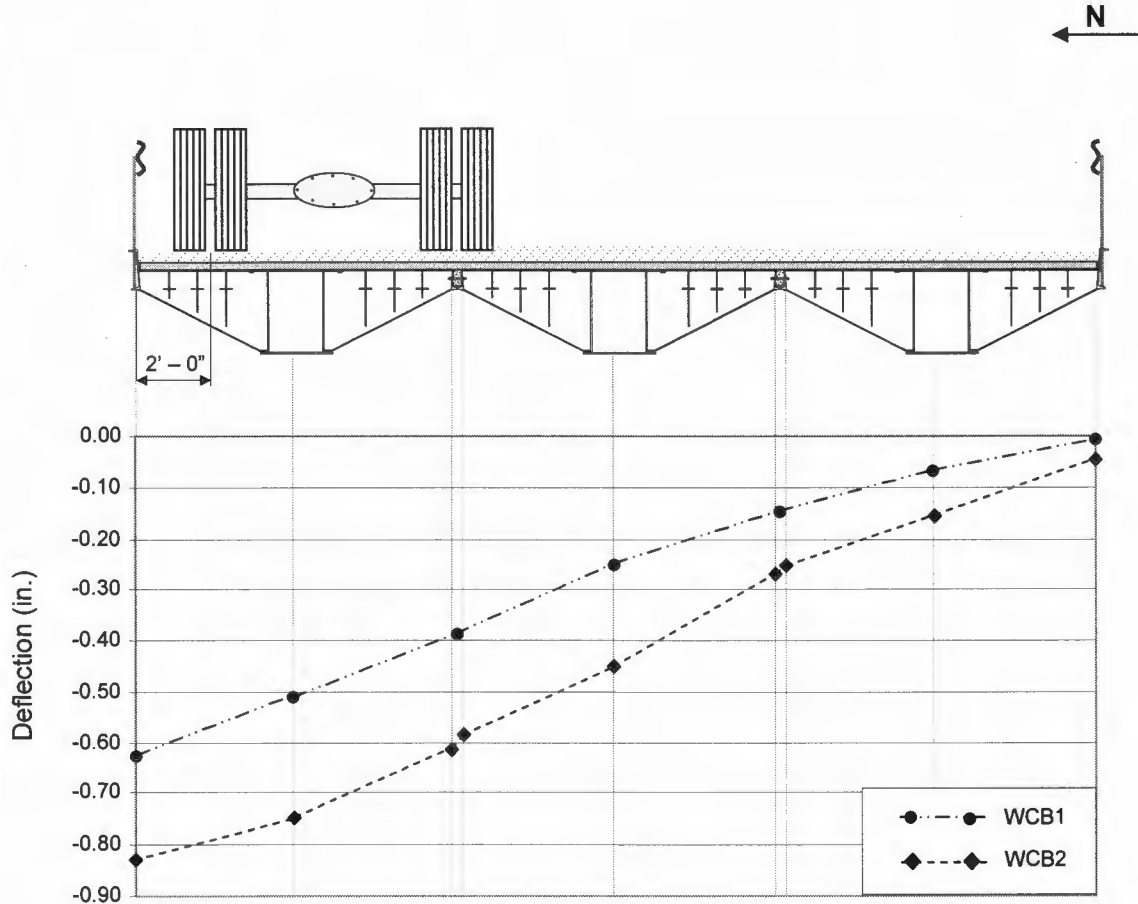
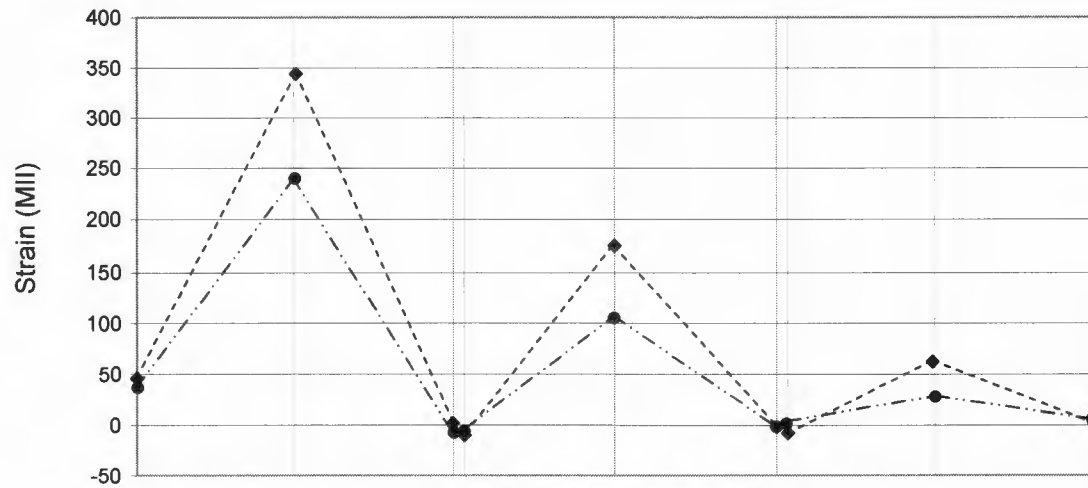


Figure 3.21. Comparison of field data from WCB1 and WCB2 (Lane 2).



a. Deflections



b. Bottom flange strains

Figure 3.22. Comparison of field data from WCB1 and WCB2 (Lane 3).

4. SUMMARY AND CONCLUSIONS

4.1 Summary

The focus of this thesis was to investigate the structural behavior of bridges constructed with RRFC superstructures. Specific objectives included investigating construction variables; testing RRFC bridges to determine live load strains (stresses) and deflections; and using field testing data to revise the design methodology developed in previous research. These objectives were accomplished by field testing two bridges - one in Buchanan County and one in Winnebago County, Iowa - and examining the data obtained from those tests.

Both the BCB3 and the WCB2 were constructed using three 89-ft RRFCs (the railcars were “trimmed” to meet the span requirements of each bridge); however, the construction details in each bridge were significantly different which greatly influenced their structural behavior. The BCB3 was 26 ft – 5 1/2 in. wide with a single span of 66 ft – 2 in. The constructed concrete abutment was 3 ft tall, 4 ft wide, and 30 ft long. Five HP 10x42 piles were extended 24 in. into the concrete cap and surrounded with spiral reinforcement within the cap. Supports at both concrete abutments were rollers and restricted only vertical movement. A bolted longitudinal connection (1 1/4 in. diameter bolts spaced on 3 ft centers) was used to join adjacent RRFCs and a gravel driving surface was added. On the other hand, the WCB2 was 27 ft – 0 in. wide with a main span length of 66 ft – 4 in. and 2 ft – 1 3/4 in. overhangs at each abutment. End abutments consisted of 6 steel HP12x53 piles and HP12x53 steel caps with sheetpile backwalls at the end of the overhangs for soil retainment. Supports at the east abutment were welded (restraining translations and rotations), while those at the west abutment restrained only vertical movement (rollers). Timber planks (3x12 planks on the north side and 4x12 tongue-and-groove planks on the south side) were added for additional transverse live load distribution. Adjacent RRFCs were joined by a

longitudinal reinforced concrete connection with threaded rods spaced on 2 ft centers. To complete the bridge construction, a gravel driving surface was installed.

The bridges tested were instrumented with deflection and strain transducers and the data collected were used to analyze the bridges' behaviors. The BCB3 was instrumented with 12 deflection and 24 strain transducers. At the bridge's midspan, deflection and strain instrumentation was placed on all interior box girders and exterior members of the three RRFCs. The interior box girder of the South RRFC was instrumented with strain transducers near each abutment, at the midspan, and also at the 1/4 and 3/4 span locations. At the 3/4 span location, deflection instruments were placed on all three interior box girders and a strain transducer was placed on the outer side of the south guardrail's top channel. Lastly, secondary longitudinal members and a transverse member near the midspan were instrumented with strain transducers. The RRFC girders of the WCB2 were instrumented with 20 strain and 9 deflection transducers. Similar to instrumentation on the BCB3, deflection and strain transducers were placed along the midspan cross-section at all the interior and exterior girders of the three flatcars. Additional strain data were collected on the interior girder of the South RRFC near the abutments and at the 1/4 and 3/4 spans. Two secondary longitudinal members, a transverse member, and the south guardrail all near the bridge midspan were also instrumented with strain transducers.

Gross truck weights of 48.2 kips and 52.0 kips were used in the testing of the BCB3 and WCB2, respectively. An HS-20 design truck, without impact, has a gross weight of 72 kips, which is approximately 49% larger than the BCB3 loading and 38% larger than the WCB2 loading. A maximum deflection of -0.88 in. occurred in the BCB3 field test, which is below the AASHTO recommendation of $L/800$ (-0.99 in. for a span length of 66 ft – 2 in.) for legal load (HS20 gross truck weight = 72.0 kip). The WCB2 had a maximum measured deflection of -0.92 in., which was also below that of AASHTO recommendations (-1.00 in

with a clear span length of 66 ft – 4 in.) If the deflections of both the BCB3 and WCB2 were increased in proportion to the test truck weights and the HS-20 design truck, the maximum deflections would be -1.31 in. and -1.27 in., respectively. These deflections are both larger than the AASHTO recommendations for both bridges, which could result in serviceability issues. The interior girders of the BCB3 during field testing had a calculated maximum total stress of +21.7 ksi, while a maximum total stress of +6.3 ksi was computed for the exterior girders. Calculated maximum total stresses for the interior and exterior girders that occurred during WCB2 field testing were +21.8 ksi and +7.1 ksi, respectively. Assuming a 40 ksi yield stress capacity, these maximum stresses fall below allowable limits of 55% of yield (22 ksi for yield stress of 40 ksi). However, if considering an HS-20 design truck loading condition, the estimated maximum total stresses for the BCB3 (+25.2 ksi) and WCB2 (+24 ksi) are above the allowable limit by 15% and 9%, respectively.

Dynamic load testing of the BCB3 and WCB2 was performed to determine the dynamic properties of the bridges, along with the dynamic amplification of their deflections and strains. The period of the BCB3 was found to be 1.3 seconds, resulting in an interior girder frequency of 0.77 Hz, and the damping of the interior girders was approximately 4%. Maximum dynamic amplification occurred at a truck speed of 25 mph on the BCB3; the maximum strain amplification was 17% and occurred in the South RRFC. Based on the free vibration of the interior girders, the dynamic properties of the WCB2 were determined. The period was found to be 1.4 seconds, resulting in a member frequency of 0.70 Hz, and the damping of the interior girders was approximately 1.5%. A truck speed of 10 mph produced the maximum dynamic amplification in the WCB2. The largest strain amplification (27%) occurred in the North RRFC interior box girder.

Using field test data, live load distribution was determined for both bridges. The additional timber planks and reinforced concrete connection in the WCB2 increased the

distribution of live load forces transversely across the bridge, thus lowering the moment distribution factor. The BCB3 distribution factor was 60% while the WCB2 has a 55% distribution factor.

4.2 Conclusions

Through the investigations involved with this thesis, the following conclusions were drawn for the use of “trimmed” 89-ft RRFCs in LVR bridge superstructures:

- The longitudinal reinforced concrete beams connecting adjacent RRFCs, along with transverse timber planks on the bridge deck effectively transfer the live load forces transversely across the bridge.
- Tongue-and-groove timber planks on the bridge deck reduce deflections and strains by increasing the distribution of live load forces to other RRFC members.
- The use of bolted longitudinal connections between RRFCs must be properly designed for minimal spacing between bolts and large transverse members due to the susceptibility of out-of-plane bending that may occur between bolts at these locations.
- RRFC bridges, with little or no overhangs at the abutments, should be restricted to clear span lengths of less than 66 ft. Increasing the clear span lengths would obviously increase the total maximum stresses beyond the allowable yield stress of the steel.
- The RRFC interior girder resists the majority of both the live and dead loads due to its large size in comparison to that of the other members. Thus, the increased importance that this member be free of any defects prior to bridge construction.
- The maximum strains (stresses) and deflections measured in both the BCB3 and WCB2 bridges during testing were below the allowable stresses and AASHTO deflection recommendations. However, the estimated strains (stresses) and deflections for an HS-20 truck loading were above these required values. It is recommended to reduce the span lengths so that girder strains (stresses) and deflections fall below the allowable stresses and AASHTO deflection recommended values, respectively.
- RRFC bridges are an economical solution to bridge replacement if the longitudinal connections and bridge span length are correctly engineered. Timber planking should also be considered for additional load distribution for wider bridges composed of three railcars.

APPENDIX A

SHEET PILE ABUTMENTS

In this appendix the feasibility and design of sheet pile abutments for RRFC bridges on LVRs are presented. A brief overview of the advantages of constructing sheet pile abutments and selected case studies of their use in both Europe and the United States will be outlined. Design considerations and recommendations obtained from previous research are also included. Last, a sample design of a sheet pile wall abutment using the WCB3 site conditions and an 89 ft, three-span RRFC bridge will be discussed.

A.1 Background

Main objectives of this project were to investigate possible design and/or construction variables along with improving performance, constructability, and cost for the RRFC bridge concept. One way to accomplish these objectives is to create an alternative, cost effective, abutment design that provides adequate bearing capacity and is easy to construct.

In previous RRFC bridge construction, steel sheet piles have been driven behind abutments only if required for soil retainment; they have not been utilized for bearing purposes. These structures, however, also possess the ability to support vertical load. Therefore, it is possible to eliminate the conventional pile abutments and utilize the bearing capacity and flexural rigidity of a steel sheet pile wall to serve as both the bridge abutment and as an earth retaining structure. It has been documented that using steel sheet piling for both bearing and earth retention has been used in Europe for years and its use in the United States is increasing.

A.1.1 Sheet Pile Abutment Feasibility

Using steel sheet piles for bridge abutments have numerous advantages over conventional methods. Sheet piles can resist both bridge bearing loads and lateral earth forces, thus eliminating the need for foundation piles. Construction may be completed sooner because the amount of earthwork is reduced, fewer materials are needed to

construct the abutment, and formwork is not required since the piles are driven. Scour, a significant issue with bridges, may be prevented with driven steel sheet piles. Through the combination of these attributes, other advantages of sheet pile abutments include substantial cost savings, less traffic disruption due to quicker construction, simplified construction, and reduced environmental impact [7].

A.1.2 Case Studies of Sheet Pile Abutments

The use of sheet pile walls for bridge abutments has been practiced in Western Europe extensively for decades in both rural and urban areas; in the past 35 years, some of these structures have been used in highway bridges over railroads, highways, and waterways. Sheet pile abutments have been built in the United States, but have been limited to mostly low volume road (LVR) bridges in rural areas. In the following case studies, various designs and wide applications of steel sheet pile abutments for bridges [7].

A.1.2.1 Highway Bridge over a Branch of the Moselle - Europe

In this application, a sheet pile abutment with a concrete cap and bridge seat supports the bridge superstructure. The steel sheet pile wall abutment penetrates through various soil stratum including backfill, gravel, and sand, while the sheet pile is embedded in stiff marl (a mixture of crumbly clays, shells, and calcium and magnesium carbonates). Tie rods are spaced 6 ft – 7 in. on centers along the length of the wall for additional support [7].

A.1.2.2 Highway Bridge over a Railroad - Europe

Due to the high elevation of bedrock, the required depth of penetration was greatly reduced. A concrete footing within the bedrock was constructed. The toe of each sheet pile was embedded into a steel channel placed in the footing which transferred the vertical loads into the reinforced concrete. The sheet pile abutments were capped with an integral reinforced concrete beam and tied back using a 2 1/2 in. diameter tie rod 46 ft long [7].

Railway transportation is widely used in European countries; hence, the swiftness of installing sheet pile abutments is a significant advantage because of train frequency.

Installation of the sheet piles for this highway bridge over a railroad was performed between the passing of trains and eliminated the disruption of train schedules [7].

A.1.2.3 Highway Bridge over a Port Facility - Europe

Large bearing forces from the 233 ft long truss bridge were resisted by a set of steel sheet pile walls. The first row of sheet piles were continuous, while the second row of sheet piles were intermittently spaced 13 ft – 9 3/5 in. apart and were utilized for added bearing resistance. A 66 ft driven and grouted batter pile was tied to the top of the sheet pile abutment and was extended into layers of sand and medium firm marl for supplementary support [7].

A.1.2.4 Taghkanic Creek Bridge, Columbia County, New York – United States

Steel sheet piling abutments were used for the 42 ft single span highway bridge. The sheet piling was driven into granular soils to an embedment depth required for adequate bearing strength (16 ft). The sheet piles were capped with a reinforced concrete beam bearing on a steel plate. Wing walls were constructed using cantilevered steel sheet piles driven to the same depth as the abutments, and were capped with steel channels [7].

A.1.2.5 Banks Road Bridge, Tompkins County, New York – United States

The 65 ft single span bridge was supported on steel sheet abutments embedded to a required depth of 45 ft at the east abutment and 22 ft at the west abutment. A total of 16 sheet pile sections were used for the abutment, but only 10 were needed to support the vertical bridge loads. The remaining six sheets were driven to a more shallow depth required for soil retainment. A steel channel overlain by a steel beam was used to cap the sheet pile abutment piles. Tie backs were used to stabilize both the steel sheet pile abutments and wing walls [7].

A.1.2.6 Sprout Brook Bridge, Paramus, New Jersey – United States

In 2000, A.G. Lichtenstein & Associates constructed the Sprout Brook Bridge (48 ft span length; 13 traffic lanes for a width of 209 ft) using permanent sheet piling abutments in an effort to reduce construction cost and time. The sheet pile abutment construction reduced the project cost by over \$200,000 and resulted in a completion date 10 weeks earlier than originally anticipated. Original construction plans included cast-in-place concrete abutments and wingwalls on piled footings which would have required temporary cofferdams along with significant excavation and dewatering for the driving of piles and footing construction. Permanent sheet piles were installed instead to support both the vertical bridge loads and the horizontal earth pressures. Installing steel sheet pile abutments eliminated the need for excavation of the existing channel, which lessened the economic impact and reduced traffic rerouting from six lane changes to only two. Steel sheet piles were driven to refusal into sandstone bedrock and stabilized with a tie back near the top attached to a deadman system. The sheet piling was imbedded 1ft – 0 in. into a cast-in-place reinforced concrete cap which was designed to transfer the 15 kip/ft of axial load from the bridge to the abutment. Design moments of 45 kip-ft/ft from earth pressures and an additional 150 kip-ft/ft for seismic activity were also considered [8,9].

A.1.3 Analysis and Design

When analyzing and/or designing a sheet pile wall abutment, both the lateral earth pressures and the bearing capacity of the abutment must be considered. Designing for lateral earth forces on sheet pile walls has been widely documented since sheet piles are commonly used for soil retainment. However, calculating the pile resistance of the steel sheets is more difficult to determine and, consequently, the use of sheet piles for bearing is less common.

To proceed with design calculations for the steel sheet pile wall, an accurate subsurface investigation must first be conducted. Soil borings near each abutment are required since soil conditions may vary across the channel. Data obtained should include the water table depth, along with soil classifications, water content, blow count, and unit weight throughout the boring depth. In poor soil conditions, adequate bearing strength may not be achieved in shallow depths; therefore, borings should extend sufficiently deep to ensure a complete soil profile for the entire depth of the sheet pile.

Lateral earth pressures on the sheet pile walls are dependent upon soil conditions, location of the water table, embedment depth, and if cantilever or anchored sheet piles are used. Guidelines for the design of steel sheet piles for use as retaining walls are documented in the United States Steel (USS) Steel Sheet Piling Design Manual [10]. Cantilevered sheet piles are designed by creating a zero net lateral pressure on the wall, thus resulting in stability of the sheet pile wall. Figure A.1 illustrates the design lateral forces exerted on a cantilevered sheet pile assuming granular backfill and penetration into clay. As described in the Design Manual previously noted, cantilevered sheet piles may be designed according either by a conventional method (Figure A.1a) or by the simplified method (Figure A.1b). The Fixed Earth and Free Earth Support Methods are the basic methods of sheet pile design, with the Free Earth Support Method being the most commonly used due to its simplicity. The Fixed Earth Support Method assumes a hinge (zero bending moment) at the point of contraflexure, and the portions above and below this point are treated as separate freely supported beams. The Free Earth Support Method assumes that there is no pivot point below the dredge line. A sketch of the design lateral forces acting on an anchored sheet pile in cohesive soil backfilled with granular soil using the Free Earth Support Method is shown in Figure A.2 [10].

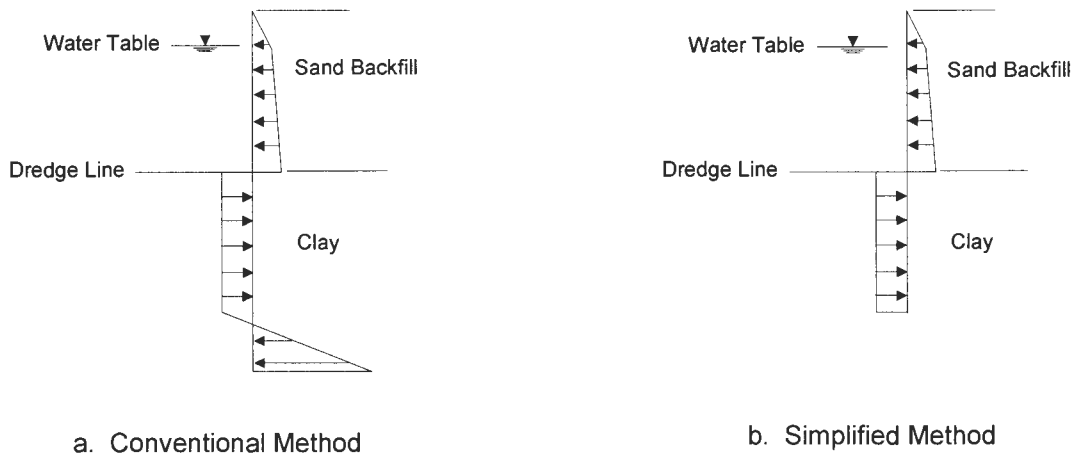


Figure A.1. Design lateral forces for a cantilevered sheet pile [10].

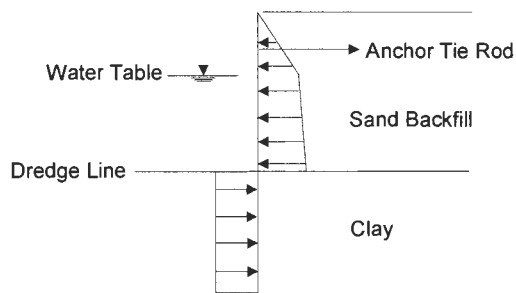


Figure A.2. Design lateral forces for an anchored sheet pile using free-earth method [10].

Pile bearing capacity is composed of both the point resistance and the skin frictional resistance of the pile (See Figure A.3). The point resistance is a function of the cross sectional area of the pile, while the skin friction is proportional to the perimeter of the pile throughout the embedment depth. The behavior of steel sheet piles may be compared to that of a steel H-pile whereas the cross section is not a boxed or circular section, but instead is an open cross section. A plug situation may be created in the void areas of the cross section when penetrated into cohesive soil conditions; however, a complete plug situation is

unlikely to occur. Therefore, it is difficult to determine the effective area and perimeter of the cross section that is effective for when calculating the point and frictional resistance of a sheet pile.

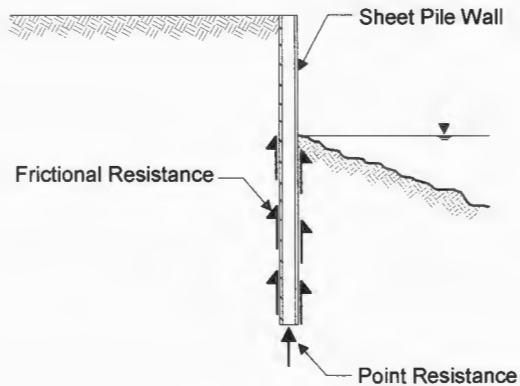


Figure A.3. Point and frictional resistance.

A.1.3.1 Point Resistance

The sheet pile cross sectional area bearing the lateral forces has been defined in numerous ways. Bustamante and Gianceselli [11] describe the bearing cross sectional area as the entire inside area bounded by the flanges of the profiles as shown in Figure A.4. However, McShane [12] considers the instance in which complete plug conditions may not exist; hence, in cohesive soils it is suggested 50% of the gross area (steel sheet pile cross sectional area + soil plug area) be considered.

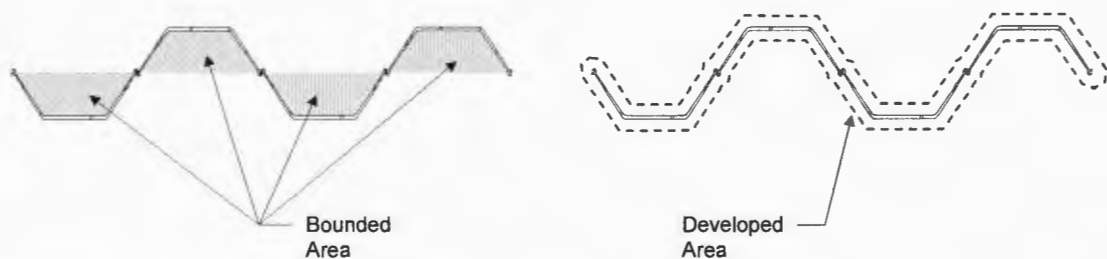


Figure A.4. Bounded and developed areas.

A.1.3.2 Frictional Resistance

As with point resistance, there are various methods for calculating the sheet pile area used in determining the frictional resistance. Bustamante and Gianceselli [11] define the area as the developed area of the wall (i.e. perimeter) (See Figure A.4); whereas, McShane [12] recommends using a surface of up to 80% of the perimeter when plug formation is not considered.

A.2 Sheet Pile Abutment Design

The WCB3 site was selected for the theoretical design of sheet pile abutments. Three, 89-ft RRFCs were used for a 3-span bridge (See Figure A.5): the middle span was 66 ft and each end span was 11 ft – 6 in. from bolster to the end of the RRFC. Sheet pile wall abutments were designed based on soil borings taken at the East and West abutment locations. The sheet pile abutments were designed for soil retainment and to transfer bridge bearing forces to the underlying soil.

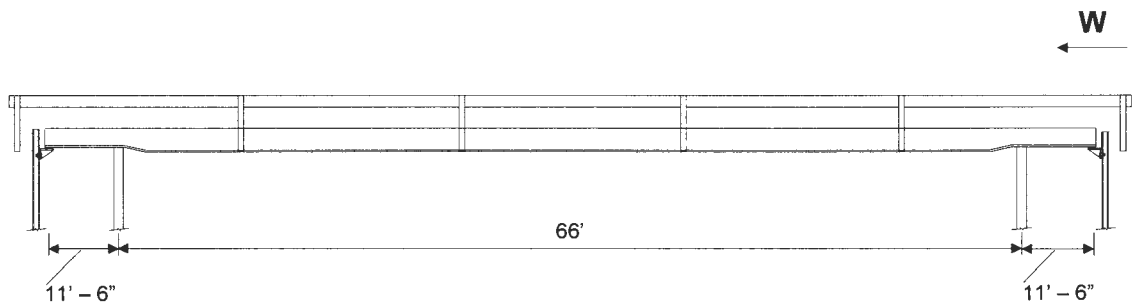


Figure A.5. Theoretical WCB dimensions.

A.2.1 Soil Properties

Borings near each existing abutment determined that fill material extended to about 5 ft below the existing road grade. Alluvial deposits extending to approximately 19 ft below existing road grade at the east abutment consisted of sandy lean clay and fine sand with silt. The alluvial deposits at the west abutment consisted mostly of a thin lean clay layer underlain by a peat layer extending from 7 ft to 19 ft – 6 in. below existing road grade, followed by silty or fine sands to a depth of 44 ft – 6 in. below existing grade. Below the alluvial deposits at both abutments were supraglacial sediments and subglacial tills consisting of stiff or very stiff sandy lean clays to a depth of about 65 ft – 6 in. below existing road grade. Supraglacial deposits typically consist of nearly equal parts of sand, silt, and clay with traces of larger particle sizes such as gravel, cobbles, or boulders. Subglacial tills have been preconsolidated by glacial activity; hence, they typically have a high density and shear strength [13]. Hence, both supraglacial and subglacial soils would provide strong bearing if embedment depths were required to extend into these layers.

Unit weights, undrained shear strength, and soil friction angles of the various soil layers were not available from the boring test results; therefore, correlations between Standard Penetration Test (SPT) blow count numbers (N values) and these unknown properties were used. The USS Steel Sheet Piling Manual was referenced for its tables relating N values and unit weights of both cohesive and cohesionless soils [10]. A relationship established by Karl Terzaghi and Ralph Peck for estimating undrained shear strength of cohesive soils from SPT blow counts was used, and Peck's estimate of soil friction angle using SPT blow counts in cohesionless soils was also utilized [14].

A.2.2 Earth Pressures

The sheet pile wall was designed for lateral earth pressures, including a surcharge load specified in article 6.5.2.4 of the Iowa Department of Transportation Bridge Design

Manual [15], and an external moment resulting from eccentric loading of the RRFC onto the abutment (See Figure A.6). A required penetration depth was found and a 40% increase, as specified in the USS Sheet Piling Design Manual [10], was applied for a safety factor to obtain the design embedment depth. The calculated stresses in the retaining wall were then used to select a required steel sheet pile section.

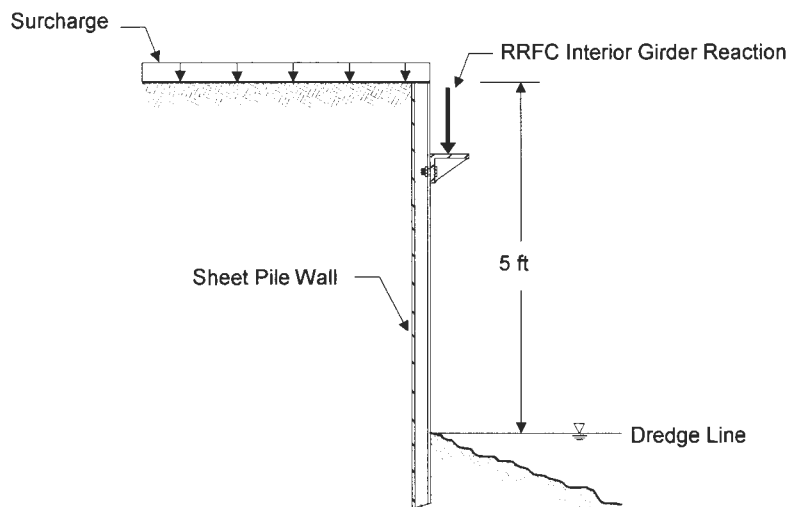


Figure A.6. Sketch of sheet pile analysis.

A.2.3 Pile Design

Pile designs for the steel sheet pile walls were performed considering both end bearing and skin frictional resistance since layered soils existed throughout both abutment profiles. The west abutment of the WCB was bearing in a sand layer, while the east abutment was in firm glacial clay. Skin friction for the sand layers in both profiles and bearing resistance of the sand layer at the driven distance for the west abutment were calculated using equations given in AASHTO 10.7.3.4.2 correlating these values to SPT

blow counts. The skin friction of the cohesive clay layers at both abutments and bearing resistance for the cohesive clay layer at the east abutment embedment depth were found using AASHTO 10.7.3.3 Semiempirical Estimates of Pile Resistance [5]. A factor of safety of 4.0 [16] was applied to all bearing and friction resistance values because of the soil property correlations that were utilized to obtain values used in the design.

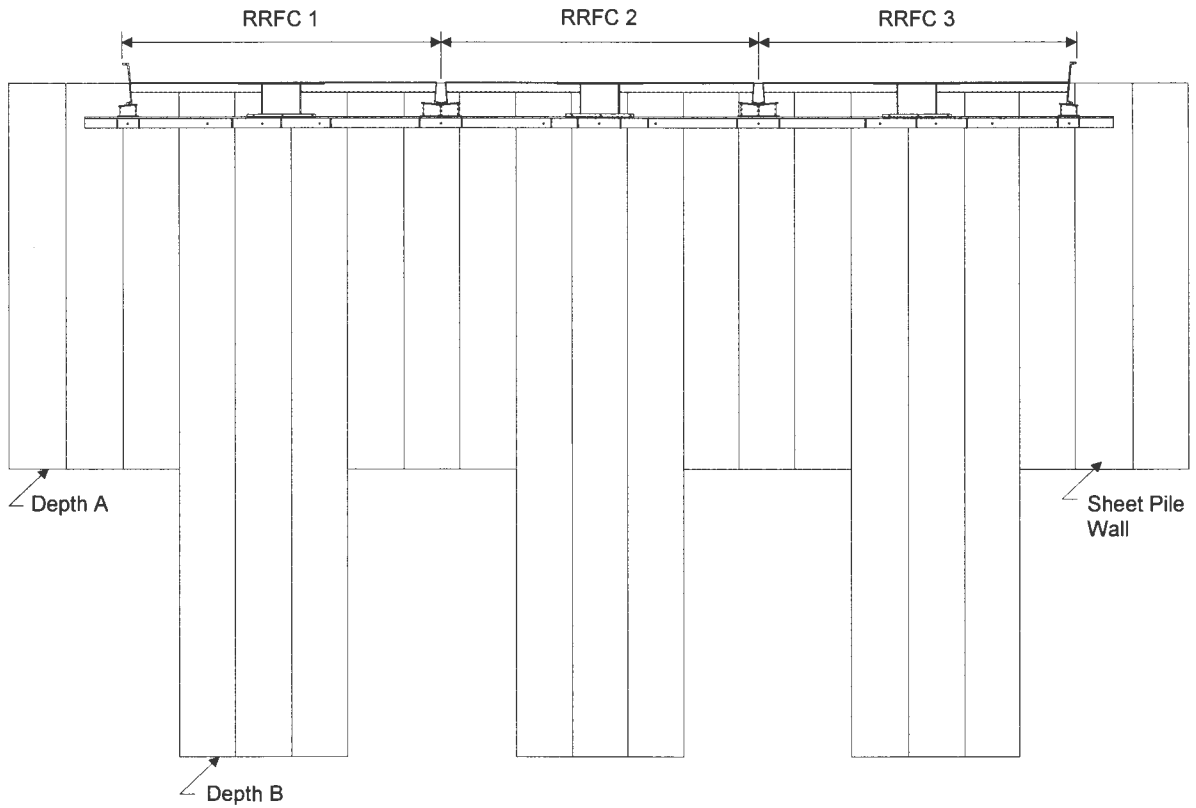
Material properties for 5-Gage metric sheeting from Contech Construction Products Inc. were used for design, including both bearing capacity and frictional resistance of the sheet piles. Because sheet piling does not have a solid cross section, like that of an H-pile, the amount of surface area in contact with the soil is unknown. Since a complete plug situation is unlikely to occur, the cross sectional area used for bearing capacity calculations was the cross sectional area of the steel sheets given in the Contech Construction Products Inc. Metric Sheeting brochure [17], and the surface area used for frictional resistance was twice the laying width, which was approximately 86% of the total surface area of each steel sheet.

The maximum required depth from the earth pressure analysis and pile design calculations was used for determining the embedment depth of each steel sheet pile section located under a bearing point. The bearing points at the sheet pile abutments were the location of the 3 interior girders, the 2 concrete beam locations, and the 2 exterior girder locations at the outer edges of the bridge. Three sheet pile sections were designed to carry the bearing under the most critical bearing locations: the interior girders. The reaction forces under the remaining locations were much less; therefore, only one sheet pile section was required for bearing at the exterior members and concrete beam bearing regions. Sheet piling must be continuous for soil retainment; hence, the sheets not required for bearing under the interior girders would be driven to a lesser depth. It is recommended that the sheet piling be extended below the peat layer at all locations in the west abutment

because of the soil's low strength. The west abutment, due to the substantial peat layer, would have a significantly deeper embedment than the east abutment to ensure a strong soil base for bearing. Design drawings of the steel sheet pile abutments for the theoretical 89 ft Winnebago County Bridge are presented in Figure A.7.

The upper surface of the sheet pile wall is not a suitable base for bearing; therefore, an attached angle support was designed to provide the required bearing. As stated in section A.1.2, previous use of sheet pile wall abutments has involved attaching an inverted channel shape on the top of the sheet pile wall to create an adequate bearing surface. However, for RRFC bridges, this approach may not be suitable since the open cross-section would not retain backfill material. This problem may be prevented by attaching a stiffened angle to the side of the wall along the length of the sheet pile to create the bearing surface (See Figure A.8). In this instance, the sheet pile wall would still retain the backfill material and would also resist the bearing forces.

Figures A.9 – A.16 show details of the support conditions for the interior and exterior girders at the piers and abutments. The height of the interior girders is larger than that of the exterior girder, so a built-up support was designed to allow the exterior girders to rest on the pier caps and abutments. Recycled H-pile sections used for the piers are also used as the built-up supports for the exterior girders at the piers. At the abutments, the H-pile built-up supports could not be used since the bearing angle does not have a sufficient bearing width; therefore, at the abutments, hollow tube sections (HSS 6x6x1/4) were designed to support the exterior girders.



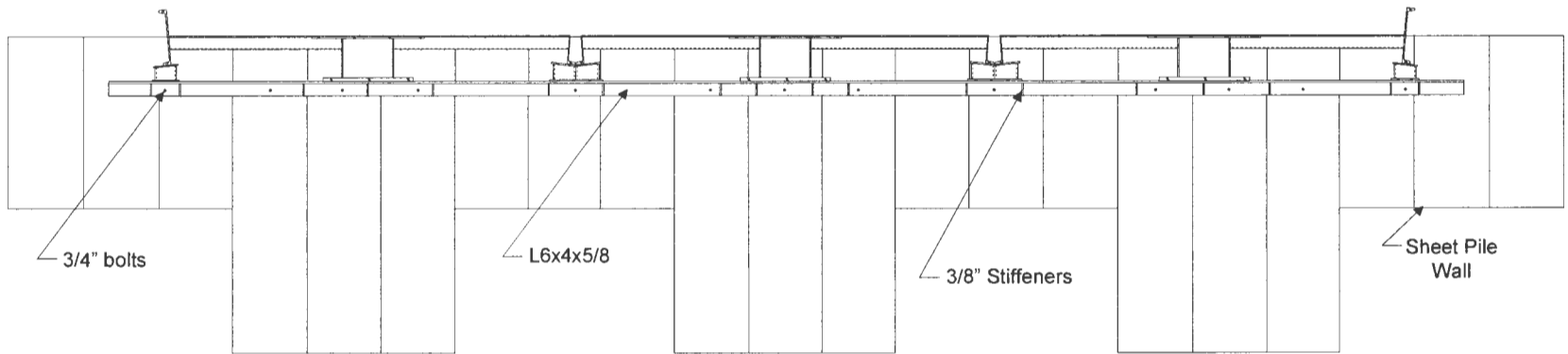
	Depth A	Depth B
East Abutment	11 ft	25 ft
West Abutment	20 ft	35 ft

Materials Summary:

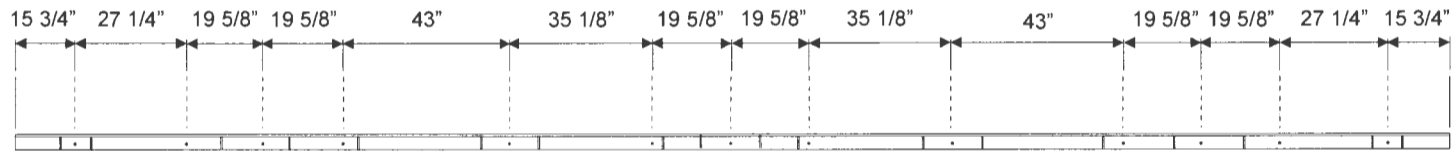
East Abutment
 9 pieces of Gage 5 steel sheets, 25 ft long
 12 pieces of Gage 5 steel sheets, 11 ft long

West Abutment
 9 pieces of Gage 5 steel sheets, 35 ft long
 12 pieces of Gage 5 steel sheets, 20 ft long

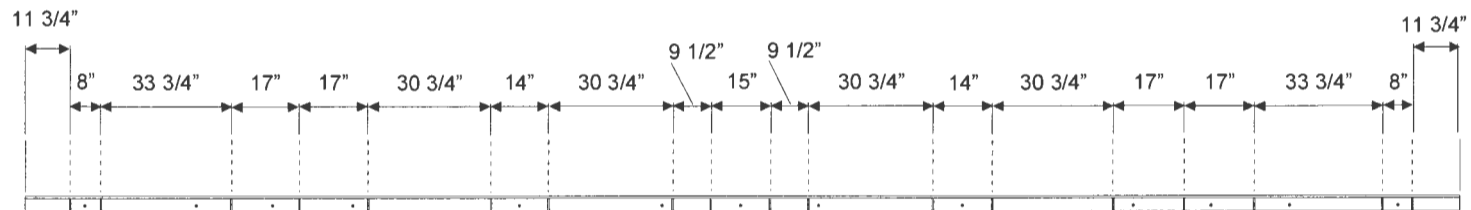
Figure A.7. Sheet pile abutment design for the theoretical WCB.



a. Cross sectional view of the RRFC stiffeners and bolt locations at the sheet pile abutments



b. Approximate spacing between centerline of bolt holes*



c. Approximate spacing between centerline of angle stiffeners*

*Dimensions may need to be adjusted for field conditions.

Figure A.8. Theoretical WCB sheet pile abutment bearing support design.

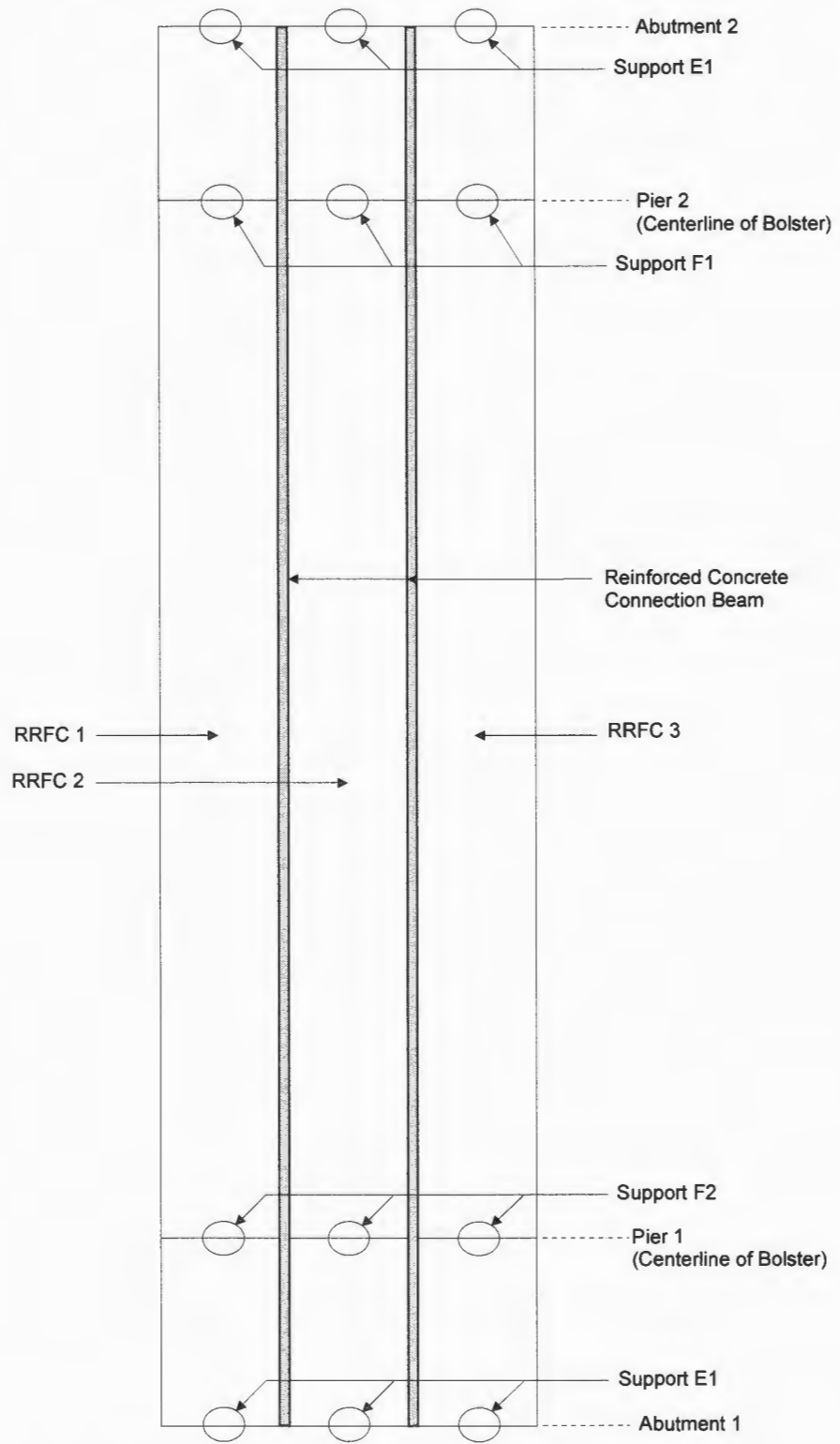


Figure A.9. Location of interior girder supports.

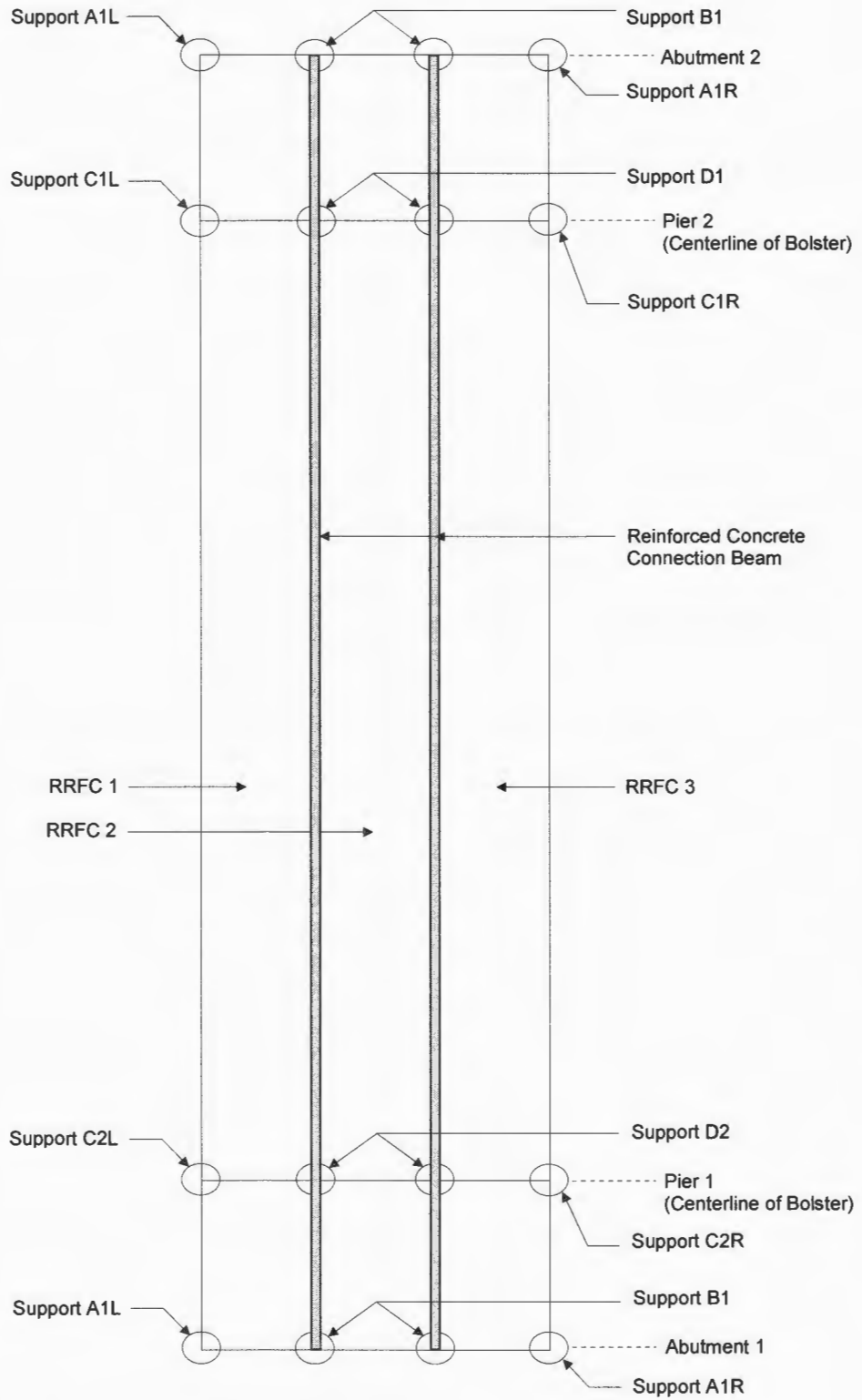
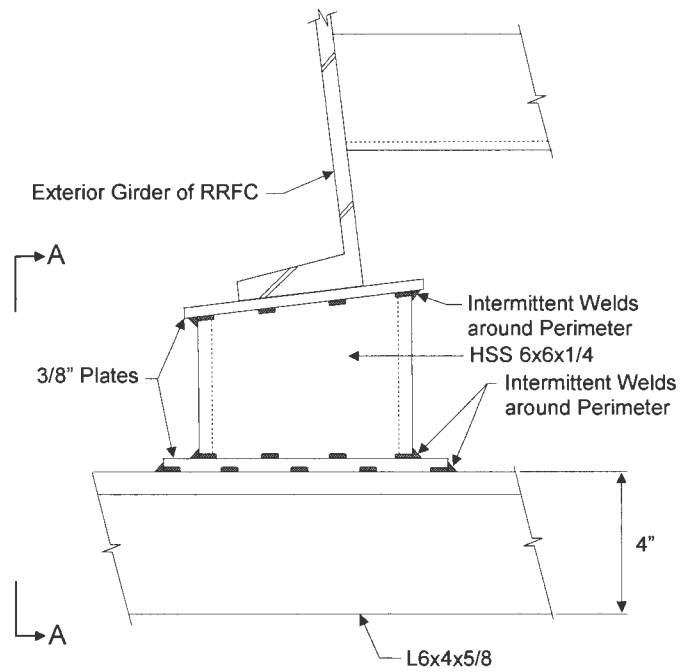
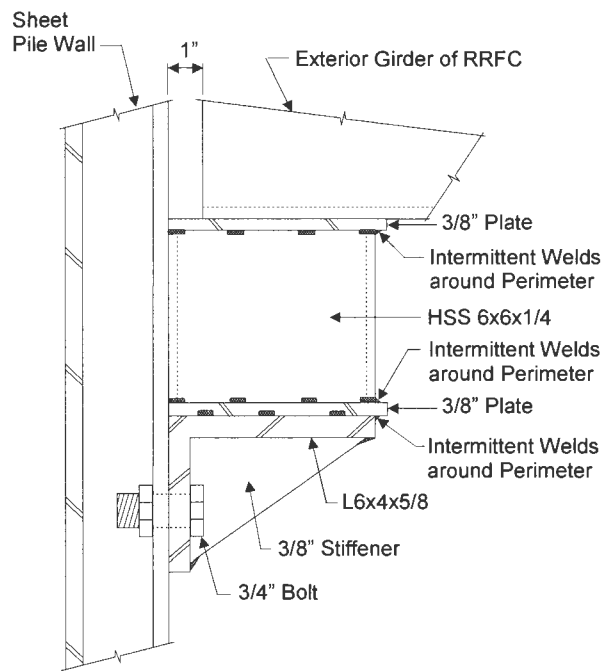


Figure A.10. Location of exterior girder supports.

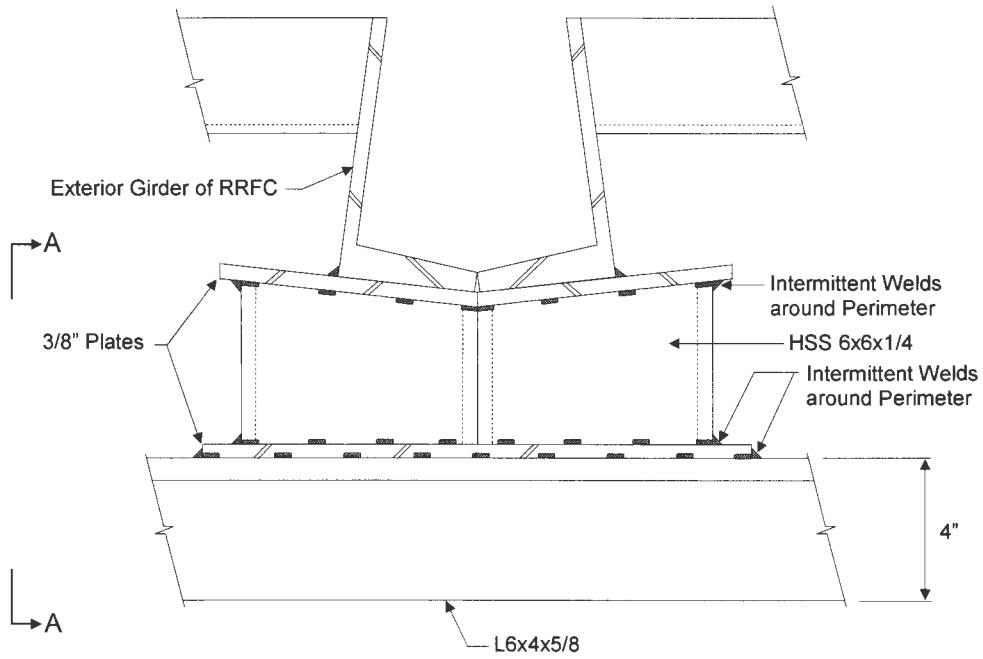


a. Support A1L

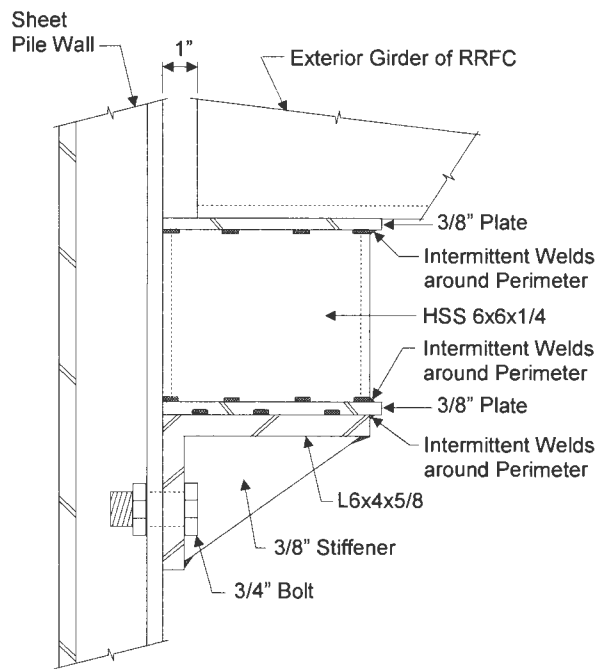


b. Section A-A

Figure A.11. Exterior girder support at the sheet pile wall abutment.

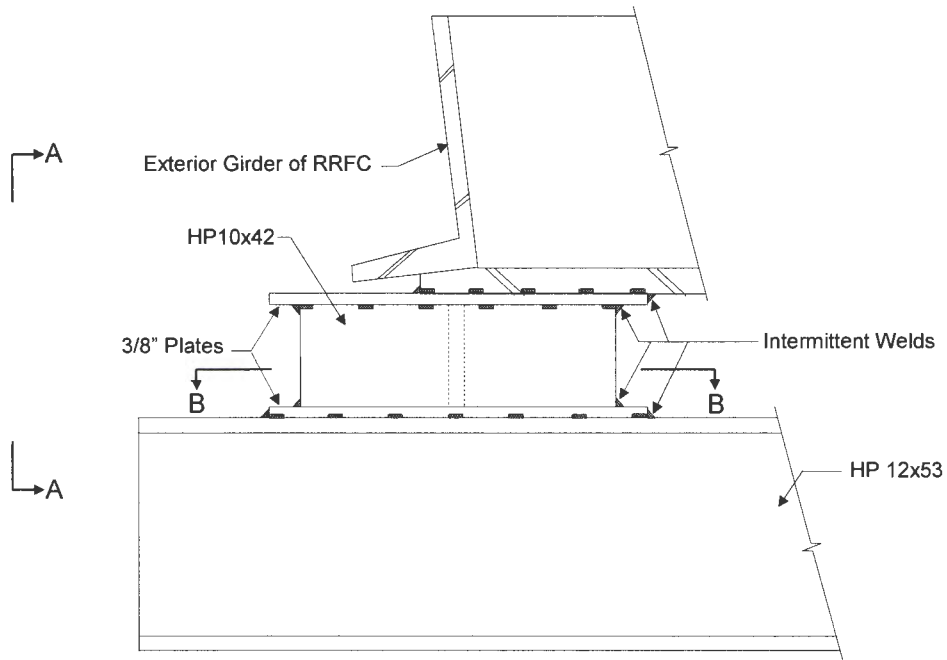


a. Support B1

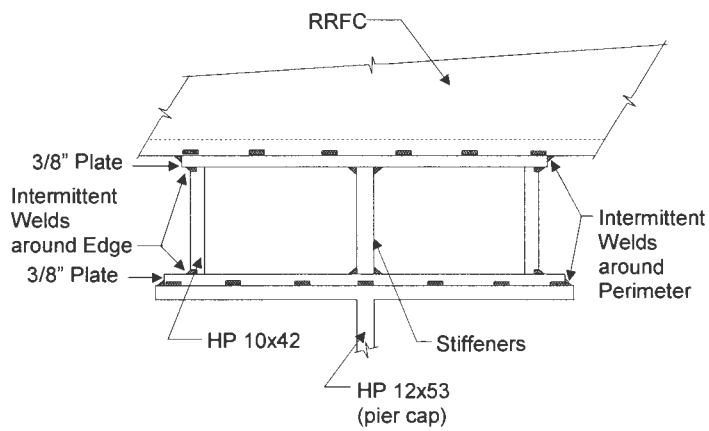


b. Section A-A

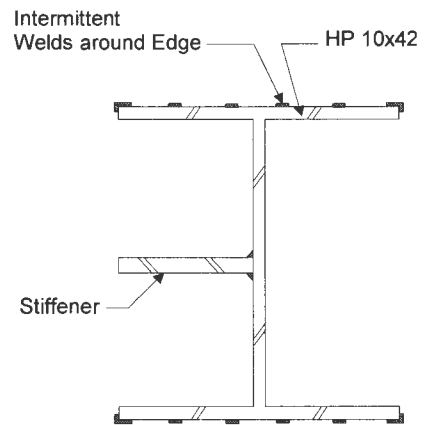
Figure A.12. Exterior girder support at reinforced concrete connection beam located at the sheet pile wall abutment.



a. Support C2L

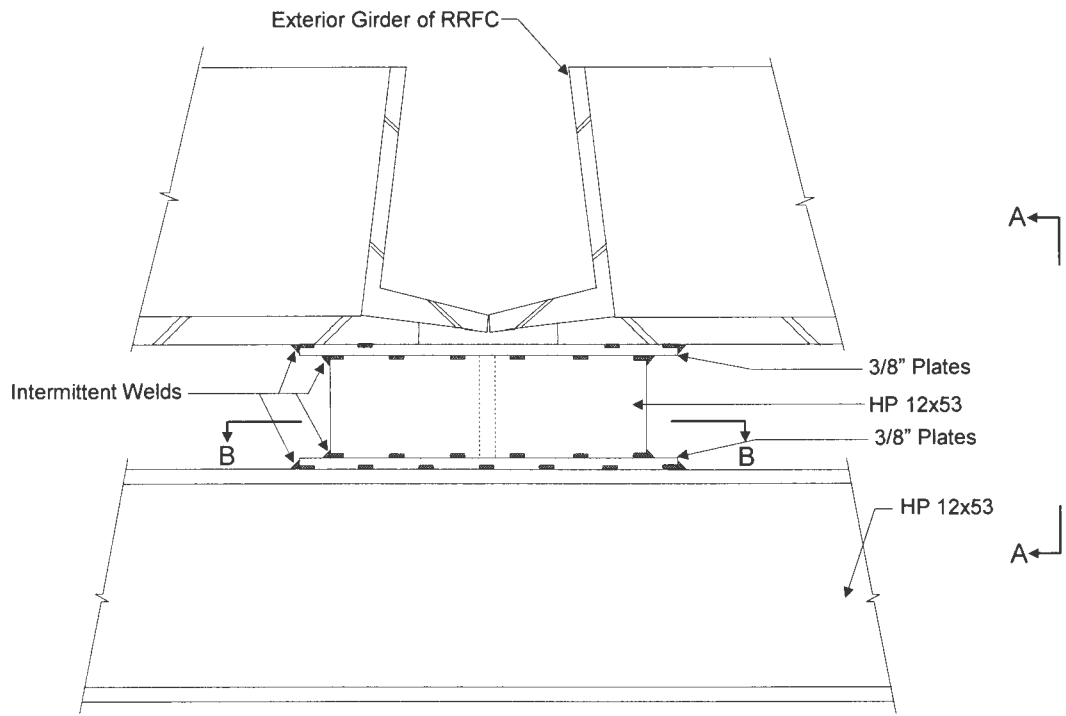


b. Section A-A

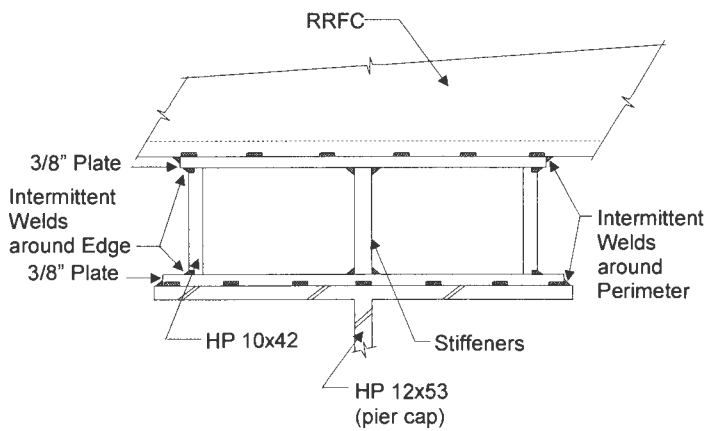


c. Section B-B

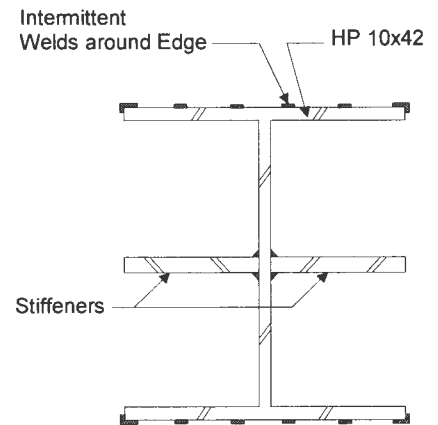
Figure A.13. Exterior girder support at the pier (bolster location).



a. Support D2

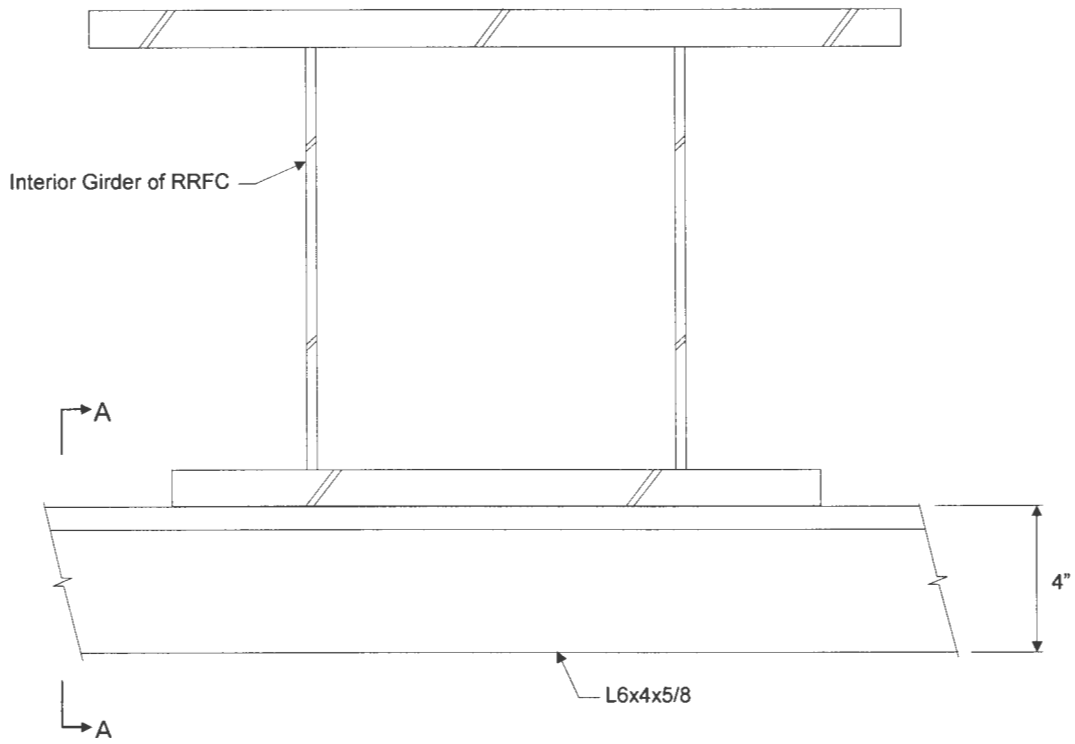


b. Section A-A

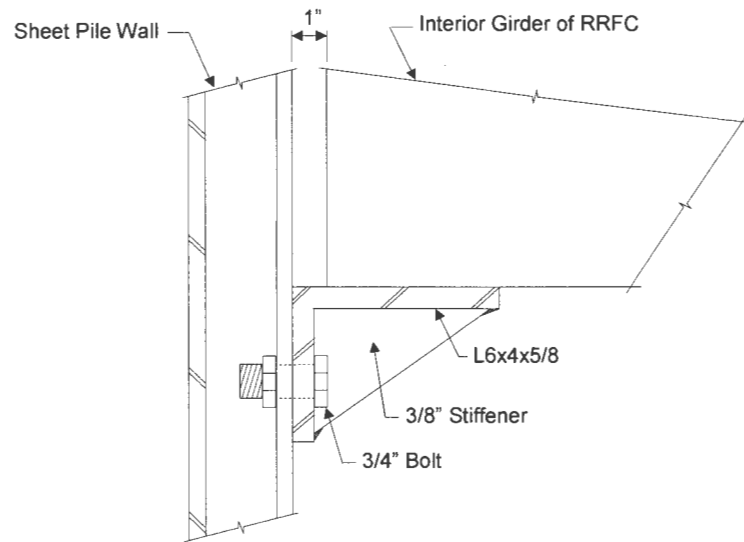


c. Section B-B

Figure A.14. Exterior girder support at the reinforced concrete connection beam located at the pier (bolster location).

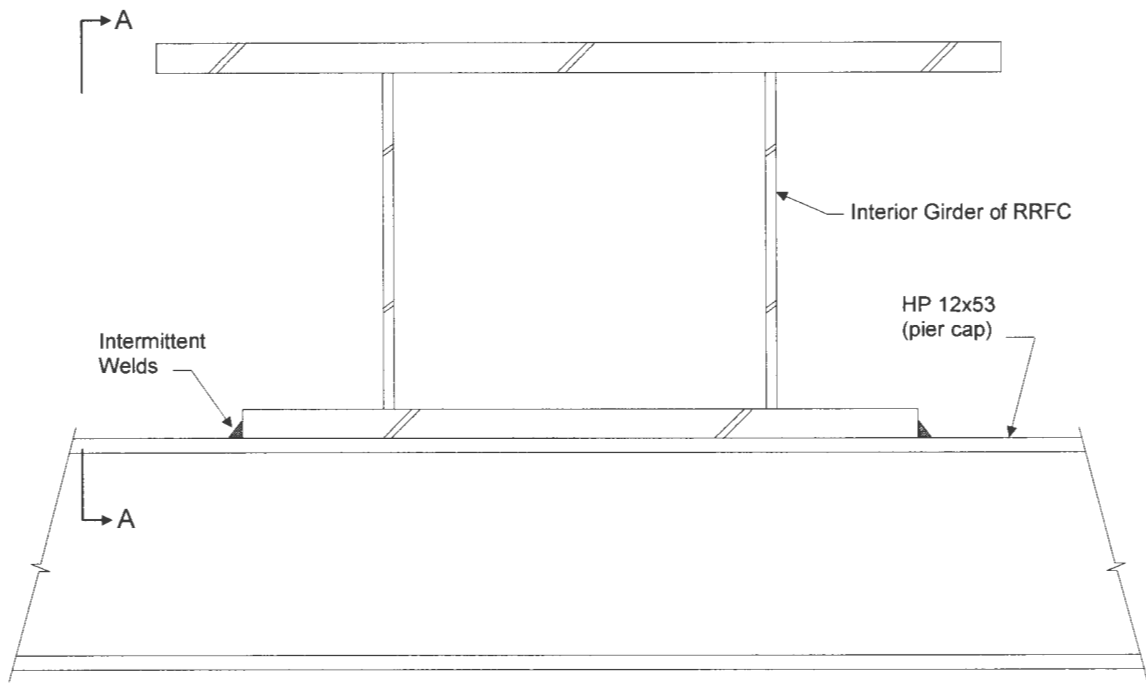


a. Support E

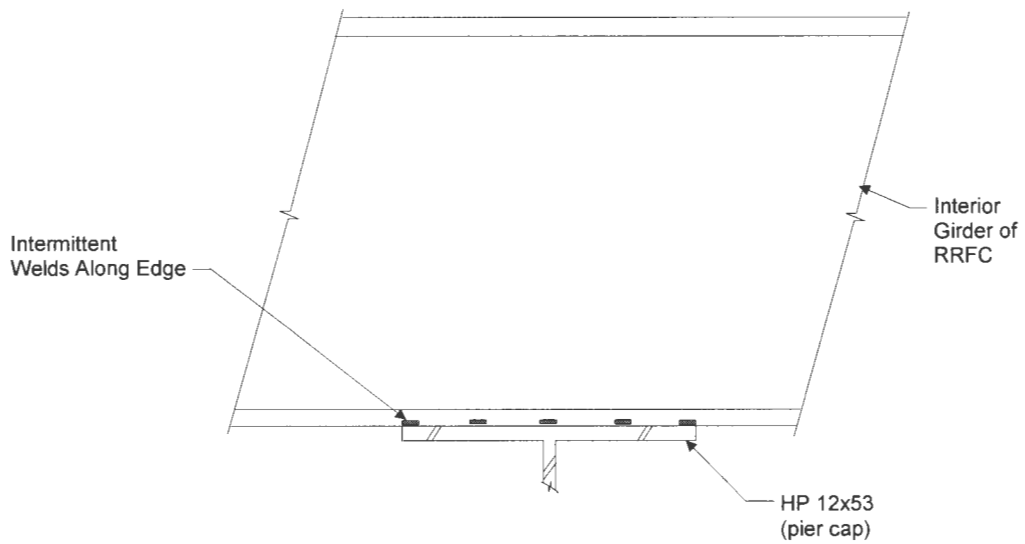


b. Section A-A

Figure A.15. Interior girder support at the sheet pile wall abutment.



a. Support F



b. Section A-A

Figure A.16. Interior girder support at the pier (bolster location).

APPENDIX B

“SHOE” DESIGN FOR CONCRETE AND STEEL ABUTMENTS

The 89-ft RRFCs used for the bridges in this thesis have a varying cross-section along their lengths. These types of RRFCs may also be used at other sites for varying bridge length; however, modifications may be required for proper bearing. Bridge lengths shorter than 47 ft – 4 in. and longer than 66 ft – 0 in. would have a flat cross-section for bearing since the RRFC interior girder is constant at these distances and therefore rests evenly on the abutments. Between these lengths the RRFC interior box girder tapers from a height of 30 1/4 in. to 13 1/4 in. (See Figure B.1). As can be seen, the transition zone begins at the edge of the bolster plate and extends 8 ft – 4 in. The distance between bolster centerlines is 66 ft; hence, when the required bridge distance spans further than the bolsters or the center 47 ft – 4 in. of the RRFC is utilized, the interior girder is constant and no alterations need to be made for bearing.

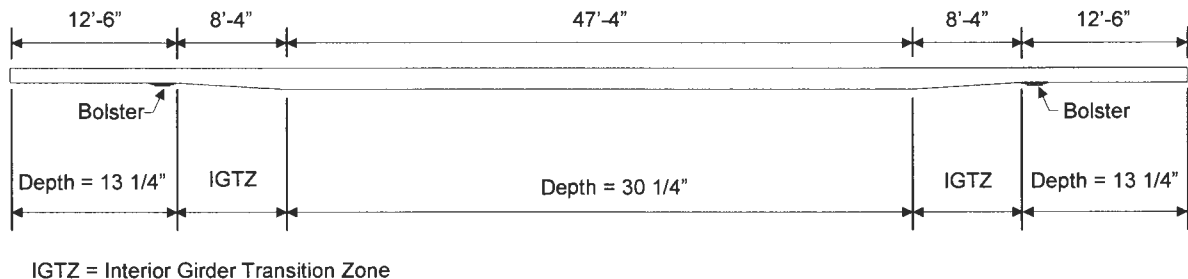


Figure B.1. 89-ft RRFC interior girder depths along length.

Modifications for bearing are required in the region in which the interior girder tapers. The inclined interior girder at the bearing locations results in a very small bearing point, instead of a flat bearing surface (See Figure B.2).

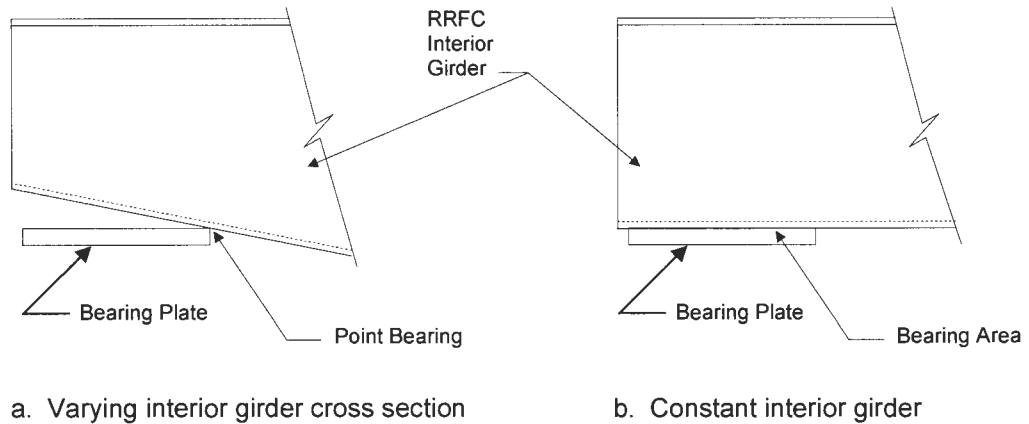
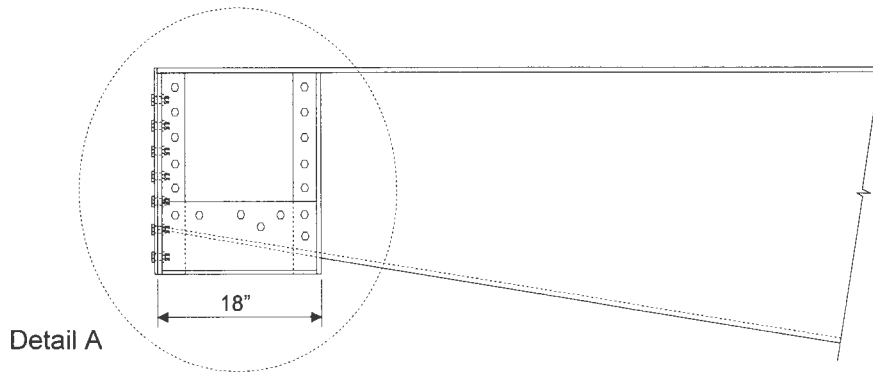


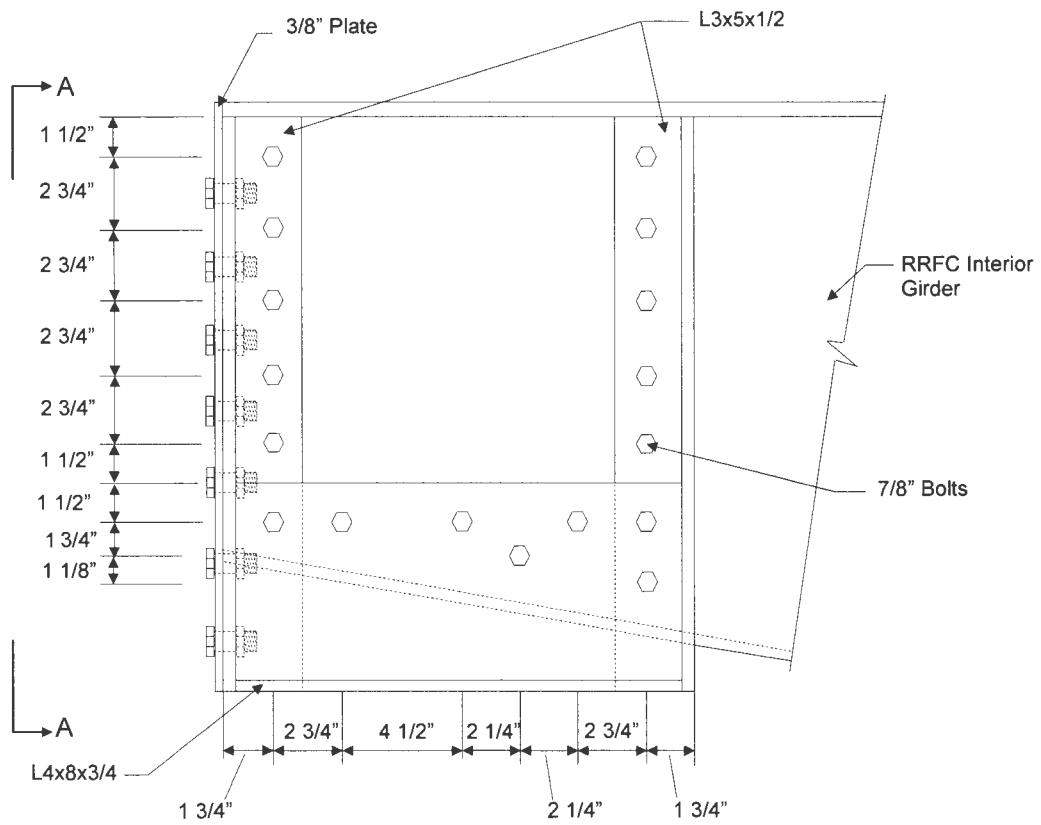
Figure B.2. Bearing conditions for the RRFC interior girders.

As can be seen from Figure B.2, at the varying interior girder cross section region, the point bearing location is at the edge of the bearing plate, causing a large eccentric loading. A condition with a flat bearing surface is ideal; therefore, a “shoe” must be constructed at the tapered interior girder ends of the RRFC to create an even surface to transfer the bridge forces to the abutments.

One possibility is to position four vertical angles, 2 on either side of the interior box girder to act as bearing stiffeners, to distribute the load evenly to the abutment. Another angle, positioned perpendicular to the bearing stiffener angles, would then be placed at the base to complete the framed box on either side of the interior girder. Detailed sketches of this design for both concrete and steel abutments are presented in Figures B.3 and B.4, respectively.

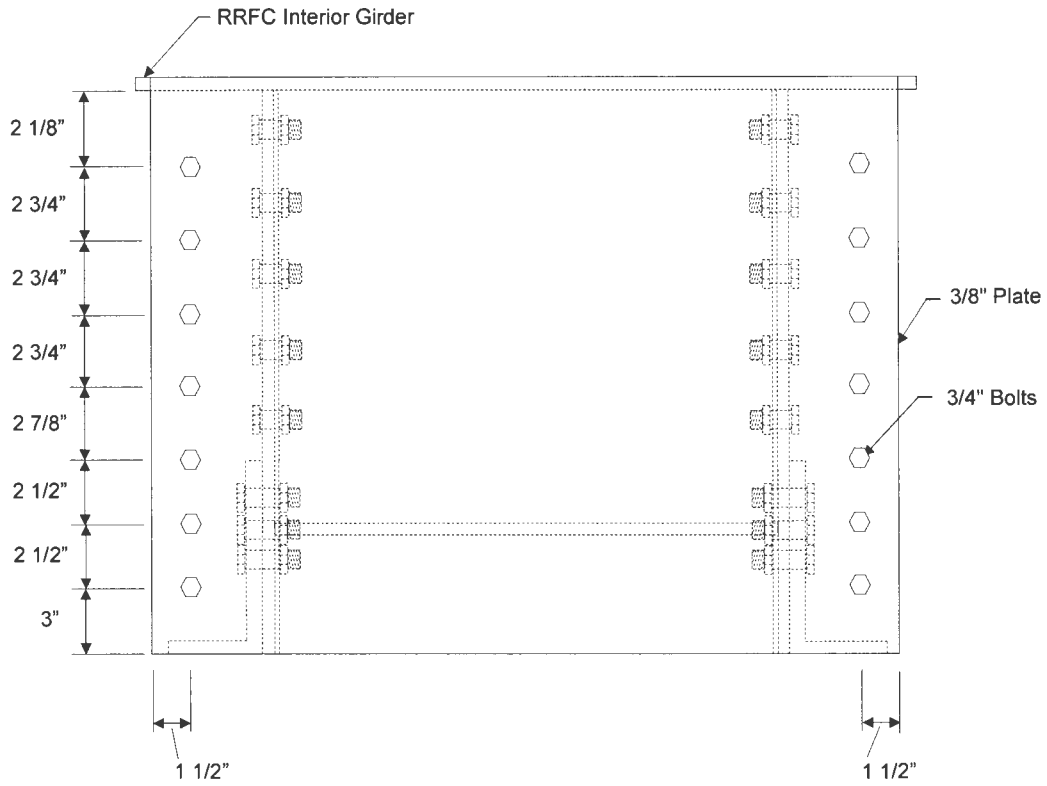


a. Concrete abutment support



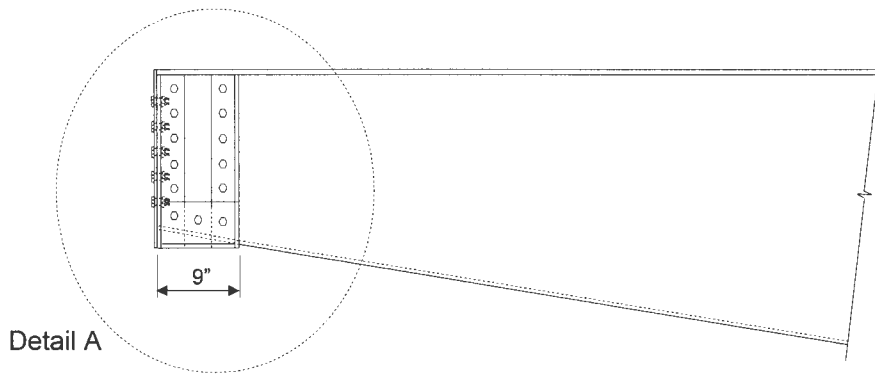
b. Detail A

Figure B.3. Support at tapered end of RRFC interior girder for concrete abutment.

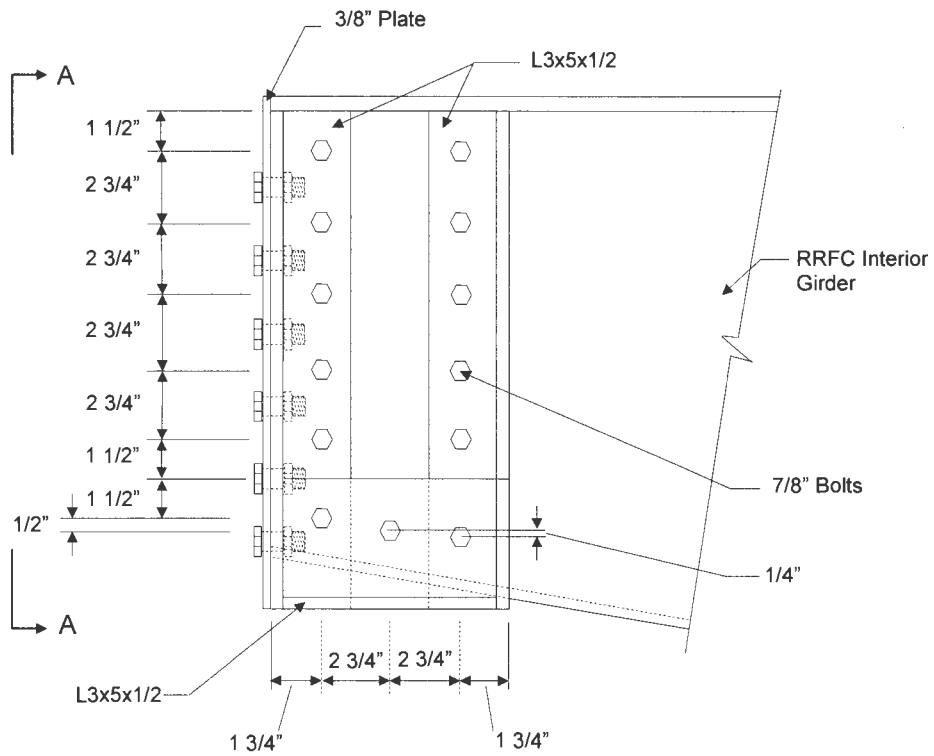


c. RRFC interior girder cross-section

Figure B.3. Continued.

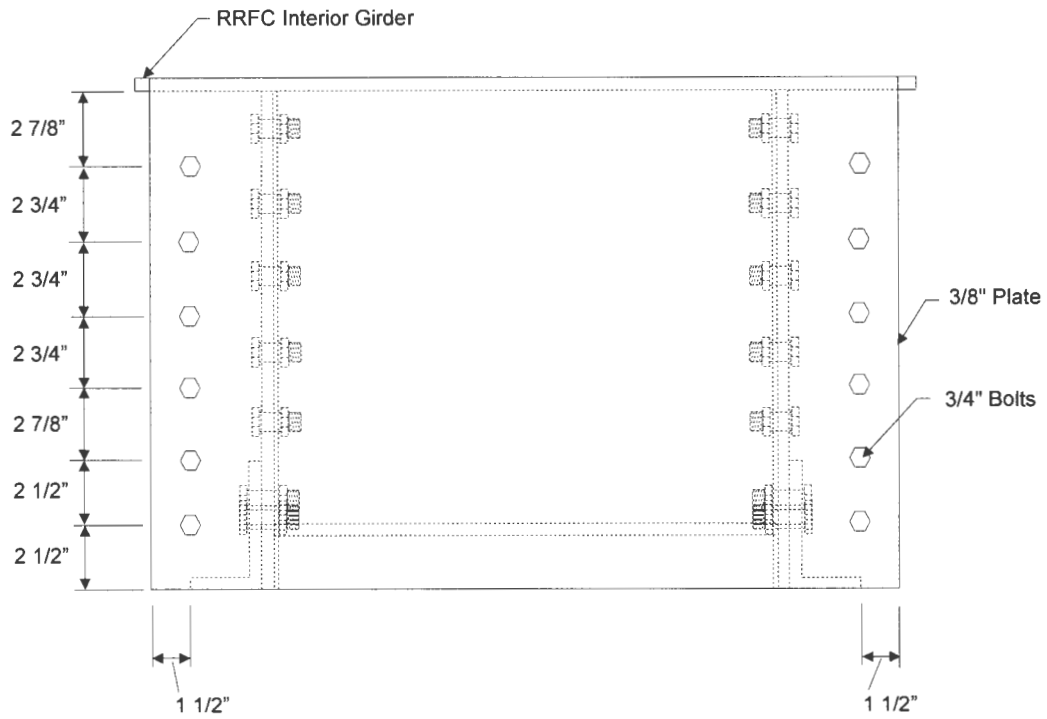


a. Steel abutment support



b. Detail A

Figure B.4. Support at tapered end of RRFC interior girder for steel abutment cap.



c. RRFIC interior girder cross-section

Figure B.4. Continued.

REFERENCES

1. Wipf, T. J., F. W. Klaiber, J. D. Witt, and T.L. Threadgold. *Use of Railroad Flat Cars for Low-Volume Road Bridges*. Iowa DOT Project TR-421. Iowa Department of Transportation. August, 1999. 141 pp. May be accessed electronically at http://www.dot.state.ia.us/materials/research/reports/ihrb_by_topic/transportation_structures.html
2. Wipf, T. J., F. W. Klaiber, J. D. Witt, and J. D. Doornink. *Demonstration Project Using Railroad Flatcars for Low-Volume Road Bridges*. Iowa DOT Project TR-444. Iowa Department of Transportation. February 2003. 193 pp. May be accessed electronically at http://www.dot.state.ia.us/materials/research/reports/ihrb_by_topic/transportation_structures.html
3. Quasqueton, Iowa [map]. <http://www.mapquest.com/maps/map.adp?searchtype=address&country=US&addtohistory=&searchtab=home&address=&city=quasqueton&state=ia&zipcode=>. Accessed October 25, 2004.
4. Iowa Department of Transportation, Highway Division. Standard Designs. *Abutment Details 0° skew – Steel Piling*, Standard No., J30C-17-87. December 2004.
5. American Association of State Highway and Transportation Officials (AASHTO). *AASHTO LRFD Bridge Design Specifications, Second Edition, Customary U.S. Units*. Washington, D.C. 1998.
6. Lake Mills, Iowa [map]. <http://www.mapquest.com/maps/map.adp?searchtype=address&country=US&addtohistory=&searchtab=home&address=&city=lakemills&state=ia&zipcode=>. Accessed September 13, 2004.
7. Carle, R., and S. Whitaker. *Sheet Piling Bridge Abutments*. Deep Foundations Institute Annual Meeting, Baltimore, Maryland. Oct. 1989, 16 pp.
8. Skyline Steel, LLC. *Case Histories: Sprout Brook Bridge: Permanent Sheet Piling provides the Answer*. Online article: http://www.skylinesteel.com/info_ch1.htm.
9. Sassel, R. *Fast Track Construction with Less Traffic Disruption*. Structural Engineer, October 2000. pp. 1-2.
10. United States Steel Corporation. *USS Steel Sheet Piling Design Manual*. Federal Highway Administration (FHWA). July 1984, 132 pp.
11. Bustamante, M., and L. Gianceselli. *Predicting the Bearing Capacity of Sheet Piles Under Vertical Load*. Proceedings of the 4th International Conference on Piling and Deep Foundations, Stresa, Italy. April 1991, 8 pp.
12. McShane, G. *Steel Sheet Piling Used in the Combined Role of Bearing Piles and Earth Retaining Members*. Proceedings of the 4th International Conference on Piling and Deep Foundations, Stresa, Italy. April 1991.

13. Doss, Robert E. and Shiping Yang. *Subsurface Exploration Bridge G-2-N Winnebago County, Iowa. TEAM No. 1-1361*. TEAM Services: Soil, Environmental and Material Consultants. March 1, 2004, 12 pp.
14. Anderson, J.B., F.C. Townsend, and B. Grajales. *Case History Evaluation of Laterally Loaded Piles*. Journal of Geotechnical and Geoenvironmental Engineering, American Society of Civil Engineers (ASCE). March 2003, pp. 187-189.
15. Office of Bridges and Structures. *Bridge Design Manual*. Iowa Department of Transportation. January 28, 2004.
16. Das, Braja M. *Principles of Foundation Engineering, 4th Edition*. Brooks/Cole Publishing Company. 1999, p598.
16. Contech Construction Products, Inc. *Metric Sheeting*. Middletown, Ohio. 1989.

ACKNOWLEDGEMENTS

This investigation was conducted by the Bridge Engineering Center at Iowa State University. The research was sponsored by the Iowa Department of Transportation, Highway Division, and the Iowa Highway Research Board as a portion of Research Project TR-498.

I would like to thank the county engineers and personnel associated with this project for their assistance and cooperation: Brian Keierleber, Buchanan County Engineer, Jim Witt, Winnebago County Engineer, and Mark Johnson from Winnebago County. Doug Wood, ISU Research Laboratory Manager, also deserves special thanks for all his help with the field testing and laboratory work performed for this project. Thanks are given to the following ISU graduate and undergraduate students who assisted with the instrumentation and field testing of these bridges: Kristine Palmer, Jeremy Koskie, Ben Woline, Travis Rengstorf, Jodie Blume, and Mark Currie. I would also like to thank Dr. Wayne Klaiber, Dr. Terry Wipf, and Dr. Loren Zachary, members of my Program of Study, for giving me this opportunity and for guiding me through this research. Lastly, I want to thank my family for their encouragement, especially my parents who have shown me that you truly can become anything you wish through hard work, perseverance, and the support of those around you.